2018

RESOLUTION OF PROXIMAL OXIDATIVE BASE DAMAGE AND 3'-PHOSPHATE TERMINI FOR NONHOMOLOGOUS END JOINING OF FREE RADICAL-MEDIATED DNA DOUBLE-STRAND BREAKS

Sri Lakshmi Chalasani

RESOLUTION OF PROXIMAL OXIDATIVE BASE DAMAGE AND 3′-PHOSPHATE TERMINI FOR NONHOMOLOGOUS END JOINING OF FREE RADICAL-MEDIATED DNA DOUBLE-STRAND BREAKS

A dissertation submitted in partial fulfillment of the requirements for the degree of Doctor of Philosophy at Virginia Commonwealth University

By

Sri Lakshmi Chalasani
MBBS, NTRUHS, 2007
MD, NTRUHS, 2012
MS, VCU, 2015

Director: Lawrence F Povirk Ph.D.,
Professor, Department of Pharmacology and Toxicology

Virginia Commonwealth University

Richmond, Virginia

February 2018

ACKNOWLEDGEMENT

I would like to give my heartfelt thanks to Dr. Lawrence Povirk who has made this possible for me by his excellent mentorship. He is an awesome advisor sharing his enormous knowledge for better understanding of the subject in the study. Being an amateur myself in this field, I had much to learn from him. Dr. Povirk has had a lot of patience to train me all the while during my projects. He has always been there continually guiding me in my each and every step of the lab work. Dr. Povirk dedication to work is beyond compare. His knowledge and approach in science has immensely inspired me. He is a wonderful scientist and a great human being. The birthday song he played for me is which I can never forget in my life. All these years of training under him has made a better at basic research.

My sincere thanks go to Dr. Konstantin Akopiants. He has been a great teacher and help in devising and enacting various experimental protocols. I appreciate his beneficial nature. He is the person one can approach for anything and sure to get it done. I was treated as his kid with many small gifts all the time. I would say he is a valued asset to any workplace. I am blessed to have been able to work with my colleague and friend Ajinkya Kawalae. Our discussions range from intellectual to futile matters and the wisdom and knowledge he displays always embezzled me. I would definitely add him to the list of my mentors for his advice and help regarding my projects are immense. I would like to thank him for his contribution in making me a better person and researcher.

I would like to extend my gratitude towards my committee members, Matthew C Hartman Ph.D., Joseph K. Ritter Ph.D., Kristoffer Valerie Ph.D., Joseph Landry Ph.D. and David Gewirtz Ph.D. for their intellectual contributions to my projects and helping to develop new research ideas to work on. I wish we had many more discussions to build up great projects.

I would like to thank Dr. Akbar Ali for accepting me into the department and guiding me all through the program. I appreciate his dedication to see that his graduate students are up to date and comfortable. I am also grateful to Dr. William Dewey for his valuable advice regarding my professional career and giving me an opportunity to be a part of this wonderful department and lab.

I am indeed lucky to have great friends who always have been a great support in my personal and professional life and made my journey in Richmond memorable. I am indebted to my friend Wisam Toma for giving me a soul-friend none other than his loving wife, Maysam Daryos. Words would not do any justification for explaining the relationship we share. This couple has left no stone unturned to give me comfort and making sure I am content and happy. They gave me home away from home and made my survival possible here. I would also like to thank Ms. Pamela O Haney, a beautiful human being for always being there, taking me out to dinners and tours and teaching me American history and culture. I am also thankful to my friend Madhavi Puchalapalli and her family for their help I would also like to thank my extended family members especially my cousin, Seshagiri Rao Surapaneni, and his family for his moral and financial support

Finally, I would like to thank my family, my mom, and dad for believing in me and supporting me in whatever decision I make. The sacrifices they made put me in this position. If not for them I would stand nowhere. May GOD give them health, peace, and prosperity.

Table of Contents

List of Figures

List of Abbreviations

AP	apurinic/apyrimidinic
APE1	apurinic/apyrimidinic endonuclease
ATM	ataxia telangiectasia mutated
ATP	adenosine triphosphate
ATR	ATM and rad3-related
BER	Base excision repair
CIP	Calf-intestinal phosphatase
CtBP	C-terminal binding protein
CtIP	CtBP-interacting protein
DDR	DNA damage response
DNA	Deoxyribonucleic acid
DNA - PK	DNA-dependent protein kinase
DNA - PKcs	DNA-dependent protein kinase catalytic subunit
dNTP	deoxynucleotides

ddCTP	dideoxycytidine
ddGTP	dideoxy guanidine
ddTTP	dideoxythymidine
DSBs	double-strand breaks (in DNA)
EndoIII	Endonuclease III
Hr	hour(s)
HRR	Homologous recombination repair
IR	ionizing radiation
LET	Linear energy transfer
MDC1	Mediator of DNA damage checkpoint
NHEJ	Non-homologous end joining
PARP-1	Poly(ADP-ribose) polymerase-1
PNKP	Polynucleotide kinase phosphatase
SCID	Severe combined immune-deficiency
sec	seconds
SDS	sodium dodecyl sulfate
SSBs	single-strand breaks (in DNA)
ssDNA	single-strand DNA

TBE	buffer solution mixture of Tris base, boric acid, and EDTA
Tg	Thymine glycol
Tg1	Thymine glycol terminally located at DSB
Tg2	Thymine glycol located at the second position of DSB
Tg3	Thymine glycol located at the third position of DSB
Tg5	Thymine glycol located at the fifth position of DSB
5′ Tg2	Thymine glycol at second position on the 5′-strand of DSB
5′-Tg3	Thymine glycol at the third position on the 5′-strand of DSB
V(D)J	variable, diversity, joining
XLF	XRCC4-like factor
X4L4	XRCC4 -DNA ligase IV complex
XRCC1	X-ray cross-complementation factor 1
XRCC4	X-ray cross-complementation factor 4

Abstract

RESOLUTION OF PROXIMAL OXIDATIVE BASE DAMAGE AND 3′-PHOSPHATE TERMINI IN NONHOMOLOGOUS END JOINING OF FREE RADICAL-MEDIATED DNA DOUBLE-STRAND BREAKS

By Sri Lakshmi Chalasani

A dissertation submitted in partial fulfillment of the requirements for the degree of Doctor of Philosophy at Virginia Commonwealth University

Advisor: Lawrence F. Povirk, Professor, Department of Pharmacology and Toxicology, Virginia Commonwealth University, Richmond, Virginia.

Clustered damage to the DNA is a signature mark of radiation-induced damage, which involves damage to the nucleobases and/or DNA backbone. Modification of the bases and strand breaks with the altered composition are a common occurrence at these clusters, imposing a difficulty in processing these lesions, requiring multiple repair pathways or repair factors to handle the lesions. Double-strand breaks created either directly or indirectly by the repair enzymes are detrimental to the cell survival, as they can lead to chromosomal translocations. Normal cells employ Non-homologous end-joining because of its faster kinetics and a limited homology requirements to suppress the

chromosomal translocations. However, the presence of complex DNA ends constitutes a significant challenge to NHEJ. One such lesion, thymine glycol (Tg), an oxidized thymine lesion was shown to be a lethal due to its propensity to block replicative DNA polymerases. Location of Tg at the 3′ overhang proved to be a potential hindrance to end joining compared to an oxidized purine lesion, 8-oxo-guanine. Positioning Tg at the 3′ end of the blunt double-strand break also inhibited the end joining, but much less when moved to the third position (Tg3) from the end. Positioning it at the fifth position (Tg5), however, reduced the end joining, due to increased removal of Tg from a DNA DSB end. Assaying for the removal of Tg by purified hNTH1 protein, Tg5 was shown to be a better substrate than Tg3, potentially explaining the increased Tg removal and decreased end joining in extracts. Moreover, Tg at second (5′ Tg2) and third (5′-Tg3) positions at 5′ end of the double strand allowed for end joining even when at the second position, unlike its 3′ counterparts, displaying no preference to processing by hNTH1.

Strand breaks caused either by radiation, chemotherapeutic drugs or as intermediates during processing other lesions, also possess unligatable ends with a 3′-phosphate with/without 5′-hydroxyl ends. Polynucleotide kinase phosphatase (PNKP) enzyme is crucial in restoring the 3′ hydroxyl, and 5′ phosphate ends, thus playing a pivotal role in the repair of single and double strand breaks. Targeting PNKP is found to be beneficial in sensitizing the cells to cancer treatment, along with being a synthetic lethal target in cancers lacking a tumor suppressor gene. Experiments done in the current study to explore the activities of PNKP in its absence have revealed surprising results. PNKP knockout derivatives of two cell lines, HCT116, and HeLa, displayed a 3′ phosphatase activity on the overhang and recessed 3′-phosphate ends, in extracts, and

also in-vivo, albeit less than the parental wild-type. Processing of the recessed ends was found to be lesser than the overhangs, even in the wild-type, with a substantial decrease in the knockouts of both cell lines. NU7441, a DNA-PK inhibitor significantly blocked the activity in both wild-type and knockout extracts, while the PNKP inhibitor, ST042164 inhibited the DNA 3′ phosphatase activity in wild-type and not the PNKP knockout. DNA 5′ Kinase activity was also evident in PNKP knockout extracts of both HCT116 and HeLa cell lines. Overall, these results suggest the presence of less efficient alternatives to PNKP for both 3′ phosphatase and 5′ kinase activities in the cells. Also, among the core NHEJ proteins, XRCC4 has been shown to potentiate both activities of PNKP, while XLF enhanced the kinase activity.

General Introduction

Deoxyribonucleic acid (DNA) is one of the four major molecules that are essential for all known forms of life. It carries the genetic information encoded in order via the four nitrogen-containing nucleobases — cytosine (C), guanine (G), adenine (A), or thymine (T), a sugar - deoxyribose, and a phosphate group (nucleotides). These nucleotides form two biopolymer antiparallel stands bound together by base pairing rules (A with T, and C with G), with hydrogen bonds and form a double helix of double-stranded DNA. This information determines the structure, function, growth and development, and reproduction of the living beings. These DNA sequences are highly conserved in evolution and persisted as genetic information despite the constant disturbing influence. These insults came from the usual cellular environments or physiological events, and natural physical agents from external sources such as UV radiation, ionizing radiation, cosmic rays or human-made reactive chemicals, potentially altering the composition and integrity of the DNA. About 18,000 purines are lost in each cell every day, and there will be a conversion of about 100-500 cytosine residues into uracil by deamination. Also, DNA aberrations can also arise from physiological processes such as base mismatches introduced during DNA replication(Jackson & Bartek, 2009), or from the release of reactive oxygen and nitrogen species (ROS/RNS) upon oxidative respiration or through redox-cycling events mediated by heavy metals. Additionally, oncogenic signaling may

cause replication stress resulting in genome instability (Sacco, 2009). On the other hand, the external genotoxic agents, such as ultraviolet light from the sun, IR from cosmic radiation and chemical agents used in cancer therapy utilizing X-rays or radiation can induce a diversity of lesions in DNA including changes or losses of bases (abasic sites), intrastrand or interstrand crosslinks between two complementary DNA strands, SSBs and DSBs. Many such damages occur in conjunction with one another resulting in "clustered lesions." These lesions have a propensity to block genome replication and transcription, and if not repaired or misrepaired, they lead to mutations or wider-scale genome aberrations that threaten cell or organism viability. To address the vast number of DNA lesions, a cell encounters each day, a myriad of elegant repair mechanisms have evolved to ensure faithful propagation of genetic material to daughter cells, and are essential for life. Hence, these repair pathways are critical and described as guardians of the human genome (Sishc & Davis, 2017). However, this DNA damage response might be a hindrance in treating cancer as DNA damage is the prime detrimental target for cancer chemotherapy or radiotherapy. Several inhibitors of specific proteins / factors involved in DNA damage response that is responsible for the survival of the cancer cells are under study, to sensitize the resistant cells to the regular treatments. Moreover, some of the tumor cells can be addicted to the protein (oncogene) for survival and/or can be defective in specific DNA damage response. These parameters serve as biomarkers to develop therapeutic strategies. Nonetheless, before considering a damage response/repair as a target, the mechanism of repair of a particular lesion should be elucidated appropriately to ensure that there is no compensatory /redundant pathway that can take over in the absence of the primary pathway. Radiotherapy is notorious to elicit a variety of repair

responses by inducing a medley of lesions in clusters and is a signature mark of radiation damage. In my current study, I will be studying the repair of clustered lesions with either an oxidized base (Thymine glycol) or modified end (3′-Phosphate) at the double strand break (DSB) of DNA.

1.1 Radiation-induced DNA damage

There has been extensive evidence from the radiation biology studies that DNA damage can result in various human pathologies such as cancer, premature aging, and chronic inflammatory conditions (Ciccia & Elledge, 2010). Radiotherapy is one of the primary modalities of cancer treatment, used either alone or in combination with surgery and chemotherapy and is considered as a 'two-edged sword' as it can induce genetic modifications in normal tissue along with the loss of clonogenic survival of tumor cells. Evidence from various animal models has shown that radiation-induced key gene losses in non-targeted cells can be of DNA damage response, apoptotic and cell cycle control genes and others, leading to secondary carcinogenesis. This damage caused by radiation is via linear energy transfer (LET), depositing energy in the biomolecules of cells it passes, causing chemical modifications. There can be either a direct deposition of energy or indirectly via formation of reactive chemical species in the surrounding of DNA (Ward, 1988) (Georgakilas, 2008). Radiolysis of water in the vicinity (10 nm) of the DNA is primarily attributed to the production of hydroxyl radicals (OH-). The nature of lesions induced is similar to endogenously (ROS) produced lesions sometimes even in a fewer number. However, what determines the lethality of radiation is the spatial distribution of lesions induced along the single radiation track. While the endogenously produced lesions are more homogenously distributed, ionizing radiation produces two or more

heterogeneous lesions within one or two helical turns of DNA (Sutherland, Bennett, Sutherland, & Laval, 2002). Radiation track structure modeling has revealed that the energy deposition of low-LET radiation leads to two or more lesions within a radius of 1–4 nM, similar to the diameter of the DNA double helix and its water layers. These signature lesions produced in a single track of radiation are considered as clustered damage, also called multiple damaged sites (MDS). These clustered lesions involve a combination of an oxidized purine or pyrimidine lesions, abasic sites with/ without single-strand breaks (non-DSB clustered lesions) and double strand breaks (DSB'S) with 3′-phosphate or 3′-phosphoglycolate ends and/or modified sugars or bases (complex DSB's) (Sage & Shikazono, 2017). These lesions can occur in the opposite strands within few helical turns termed as "bistranded clusters." High LET radiation (e,g., α-particles, protons, and carbon-ions) has an elevated propensity to form clustered DNA lesions of higher complexity (much denser), even though the overall number of DSB and non-DSB clustered lesions does not increase, and sometimes even decreases in comparison with low-LET radiation (M. Hada, 2006) (Georgakilas, O'Neill, & Stewart, 2013b).

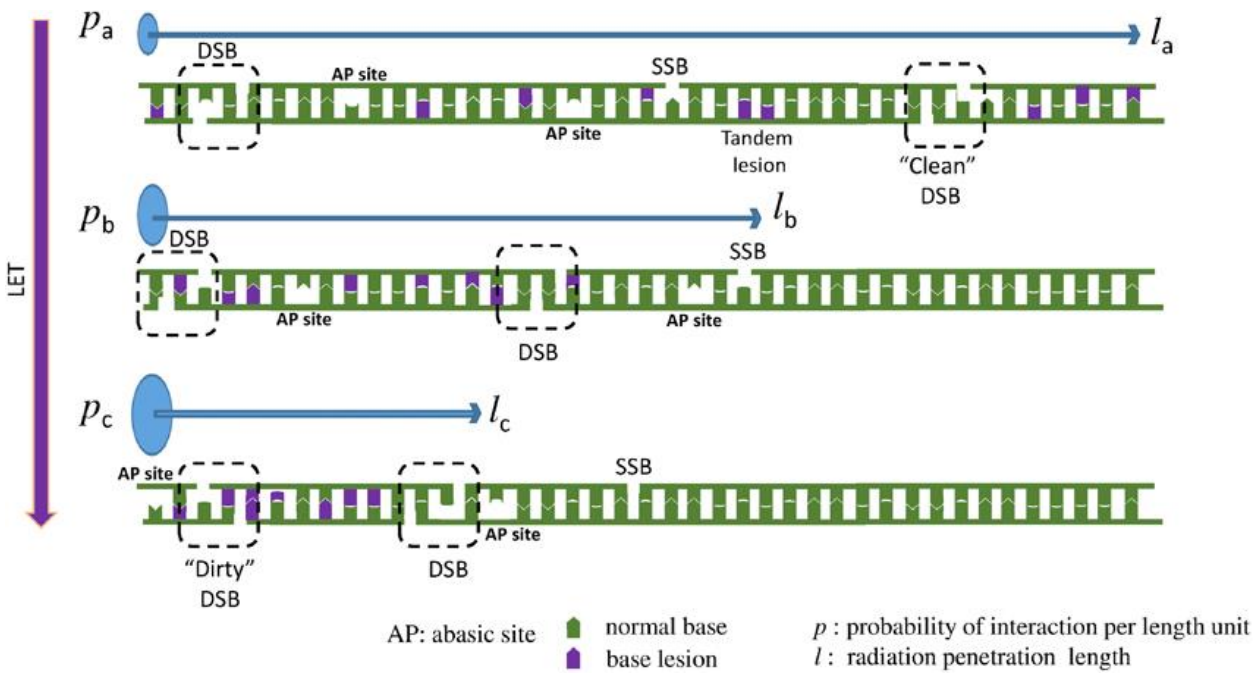

Fig. 1.1: Increase in LET increases the density but not the number of lesions: Schematic representation of increase clustering of lesions due to High Linear energy transfer (LET), depositing the same energy in a limited length inducing same number different types of DNA lesions, similar to low LET. Figure adapted with permission from Nikitaki et al., 2015.

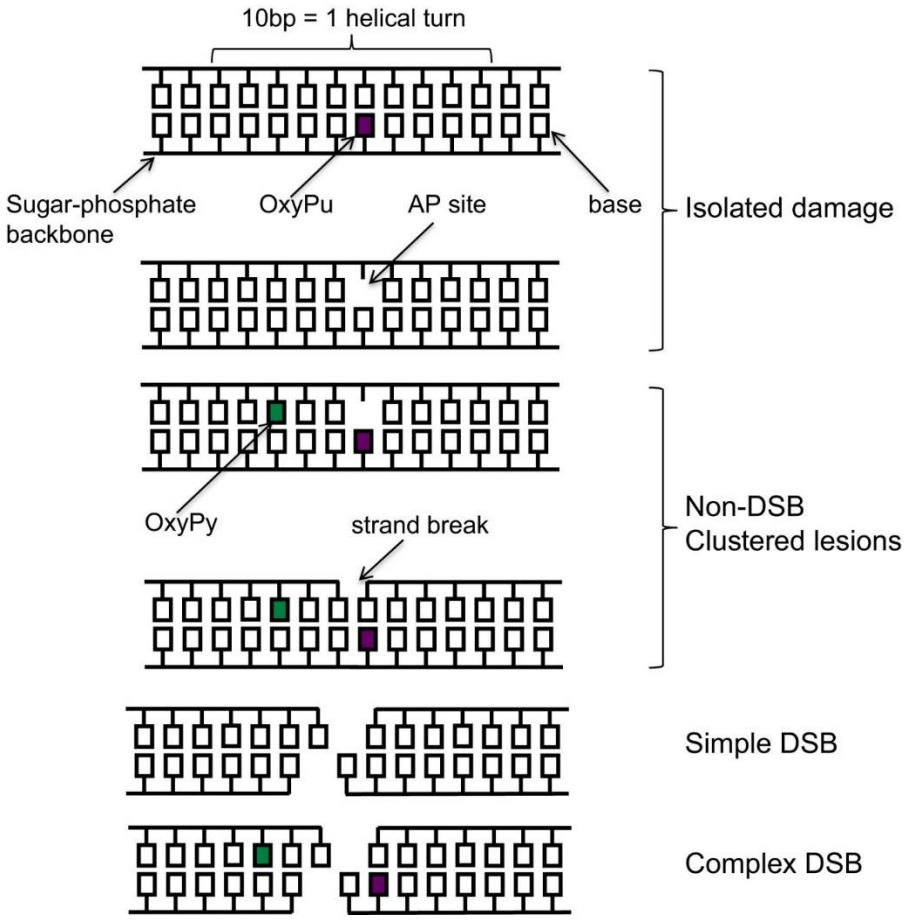

Fig. 1.2: Schematic representation of oxidatively generated DNA damage induced by ionizing radiation: Oxidatively generated base damage (noted oxyPu, oxyPy, U), abasic site clustered lesions at the with no DSB, SSB within one or two helix turns of DNA, produced by a single radiation track, the complexity of which increases with increasing LET. Complex DSB are DSB associated with several oxidized bases and abasic sites. Figure adapted with permission from Evelyne Sage and Naoya Shikazono 2017.

1.2 Biological significance and Repair of clustered lesions

As explained above a single radiation track has the propensity to cause two main categories of lesions appearing in a cluster, DSB and non-DSB lesions, usually referred to as oxidatively-clustered DNA lesions (OCDLs). The repair of the non-DSB cluster lesions is attempted by BER proteins, Apurinic/apyrimidinic endonuclease1 (APE1) or Poly(ADP-ribose) polymerase-1 (PARP1), as evidenced from recent studies using primary human fibroblasts (Das & Sutherland, 2011) or cell extracts (Kutuzov et al., 2011). The type of lesion, the inter-lesion distance and the orientation of nearby lesions (e.g., bi-stranded or tandem lesions) are a rate limit to the repair process, resulting in a reduction or inhibition of the processing enzymes such as the glycosylases and nucleases at these cluster sites. This slow processing of the lesions leads to the persistence of these lesions until they hit a replication fork leading to the formation of chromosome breaks, mutations, and misrepair (J. V Harper, Anderson, & O'Neill, 2010)(Eccles, Lomax, & O'Neill, 2010). There will be a formation of inadvertent DSB from these clustered lesions during the repair or replication (J. V Harper et al., 2010). Human AP-endonuclease-1 (hAPE1) is also capable of producing a DSB by cleaving the two opposite stranded AP sites. DSB can also result from the formation of nick in the intact strand, during processing of the apyrimidinic site on the opposite strand. There is a hierarchy of the repair of the lesions in case of three or more complex lesions to avoid the formation of DSB (Georgakilas, O'Neill, & Stewart, 2013a). There is a severe impairment of the excision of a base lesion such as 8-oxo-guanine, opposing an AP site or strand break until the AP site/strand break is repaired, though it occurs slowly due to the damaged opposed base (Lomax, Cunniffe, & O'Neill, 2004). While the radiation-induced simple prompt DSB, although carrying 3′-

ends phosphate and phosphoglycolate can be efficiently and accurately repaired within 1–2 h by non-homologous end joining (NHEJ), DSB clustered DNA lesions resulting from either direct action of the radiation or as a result of processing of non-DSB clusters are repaired by non-homologous (NHEJ) or microhomology-mediated end-joining (MMEJ) (Behjati, et al., 2016). When the DSB is due to replication fork hitting the clustered SSB lesion, the repair is by homologous recombination (Groth et al., 2012)(Arnaudeau, Lundin, & Helleday, 2001). Among the DNA lesions, DSB's are considered to be most lethal as their misrepair can lead to genomic instability. Thus, the biological significance of clustered DNA damage is not only due to the difficulty encountered by the different DNA repair proteins that process these closely spaced DNA lesions, but also because several of these OCDLs can be converted into de novo DSBs during repair. A small fraction of radiation-induced DSBs, and in particular those induced by high LET radiation, have a slow rate of repair and to require DNA damage response via the ATM pathway. Thus, there is a possibility of chromosomal abnormalities arising from the repair of radiation-induced DNA damage via the less accurate non-homologous (NHEJ) or microhomology-mediated end-joining (MMEJ) (Behjati et al., 2016). leading to leading to structural abnormalities and subsequently to genomic instability (GI) and cancer.

1.3 DNA Damage Response:

Sophisticated cellular networks sense, signal, and repair DNA lesions, constantly monitoring genome integrity. Depending on the type of the lesion, the repair can be by, but not limited to Nucleotide excision repair, Base excision repair, Homologous repair, or enjoining, and can function in a partial overlap. The proteins detect and bind to DNA lesions (sensors), activating the signaling pathways via post-translational modifications

of downstream proteins. Any genetic defects acquired in these response pathways induce a plethora of consequences affecting normal development, immunological problems, aging, and cancers. In response to DNA damage, three distinct functionalities are activated: (1) damage detection, (2) control of cell cycle and transcriptional programs of damage response, and (3) mechanisms for catalyzing the repair of the lesion (Lamarche, Orazio, & Weitzman, 2010). Cell cycle progression and DNA repair are tightly regulated via cell cycle checkpoints due to activation of orchestrated cell signaling pathways (J. W. Harper & Elledge, 2007). Minimal damage in the cell activates repair but not arrest, however with higher levels of damage there will be induction of arrest, in G1 or S, to prevent replication fork encounter with lesions (D. Branzei, 2009), and in G2 to prevent mitotic catastrophe (H. Vakifahmetoglu, M. Olsson, 2008). If the damage can't be repaired, cells enter one of several programmed death pathways (necrosis or apoptosis). In the DNA damage spectrum, DSB's are considered to be fatal as there is no complementary strand to be used as a template for repair, which can lead to translocations and chromosomal rearrangements due to aberrant end joining. In any phase, Ku 70/80 heterodimers and MRN sensor complex are the first to detect DSB's to activate and recruit apical DDR kinase ataxia telangiectasia mutated (ATM) (Uziel et al., 2003). In S/G2 phase RPA recruits the ATM and Rad3-related (ATR) kinase via its partner protein, ATR-interacting partner (ATRIP) at the regions of ssDNA exposed by DSB processing or ssDNA at stalled replication forks (Rouse & Jackson, 2002). A third signaling pathway involves ATM, p38MAPK and MK2 kinases, converging on to similar cell cycle regulation targets such as Chk1/2. DNA PKcs, a central protein in C-NHEJ, also belonging to the same class Phosphatidylinositol 3-kinase-related kinase (PIKK) as ATM

and ATR has also been discovered to play a central role in DDR signaling, especially during replication stress (R.-G. Shao et al., 1999). Although there was an initial compartmentalization of ATM and ATR response to frank DSBs and replication stress, respectively, in initial studies, there is always a functional crosstalk and overlap in the DDR. Mediator proteins for ATM such as BRCA1, MDC1 (mediator of DNA damage checkpoint) and 53BP1 (p53-binding protein 1) activate the effector kinases Chk1 and Chk2, spreading the signal throughout the nucleus stalling the progression of cell cycle (Blackford & Jackson, 2017).

1.4 Repair of double strand breaks:

Repair of DSB's is by four possible mechanisms. Classic-NHEJ end ligation independent of sequence homology, by many factors such as Ku70/80, DNA-PKcs, and DNA ligase IV. Alternatively, the DSB end can be resected leaving 3′ single-stranded DNA (ssDNA) overhangs can be repaired by three possible mechanisms: HR, SSA, and alt-EJ. However, recently a resection dependant NHEJ was discovered which is end initiated by Plk3/CtIP/Brca1, executed by Mre11 exonuclease, EXD2, and Exo1 execute resection, and completed by Artemis (Biehs et al., 2017). These repair pathways are not complementary and function under different circumstances. NHEJ does not require a template and is functional throughout the cell cycle, faster kinetics of resection independent repair suppressing chromosomal translocations (Difilippantonio et al., 2000) with resection-dependant form increasing them.(Barton et al., 2014) HR predominates in the mid-S and mid-G2 cell cycle phases, when a sister template is available and is typically error-free (Ketki Karanam , Ran Kafri, Alexander Loewer, 2012). When classical NHEJ or HR is impeded because of a missing or mutated component, alternative end-

joining pathways operate. These alternative end-joining pathways utilize the factors such as the MRE11–RAD50–NBS1 (MRN) complex, poly(ADP-ribose) polymerase-1 (PARP-1), XRCC1, and DNA Ligase I or III that are involved in SSB repair (SSBR) or HR and there is reliance on terminal micro-homologies for the joining reactions (McVey & Lee, 2008). SSA mediates end joining between interspersed nucleotide repeats in the genome and involves reannealing of Replication Protein A (RPA)-covered ssDNA by the RAD52 protein. The intervening sequence between the repeats is deleted in the repair product, thus resulting in loss of genetic information (Heyer, Ehmsen, Liu, & Heyer TEL, 2010).

1.5 Repair Pathway Selection:

In normal cells, DNA DSB's are repaired by two major pathways- NHEJ and HR. Many factors decide the choice of repair. One major factor being the cell cycle, NHEJ being active in all phases of cell cycle, except M-phase, and HR functioning only in S/G2 phase. Even in G2-phase, 70% of the two ended DSB's are repaired by NHEJ, and the remaining 30% by HR (Beucher et al., 2009). Irrespective of the stage of the cell cycle NHEJ factors Ku 70/80 and 53bp1 are the first responders to protect the free DNA ends from extensive resection. ATM-mediated phosphorylation of 53BP1 recruits RIF-1 protein which inhibits accumulation of BRCA 1 (HR factor), possibly by modulating the recognition of the ubiquitylated chromatin due to compaction of 53BP1 at the DSB (Escribano-Díaz et al., 2013). BRCA1 promotes 53BP1 dephosphorylation via protein phosphatase 4 (PP4) and RIF1 release to favor homologous recombination (Isono et al., 2017). Further, Ku should be displaced from the ends for HR to be initiated by RAD51 loading (Chanut, Britton, Coates, Jackson, & Calsou, 2016). This process is intricately regulated by neddylation, proteasome-mediated NHEJ complex degradation, phosphorylation, and MRE11-

dependent nuclease digestion of the DNA ends. The MRN complex plays a pivotal role in directing a DSB down the appropriate repair pathway, via its DNA end-processing activities (Huertas, 2010). Mre11 with its endonuclease (HR) and exonuclease functions (HR, NHEJ), along with other exonucleases, initiates a nick or resection of the DNA strand, respectively, and processes it downstream. One of these exonucleases, C-terminal binding protein 1 (CtIP) is phosphorylated at Ser327 position in a Plk3 (G1) or CDK (G2), promoting a complex formation between CtIP, Mre11 and BRCA1 (You & Bailis, 2010) (Barton et al., 2014). In HR, following the initial processing, other nucleases and helicases (i.e., DNA2, BLM, WRN) produce further resection of DSB generating extensive 3′ ssDNA overhangs on each side of the break. The ssDNA thus generated is an excellent substrate for the HR-specific ssDNA-binding factors RPA and Rad51, (Huertas, 2010) and a poor one for NHEJ-specific double strand DNA termini binding factor Ku70/80 (Dynan & Yoo, 1998). Several factors such as nuclear architecture, chromatin and transcriptional context influence repair-pathway choice. The list of the regulatory proteins and post-translational modifications which play a role in determining the destiny of the DSB's has been increasing recently (Drané et al., 2017) (Li et al., 2017)(Isobe, Nagao, Nozaki, Kimura, & Obuse, 2017) (Mackay, Howa, Werner, & Ullman, 2017) .

1.6 Homologous recombination:

Homologous recombination is the DNA repair process which utilizes a homologous sequence, on a homologous chromosome or a sister chromatid for accurate DNA repair. This is a highly conservative process. As discussed above, the initial sensor and responder to localize at the DSB is the MRN complex (Uziel et al., 2003) which forms

nuclear foci. MRN complex incites the further steps in HR mechanism by recruiting a phosphatidylinositol-3-related kinase, ATM, which phosphorylates histone H2AX at Ser139 position forming γH2AX. MDC1, a mediator protein facilitates the binding and phosphorylation between ATM and H2AX. By marking one or more megabases of DNA surrounding the break, γH2AX serves as a molecular beacon signaling the presence of damage (Davis & Chen, 2013), and forms a scaffold protein for the accumulation of other proteins in the repair pathway. Formation of NBS1/MRE11/Rad50, 53BP1, and BRCA1 foci is regulated by MDC1. The RING-finger ubiquitin ligase, RNF8, interacts with phosphorylated MDC1 with its FHA domain (Mailand et al., 2007), ubiquitinylates H2AX and facilitates the accumulation of BRCA1 at the site of damage. BRCA1-C complex, BRCA1-CtIP, is formed by the direct interaction of BRCA-1 and phosphorylated CtIP, and is recruited by MRN complex (Williams et al., 2009).

Cyclin-dependent kinase's phosphorylation of CtIP on Ser327 is essential for physical interactions between CtIP and BRCA1, which occurs during G2 phase of cycle. Upon binding to the MRN complex, CtIP catalyzes Mre11 endonuclease activity to introduce nicks on the DNA duplexes as far as 300 nt from DSB ends. The nick thus produced triggers Exo1-dependent 5′ -3′ resection, while the Mre11 exonuclease mediates 3′ -5′ degradation of the nicked strand toward the break releasing any other proteins such as Ku (NHEJ factor) bound to the DSB, thus blocking NHEJ. This extensive DSB end resection generates single strand DNA (ssDNA) overhangs. ssDNA binding complex RPA (replication protein A) coats these ssDNA overhangs initially, later substituted by RAD 51, forming a nucleoprotein filament. Other recombinant proteins such as RAD52/RAD54 stabilize this interaction. This RAD51 nucleofilament, together

with various other HR factors, mediates strand invasion near a homologous sequence in sister chromatid or homologous chromosome. Once the strand is copied and filled in by DNA polymerases and ligated by Ligase I, while DNA helicase and resolvase enzymes mediate the cleavage and resolution of HR intermediates.

1.7 Nonhomologous End Joining:

NHEJ, as the name suggests, involves direct joining of the DNA ends with minimal processing of the ends. DSB repair in mammals appears to be primarily by NHEJ and has been traditionally regarded as the guardian of the genome as it prevents genomic instability by means of its faster kinetics of repair. Moreover, NHEJ is a flexible and dynamic process that can respond to variable types of DSBs (Davis, Chen, & Chen, 2014). Physiologically, NHEJ factors in addition to protection from damage of internal ROS, are also crucial for V(D)J recombination for ensuring maturation of immune cells and for the telomere maintenance. The three main steps of NHEJ are: (I) DNA end recognition and assembly and stabilization of the NHEJ complex at the DNA double-strand break; (II) Bridging of the DNA ends and promotion of end stability; (III) DNA end processing; and (IV) Ligation of the broken ends and dissolution of the NHEJ complex (Davis & Chen, 2013). Fifteen or more proteins can be involved in the processes assembling in a confined space around the DNA ends. XRCC5, XRCC6, and XRCC7 are the genes that encode some of the core NHEJ proteins that form DNA-dependent protein kinase (DNA-PK). XRCC5 and XRCC6 encode the 80 and 70 kDa subunits of the Ku70/80 heterodimer (the DNA-binding subunit of DNA-PK), and XRCC7 encodes the 470 kDa DNA-catalytic subunit of protein kinase DNA-PKcs (Critchlow & Jackson, 1998). In addition to the above factors, a heterodimer XRCC4/LigaseIV ligates the strands

(Critchlow & Jackson, 1998) and Cerrunnos/XLF activates the ligase activity (Critchlow & Jackson, 1998). Various end processing factors such as Artemis, TdT, WRN, PNK, hTDP1, FEN1 are required to clean the ends of the DNA of any complexities that hinder the direct joining and DNA polymerases λ/μ fills in the gaps created in the process. Proteins such as PARP-3 and APLF accelerate the NHEJ by retaining the XRCC4/Ligase-IV complex at the site of break (Rulten et al., 2011). Since there is involvements of so many factors in the repair complexes, some of them required to compete for the same binding site, these factors have conserved protein domains or motifs such as XLF-like motifs (XLMs), FHA domains, Ku-binding motifs (KBMs) and BRCT domains (Rulten & Grundy, 2017).

1.8 NHEJ Pathway:

DSB associated with V(D)J recombination, irradiation or chemotherapy damage are primarily recognized by the MRN complex, which by further signaling via ATM, phosphorylates and activates H2AX to γH2AX. γH2AX recruits BRCA-1 or 53bp1, the deciding factors for the pathway of repair. In G1/M oligomers of 53bp1 flank on either side of the DSB bound to the histones modified by acetylases and methyl transferases. The chromatin conformation is thus maintained limiting access to transcription and HR factors (Chapman, Taylor, & Boulton, 2012), promoting NHEJ. Whenever there is a DSB, irrespective of the cell cycle Ku is the initial protein (Reid et al., 2015) to translocate to the site and binds dsDNA ends with extremely high affinity (Lieber, 2010) and encircles the DNA with its preformed channel (Walker, Corpina, & Goldberg, 2001). This binding occurs in an ATP dependent manner (Dynan & Yoo, 1998) and prevents the DNA ends from further damage. Ku functions as a signal molecule for the recruitment of further NHEJ

proteins. Recently, it has been shown that Ku can process the ends of the DNA by virtue of its 5′-dRP/AP lyase activity, processing the abasic sites by nicking DNA 3′ of the abasic site via a Schiff-base covalent intermediate (Fell & Schild-Poulter, 2015). After its binding to the ends, there will be an inward translocation of Ku and recruitment of DNA-PKcs to form a Ku-DNA-PKcs synaptic complex (DNA-PK) which tethers the DNA ends together and offers protection from premature nucleolytic degradation (Smith & Jackson, 1999). Further, synapsis of the juxtaposed DNA ends stimulates autophosphorylation of DNA-PKcs by DNA-PK kinase activity, inducing a conformational change in the DNA-PK complex, mobilising it internally away from the DNA strand breaks, providing access to other factors (Calsou et al., 1999). In addition to DNA-PKcs, DNA bound Ku also recruits XRCC4/Ligase IV complex and XLF independently (Yano & Chen, 2008). The recruitment of the proteins does not require any protein-protein interactions but the assembly of the proteins does. XRCC4 requires DNA-PKcs, and XLF requires XRCC4 to be retained at the repair loci. Once recruited, XLF and XRCC4 form a nucleo-filament around the DNA ends by interacting in a head-head manner. The architectural channel thus formed with the synergy of Ku-XLF-XRCC4 interaction, stabilizes DSBs and provides accessibility and activation of Ligase IV (Hammel et al., 2011). Ligase IV is ATP-dependent and uses ATP to adenylate itself to transfer AMP to the 5′- phosphate of one end of DSB. AMP gets removed by the nucleophilic attack by the 3′ hydroxyl group of the second DSB end, yielding a ligation product. XLF stimulates LIG4-mediated ligation via promoting re-adenylation of Ligase IV (Davis et al., 2014). One distinctive feature of Ligase IV is its ability to ligate incompatible DNA ends across gaps. Ligation of mismatched and non-cohesive ends is stimulated by XLF. As expected of it, NHEJ is an error-prone pathway

(Lieber, Ma, Pannicke, & Schwarz, 2004), as there will be often removal of the nucleotides and fill in without the guidance of a template. Loss of nucleotides during the process makes the DSB repair inaccurate. Except for the recruitment of the Ku heterodimer, the order of recruitment of other factors is flexible depending on the complexity of the DNA damage (Reynolds et al., 2012). The recruitment of the NHEJ machinery to the site of the DSB occurs via a dynamic assembly (Yano, Morotomi-Yano, Adachi, & Akiyama, 2009), rather than a step-wise sequential manner. Ku heterodimer, XRCC4, Ligase IV and XLF are sufficient for the repair of simple DSB, whereas complex breaks require DNA-PKcs and ATM activation of a multitude of repair factors to enhance processing of the damage. As the IR produces complex DSB's with 3′-phosphate or 3′-phosphoglycolate groups, 3′ and 5′ overhangs with damaged bases and/or ribose units in the vicinity of the break ends (Nikjoo, O'Neill, Wilson, & Goodhead, 2001), the DNA ends must be processed before ligation. Enzymes such as Polynucleotide Kinase 3′-Phosphatase (PNKP), Artemis, FEN-1, WRN, hTDP1, Polymerases belonging to Pol X family (μ and λ), aid in the processing of the complex DNA ends. DNA Polymerases serve two important roles, fill-in synthesis of gaps and nucleotide addition to broken DNA ends. Pol μ primarily adds nucleotides in a template-independent manner, whereas Pol λ primarily has template-dependent polymerase activity. While Pol PNKP removes the 3′- phosphate from the DNA ends, Artemis removes the hairpin bend at the the V(D)J associated DSB, metnase trims the damaged ends (Mohapatra et al., 2013), nucleases remove several nucleotides from single-stranded overhangs at the DSB ends termini, aprataxin removes adenylate groups from the 5′ end (Ahel et al., 2006b) , the phosphodiesterases TDP1 and TDP2 process DNA topoisomerase adducts (Lee et al., 2012), DNA poly merases

belonging Pol X family fill in the gap, FEN-1 has an exonuclease function, WRN (Werner syndrome helicase) and BLM (Bloom syndrome helicase) are the unwinding enzymes (Lee et al., 2012). This extensive processing of the DNA end can result in deletions and insertions leading to inaccuracy in repair. Even though cNHEJ is inherently error-prone, there are greater risks associated with cNHEJ defects as the back-up alt-NHEJ pathway creates larger deletions, mediating translocations (Corneo et al., 2007) (Deriano & Roth, 2013).

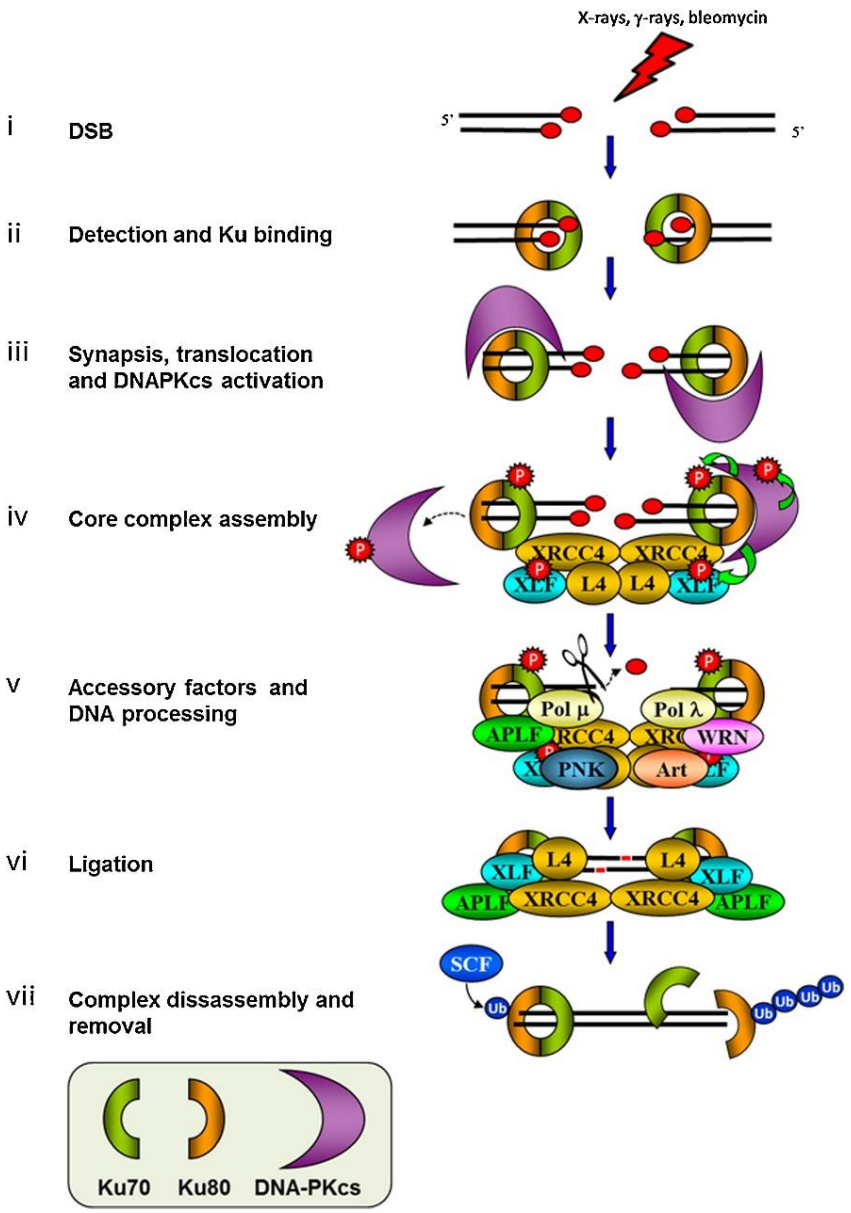

Fig. 1.3: Schematic overview of NHEJ: i) Illustration of a double-strand break (DSB). ii) Recognition of the DSB produced by an by the heterodimer protein Ku. iii) Recruitment of the DNA PKcs by Ku and formation of DNA-PK complex by the activation of its kinase activity. iv) Autophosphorylation of DNA-PKcs shifts the complex inwards exposing the DNA ends for the processing enzymes. XRCC4-Ligase IV complex in combination with XLF forms a filament around the broken ends, and vi) once the ends are processed by specific accessory factors, DNA Ligase IV ligates the ends, vii) followed by disassembly of the complex after restoring the DNA integrity. Figure adapted with permission from Grundy et al., 2014.

1.9 NHEJ – Guardian or Disruptor of the genome?

There is contrasting evidence giving rise to the debate if NHEJ is indeed a protector from genomic instability. There are numerous studies undermining the role of core NHEJ factors in promoting healthy neurological and immunological development of the organism, protection from premature aging and the development of carcinogenesis as evidenced by increased tumor rates in mouse-models lacking core NHEJ factors(Buck et al., 2006)(Yan et al., 2006) (Espejel et al., 2004)(Gao et al., 2000). Surprisingly, studies in human cells, in which site-specific DSBs are introduced using nucleases at endogenous loci, translocation reporter assays, or DSBs induced by radiation, found that NHEJ is responsible for the generation of translocations (Rothkamm, Kühne, Jeggo, & Löbrich, 2001) (Weinstock, Richardson, Elliott, & Jasin, 2006)(Lieber, Gu, Lu, Shimazaki, & Tsai, 2010). Furthermore, NHEJ is found to be the culprit behind the translocations in human lymphoid cells and renal cell carcinoma (RCC), with the characteristic small deletions near the DSB sites, and DNA polymerase μ or Pol λ mediated template-independent nucleotide insertion (Lieber et al., 2010) (Ali et al., 2013). Chromosomal translocations can be a consequence of inaccurate end joining of two independent DSBs on different chromosomes by NHEJ. The probability of this will increase during an attempted repair of highly complex lesions, or repair of one ended DSBs due to a failure of HR or pathways such as Fanconi anemia pathway which directs this one ended DSBS towards HR (Romick-Rosendale et al., 2016). Interestingly, DNA-PKcs-dependent NHEJ is found to play a role in Chromothripsis, a result of randomly rejoined multiple DSBs of a chromosome (Ali et al., 2013). Probing into this controversial data researchers have also found out the role of differential regulation and single nucleotide polymorphisms (SNPs)

in the core NHEJ genes that correlate with cancer incidence, tumor aggressiveness, and responsiveness to conventional radiation and chemotherapy. Some tumors have shown either a decrease of Ku70 levels or DNA-PKcs levels (colon, endometrial, breast and lung) (Beggs et al., 2012) (Lomnytska et al., 2012) (Lomnytska et al., 2012) (Auckley et al., 2001), or increase of Ku70 levels or DNA-PKcs levels (myeloid, gastric and colorectal) (Gaymes, Mufti, & Rassool, 2002) (H. Hu, Zhang, Zou, Yang, & Liang, 2010) (Auckley et al., 2001), which drive carcinogenesis. Similarly, high Ligase IV expression (prostate cancer) (GRUPP et al., 2015) or reduced Ligase IV expression, (colorectal cancer) (Kuhmann et al., 2014) causes tumorigenesis. Also, XLF overexpression in HPV(+) HNSCCs and down-regulation in HNSCC cells expressing high levels of mutant p53, promote chromosomal instability and cancer (Feng et al., 2016). Further, genetic single nucleotide polymorphisms (SNPs) in the core NHEJ factors are found to be associated with either carcinogenesis (Feng et al., 2016) (Schildkraut et al., 2010) (Wang et al., 2008) (Hsu et al., 2009), or reduced risk of cancer (Adel Fahmideh et al., 2016) (Andrew et al., 2015) (Roddam et al., 2002). Differential expression of the NHEJ core factors also influences the therapeutic responsiveness. While the reduced levels of expression increase the sensitivity to therapy (Hu et al., 2013) (Tarish et al., 2015) (Jin et al., 2016), increased levels promote resistance (Jin et al., 2016) (C.-J. Shao, Fu, Shi, Mu, & Chen, 2008) (Shintani et al., 2003). Though traditionally NHEJ is error-prone in the repair of non-compatible DSBs, it is likely to be much more precise than previously believed due to the flexibility of the NHEJ factors. Nonetheless, cells that are deficient in HR and FA pathways direct the one-ended DSBs towards NHEJ resulting in chromosomal aberrations, promoting carcinogenesis. This is because the cell would rather tolerate a chromosomal

aberration than having an unrepaired DSB which can result in the cell demise (Douglas, Moorhead, Ye, & Lees-Miller, 2001). Therefore, FA and HR-deficient cells, as a compensation often overexpress NHEJ factors and become addicted to NHEJ to deal with a large number of DSBs generated during rapid cell proliferation. Considering the above scenarios, one can conclude that normal cells use NHEJ to stabilize the genome, but precancerous and cancer cells utilize NHEJ to drive genomic instability and carcinogenesis.

All the above observations have led to manipulating, either genetically or pharmacologically the NHEJ factors to sensitize and improve the responsiveness of individual cancers to therapy (Jun et al., 2016) (Riabinska et al., 2013) (Winkler, Hofmann, & Chen, 2014). However, only pharmacological intervention is clinically applicable currently. Molecular compounds that inhibit either protein-protein, protein-DNA interactions (Douglas et al., 2001), or activity of the factors with a kinase and/or phosphatase activity are being explored (Leahy et al., 2004) (Douglas et al., 2001). One potential problem to translate the in-vitro inhibitor studies to in-vivo is the reduced drug uptake. Strategically, these inhibitors can be utilized for inducing synthetic lethality. This approach is recently applied by using DNA-PKcs inhibitors in the treatment of various cancers including ATM-defective tumors, HR-deficient tumors, and MSH3 deficient tumors (Lan et al., 2016) (Yanai et al., 2017) (Douglas et al., 2001). DNA-PKcs inhibitor, CC-115 (Tsuji et al., 2017) is undergoing Phase I clinical trial to be used as an adjunct to radiation therapy or chemo-radiation therapy.

1.10 Base Excision Repair

DNA base damage frequently occurs in the cells, at least 10,000 times every day, spontaneously or by oxidative stress induced by ROS generated by endogenous and exogenous sources. Oxidation, alkylation, or deamination are the common ways modifying these bases. Some examples of the modified bases are 7,8-dihydro-8-oxoguanine (8-oxoG), 5-methylcytosine (5-meC), (6-meG), N7-methylguanine (7-meG), or N3-methyladenine (3-meA). While some of these lesions are premutagenic, some of them are cytotoxic due to their propensity to block replicative polymerases (Lindahl & Wood, 1999). Various repair pathways take care of these lesions depending on the nature and complexity of the lesions. One such highly evolved pathway is the Base Excision repair (BER) pathway mends single oxidized base lesions. There are three functional processes involved in the repair, 1. Lesion Recognition/Strand Scission, 2. Gap Tailoring, and 3. DNA Synthesis/Ligation. Each step involves specific protein(s) in a coordinated fashion such as DNA glycosylases (mono or bi-functional), AP-endonuclease, DNA polymerases, and ligases. There is about 11 DNA glycosylase discovered and classified into four structurally distinct superfamilies, the uracil DNA glycosylases (UDGs), the helix-hairpin-helix (HhH) glycosylases, the 3-methyl-purine glycosylase (MPG), and the endonuclease VIII-like (NEIL) glycosylases. These DNA glycosylases scan the DNA via 4Fe4S, employing a damage pre-selection strategy to minimize the effort (Banerjee, Yang, Karplus, & Verdine, 2005). Mono-functional glycosylates such as UDG, excise the N-glycosidic bond by hydrolysis (Mol et al., 1995) releasing damaged base creating an apurinic/apyrimidinic sites (AP-site). AP endonuclease (APE1), cleaves the AP-sites on the 5′ side of the lesion leaving a 3′-hydroxyl and 5′ deoxyribose phosphate termini (5′-

Rp). The 5′-dRp termini are taken care of Pol β in case of short patch BER. Bi-functional glycosylases, on the other hand, have an AP-lyase activity which cleaves the AP-lesion on the 3′side producing a 3′- unsaturated aldehydic end (β-elimination) with a 5′phosphate end (NTH1) or a 3′-phosphate and a 5′phosphate end (β and δ elimination) (NEIL). The 3′- the unsaturated aldehydic end is further cleaved by APE1, and the polynucleotide kinase phosphatase (PNKP) converts the 3′-phosphate end to 3′-hydroxyl end. After processing the removal of the damaged base, the glycosylases are tightly bound at the AP-site and requisite APE1 for their release and turnover (Almeida & Sobol, 2007). The nick and the gap in the DNA strand are further recognized by the XRCC1, which along with Ligase III and Pol β fills in the gap and ligates the strand as a part of short patch BER. Under the conditions when a 5′ lesion is refractory to pol β lyase activity, long patch base excision pathway kicks in (Gary, Kim, Cornelius, Park, & Matsumoto, 1999). During long patch repair the polymerases δ, ε or β function in concert with other proteins such as proliferating cell nuclear antigen (PCNA), structure-specific flap endonuclease (Fen1), poly(ADP-ribose)polymerase 1 (PARP1) and LigI, to synthesize DNA to fill in the gap up to a length of 13 bases. This newly synthesized DNA displaces the 5′ end blocking strand creating a flap which will be cleaved by FEN1.

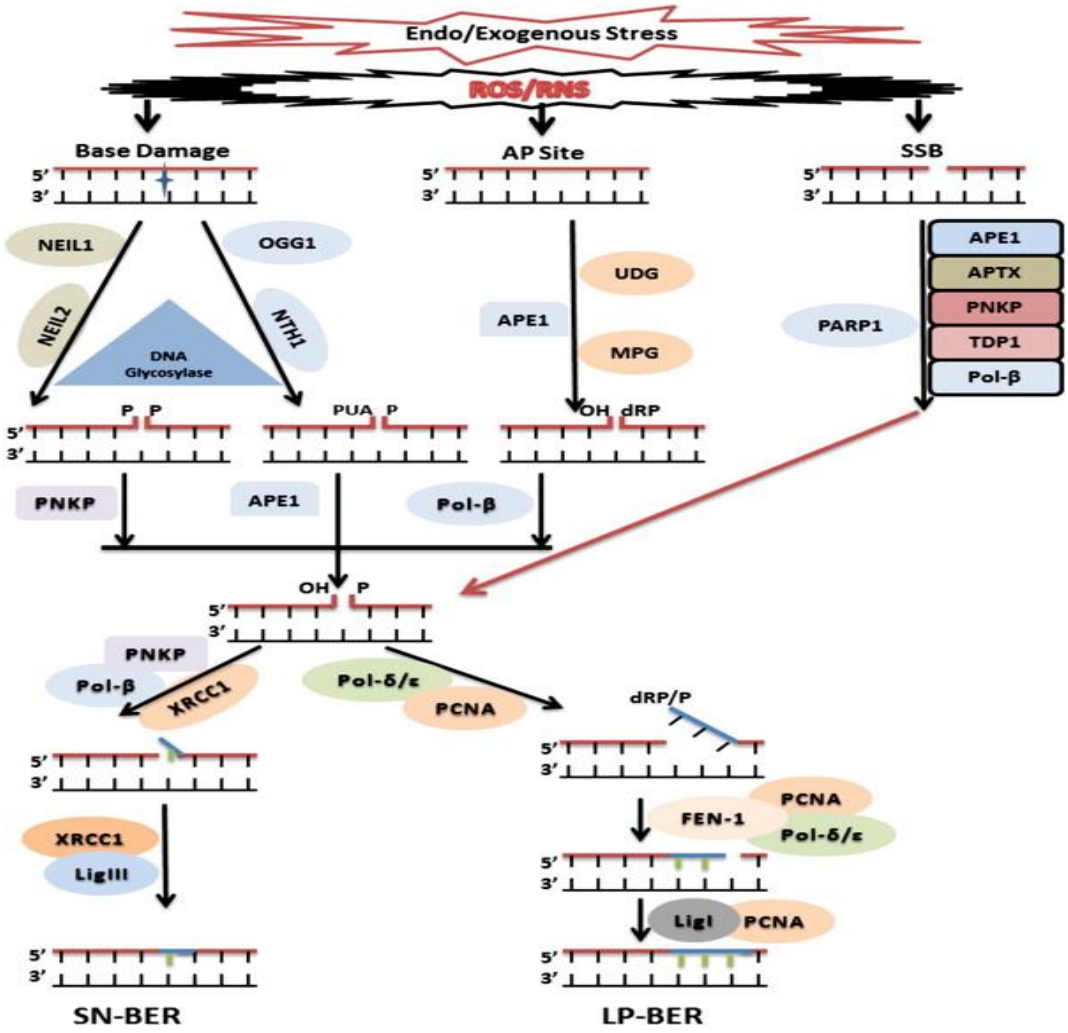

Fig. 1.4: Oxidative DNA base damage repair through BER-pathway: Initiation of BER is by removal of the modified base by either a monofunctional (M) or bifunctional (B) DNA glycosylase (DG), which leaves an AP site. If monofunctional enzyme cleaves the glycosidic bond APE1 incises the DNA backbone 5′ to the AP site. The single strand breaks (SSBs) left by the both DG and MG contain either a 3′ or 5′ obstructive termini. These end breaks are recognized by PARP1and processed by pol-β, APE1 or PNKP depending on the specific nature of the terminus. When 3′-OH and 5′-P termini result from end processing, the BER and SSBR diverge into two sub-pathways, short-patch (SN) and long-patch (LP) BER/SSBR. In SN-BER/SSBR, the single nucleotide gap is filled in by pol β aided by the XRCC1 scaffold in the presence of PNKP and ligated by Ligase III. In LP-BER/SSBR, Pol δ/ε with the aid of PCNA, 2 to 13 nucleotide gap is filled in, and the resulting 5′ flap is removed by FEN-1. As with the SN-BER final ligation step is accomplished by Ligase I. Figure adapted with permission from A.K. Mantha et al. 2014.

Chapter1

RESOLUTION OF PROXIMAL THYMINE GLYCOL AT DSB TERMINI BY BASE EXCISION REPAIR AND ITS INTERFERENCE IN NONHOMOLOGOUS END JOINING OF FREE RADICAL-MEDIATED DNA DOUBLE-STRAND BREAKS

II. Introduction

2.1 Thymine glycol lesions:

As discussed before, the formation of oxidative lesions is not uncommon even under normal physiological conditions. During irradiation, the energy deposition is proportional to mass, and hence the purines (adenine and guanine) and pyrimidines (cytosine and thymine) are about equally likely to sustain damage through the direct mechanism (JF, 1988). Thymine glycol is the most easily damaged base formed due to oxidation of thymine or deamination and oxidation 5-methylcytosine by ionizing radiation or cancer therapy (Adelman, Saul, & Ames, 1988). Radiation generates oxidants that can react with thymine leading to the formation of thymine glycol, thymine peroxide, thymine hydro peroxide, and other oxidized forms of the base. Further reaction to these products yields urea. Approximately 10%-20% of the radiation or radiotherapy-induced damage results in thymine base oxidation and DNA fragmentation(Kung & Bolton, 1997). Thymine glycol has four diastereomers of, i.e. (5R, 6S), (5R, 6R), (5S, 6R) and (5S, 6S), but in solution

exists as either the 5R cis-trans pair [(5R, 6S) and (5R, 6R)] or the 5S cis-trans pair [(5S, 6R) and (5S, 6S)], due to epimerization at the C6 position (Lustig, Cadet, Boorstein, & Teebor, 1992). Oxidation of free thymidine or thymidine in the oligonucleotides preferentially yields (5R, 6S)-thymine glycol (Kao, Goljer, Phan, & Bolton, 1993a) (Vaishnav, Holwitt, Swenberg, Lee, & Kan, 1991). According to calculations, cis-(5R,6S) diastereomer is the most stable one amongst all the isomers of thymine glycol. Depending on the original base that is oxidized, Tg is found to pair with either A (Thymine) or G 9methyl-cytosine). Thymine glycol has the propensity to cause both structural and functional perturbations of the DNA. The free radical addition to the C (5)C (6) double bond of thymine produces a nonplanar ring-saturated lesion making it extra helical as shown by NMR studies and by its accessibility in the solution (Kao, Goljer, Phan, & Bolton, 1993b) (Kao et al., 1993b). Two possible consequences of Tg lesions are either it blocks the DNA polymerases or gets bypassed by translesional synthesis and become mutagenic.

Unlike 8 oxo-guanine, Tg is a weak mutagen (Ashis K Basu et al.,1989), but a potent blocker of both DNA repair and replicative polymerases, proving lethal to the cells in the absence of translesional synthesis or recombination (Wallace, 2002). Studies using a template containing thymine glycol for primer extension with several DNA polymerases have shown that the extension occurs up to the site of Tg with adenine insertion and not beyond, especially if the 5′-neighbor is a purine as the protruding C5 methyl group of Tg pushes the purine extra-helical. This displaced base will be stabilized by the hydrogen bonds between NH2 and N3 of G on the minor groove's side and C4 and C5 hydroxyls of Tg on the major groove's side. This limits the next incoming dNTP incorporation into the

primer strand, providing a rationale for the strong bock to replication (Ide, Kow, & Wallace, 1985) (R C Hayes & LeClerc, 1986). This effect is less evident if the 5′-neighbor is a pyrimidine. Meanwhile, there are several contexts in which thymine glycol is bypassed by certain DNA polymerases in vitro (R C Hayes & LeClerc, 1986) and in vivo (A K Basu, Loechler, Leadon, & Essigmann, 1989).

Repair of a simple thymine glycol lesion is major via single nucleotide patch base excision repair pathway (A K Basu et al., 1989) and in part by Nucleotide excision pathway (NER) and by recombination. Enzymes Endonucleases III and VIII in E.coli and their human homologs Nth1 and NEIL (1,2,3) respectively, stereoselectively repair thymine glycol lesions (Katafuchi et al., 2004). 5R Tg is preferentially removed from chromosomal DNA in irradiated human cells, whereas 5S Tg is preferentially excised in irradiated E. coli cells (Shibata, 2017). The repair is sequence and counter-base dependent, Tg.G being repaired more efficiently than Tg.A by NEIL 1 (Marenstein et al., 2003). The counter base and the accompanying sequences have the propensity to either block the replication or promote misinsertion during translesional synthesis (Dolinnaya, Kubareva, Romanova, Trikin, & Oretskaya, 2013a).

In tandem lesions of 5′- abasic site and Tg, there is a severe replicative block and if at all bypassed the lesion becomes highly mutagenic, especially if accompanied by 3′-G due to a misalignment-realignment mechanism (Huang, Imoto, & Greenberg, 2009). If the tandem lesions have 5′-(8-oxoG)Tg and 5′-Tg (8-oxoG), there is enhanced mutagenicity of these lesions compared to 8-oxoG alone. In contrast, there is enhanced repair of 8-oxo G by hOGG1 in case of 3′-Tg but unaffected by 5′-Tg. In case of bistranded lesions, if Tg is opposite the abasic site, BER or replication induce a double strand break, while the 8-

oxo G protects at the expense of increasing mutations. At the double strand break, if present in an overhang, 8-oxoG is more tolerant than thymine glycol (R.-Z. Zhou et al., 2008a). In the current study, we are evaluating the role of Tg in end-joining when present at a blunt double-strand break.

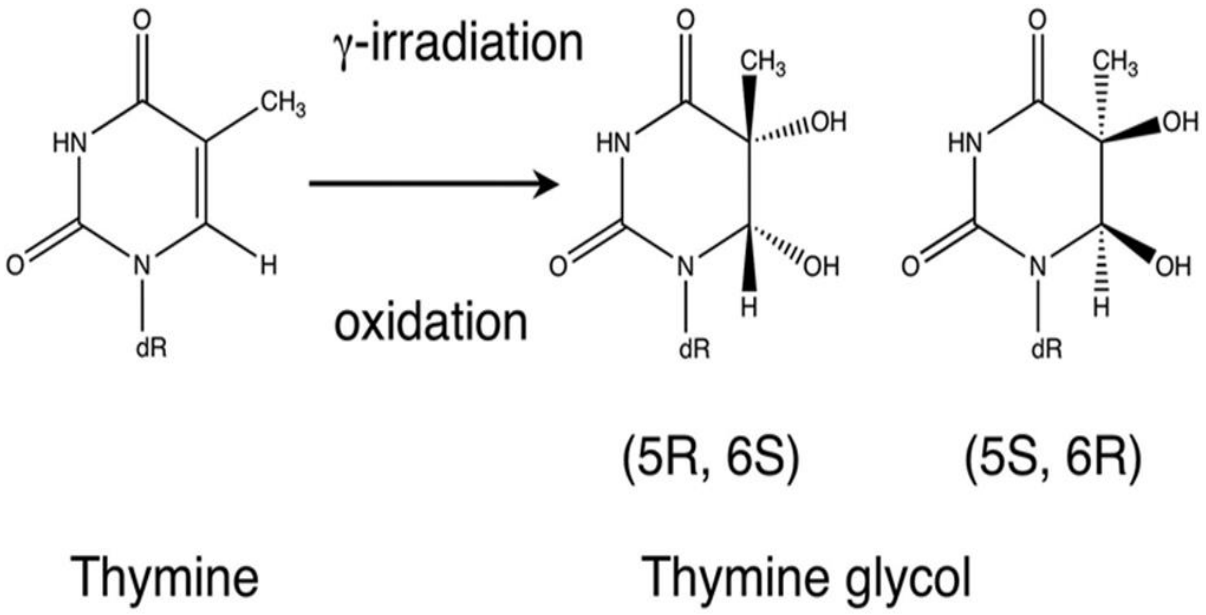

Fig. 2.1: Formation of thymine glycol: Reactive oxygen species (ROS), such as peroxide and hydroxyl radicals, are generated as byproducts during normal oxidative metabolism, and ionizing radiation modifies DNA bases. A typical product of thymine oxidation is thymine glycol. Figure adapted from Aller et al. 2007.

2.2 Human EndoIII like protein (hNTH1):

hNTH1 enzyme is a bifunctional DNA N-glycosylase/apurinic/apyrimidinic (AP) lyase and a human homolog of E. coli endonuclease III. hNTH1 removes ring-saturated pyrimidines, be they hydrated, reduced, or oxidized, from the DNA backbone as the initial step of base excision repair (BER). It is a product of the OCTS3 gene, 312 amino acids in length with a calculated molecular mass of 34,300 Da. Like its other homologs, the hNTH1 sequence has highly conserved four cysteine residues donning a binding motif for the [4Fe-4S] cluster, and a helix–hairpin–helix motif that has been shown in the case of E. coli endonuclease III to contribute to DNA binding of the enzyme (Thayer, Ahern, Xing, Cunningham, & Tainer, 1995). The Lys-220 in the helix–hairpin–helix motif interacts with the flipped out damaged base, thymine glycol in the current scenario but is not a specific substrate. The ε-amino group of this lysine catalyzes the formation of N-acylimine (Schiff's base) enzyme-substrate intermediate, which is essential for the enzymatic catalysis of the β-elimination, a characteristic of an APlyase. The hydrolysis of the Schiff base intermediate by acid-base catalysis at the active site produces an AP site with the release the damaged base and abstraction of the deoxyribose pro-S-2′-hydrogendeoxyribose sugar at the site results in a strand break with 3′ α,β unsaturated aldehyde and a 5′phosphate (Marenstein et al., 2003). It was noted that AP-lyase function is 7 times slower than the DNA glycosylase activity (Ikeda et al., 1998). The 3′-dRp generated at the AP-site is later cleaved by APE1 to produce a 3′-hydroxyl end which can further be filled in by Polβ, and ligated by Ligase IIIα.

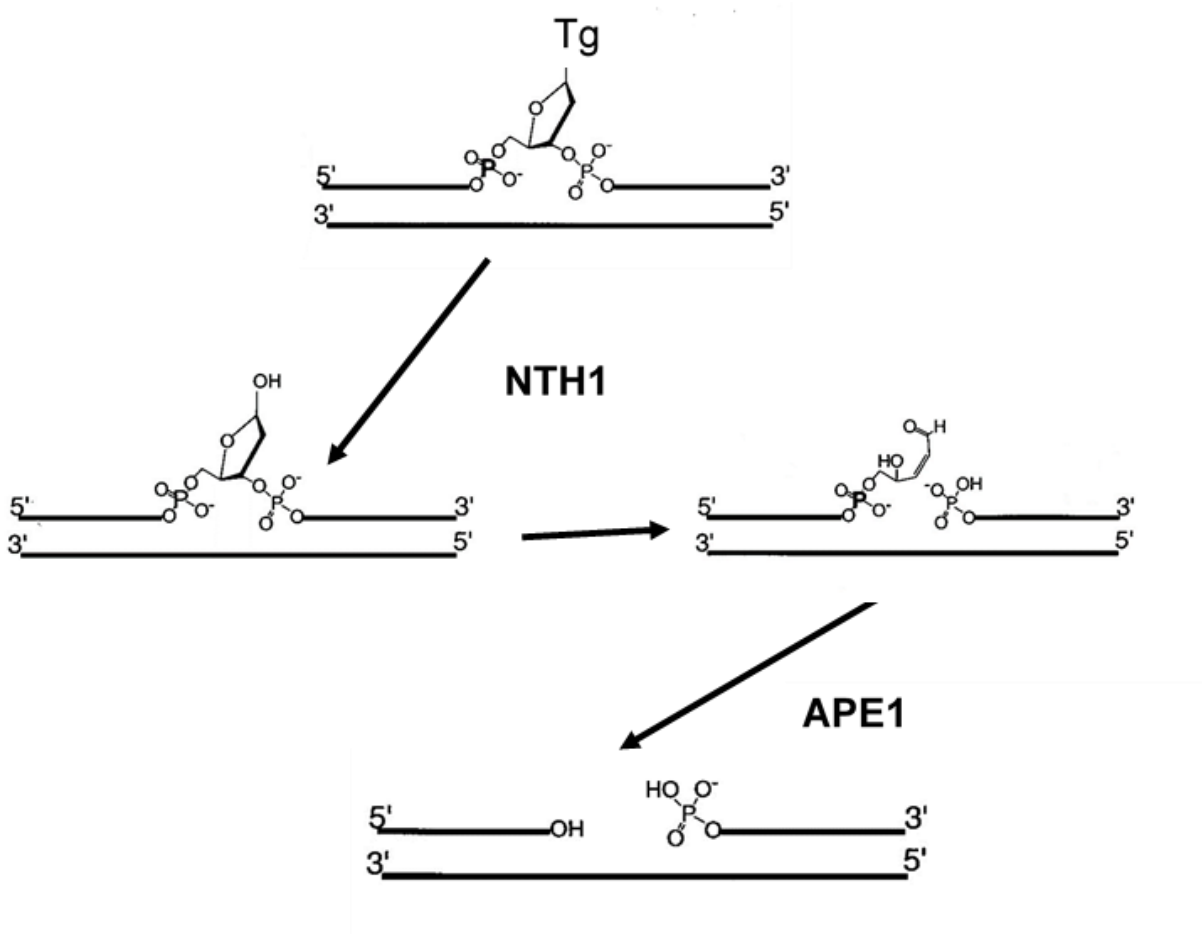

Fig. 2.2: Schematic representation of removal of Thymine glycol by NTH1 protein: The flipped out Tg lesion on the DNA strand is recognized and removed by NTH1, followed by β-elimination of the AP-site producing a 3′-deoxyribose phosphate (3′-dRp) as a unsaturated aldehyde. 3′dRp is further cleaved either by APE1 to leave a 3′ hydroxyl end. The resulting gap is filled in by Polβ and LigaseIIIα ligates the strand.

Hypothesis

Thymine glycol (Tg) is better removed from the substrate when placed away from the double strand DNA break by Base Excision Repair with possible interference with Nonhomologous end joining.

Background:

Previous experiments done with Tg positioned at various positions, first (Tg1), second (Tg2), third (Tg3) and fifth position (Tg5) at the blunt DSB have shown the end joining in the order of Tg3>Tg5>Tg2>Tg1, in Bus whole cell extracts. This observation was in contrast to our expectation that Tg5 will be joined efficiently due to Tg placement away from the break. Also, we saw an extra product, 3 or 5 bases lesser, being formed during repair of Tg3 and Tg5, respectively, corresponding to a product that would result from the removal of Tg from the third or fifth position of the corresponding substrate. This product was more prominent for Tg5 than for Tg3. Since Tg is a substrate for hNTH1 of BER, we wanted to verify if Tg5 is a better substrate for hNTH1, which might have resulted in the reduction of the end a joining due to the interference of BER with NHEJ. Similarly, we wanted to test the preference of hNTH1/BER for 5′-Tg's.

2.3: Specific aims

1. To compare the processing of the substrates with Tg placed at third position from the 3′-end of the DSB (Tg3) to that of Tg placed at fifth position (Tg5) by the recombinant hNTH1 protein

2. To compare the processing of Tg placed at second position from the 5′-end (5′-Tg 2) o that of Tg at third position at the 5′-end (5′-Tg 3) in Bus cell extracts with XLF and by the recombinant hNTH1

3. To verify the processing of 3′ and 5′-Tg substrates in HCT116 cell extracts

III. Materials And Methods

3.1 Substrate

The oligonucleotides, 5′-ATGCGGATCGCGTTGTCTg-3′ (Tg1), 5′-ATGCGGATCGCGTTGCTgC-3′ (Tg2), 5′-ATGCGGATCGCGTTG-Tg-CT-3′ (Tg3) and 5′-ATGCGGATCGCGT-Tg-GT CT-3′ (Tg5) were ordered from Midland Certified Reagents (Midland, TX). They were re-suspended in TE (10 mM Tris–HCl, pH 8, and 0.1 mM EDTA). 1mCi of [γ-^{32}P] ATP was used to label 50 pmoles of the oligonucleotide, using Polynucleotide kinase (PNK) and incubated for 1 hr at 37 °C. Each oligomer was then annealed to an equal quantity of a complementary 5′- phosphate containing, 3′-GTATACGCCTAGCGCAACGAGp-5′ or 3′-GTATACGCCTAGCGCAACAGAp-5′, via heating to 80 °C followed by slow cooling to 10 °C. The duplexes generated by this annealing process included, on one end a 3-base 3′overhang that was complementary to the 3′ overhang created by BstAPI digestion of pUC19.

3.2 Ligation of oligomeric duplexes to the KasI/BstAPI cleaved pUC19:

17 µg of the plasmid pUC19 DNA is digested with 50 units of KasI (NEB) in 0.3 ml of NEB CutSmart buffer for 3 hr at 37 °C and then digested with 50 units of BstAPI in the same buffer for 3 hr at 60 °C. The 2.6-kb KasI-BstAPI fragment was purified on a 0.8% agarose gel, electro eluted and concentrated with an ultracel 100k centrifugal filter.

10 pmole of the annealed oligomers were combined with (~1.7 pmole) of KasI/BstAPI fragment and treated with 12,000 units (4 µl) T7 DNA ligase in to ligate them at the BstAPI end in 130 µl of ligation buffer for 2 hr at 25 °C. Proteolysis and ethanol precipitated extraction of the ligation products is done. These products are then digested with SmaI (500 units) for 2 hours at 25 °C in 50 µl CutSmart Buffer. This removes 177 bp from the KasI-end and leaves a blunt end. The resulting 2.6-kb substrate has one Tg-modified end. This substrate is electro eluted and concentrated as above. T7 ligase was used for ligase instead of T4 ligase due to its preferential ligation of only cohesive and not the blunt ends (Doherty at al. 1996; Subramanya et al.1996). Some self-ligation was detected in case of the unmodified control oligomers, and therefore for these oligomers, the T7 Ligase was reduced to only 2400 units. In the case of Tg5 plasmid there some ligation seen between head-head blunt ends, and cutting the plasmid with Sma I enzyme would have eliminated any head-tail ligation. The ligation products were purified by agarose gel electrophoresis and electroelution (Bennett et al. 1996).

3.3 Electroelution of the modified substrate:

The nucleotide is electroeluted using an 11-inch segment of pretreated dialysis tubing (6,000-8,000 molecular weight) filled with the buffer composed of 20 mM Tris, pH8 and 1 mM EDTA (the elution buffer). The gel slice containing the desired DNA band was placed in the dialysis tubing, and the other end of it was knotted after removal of air bubbles. The dialysis tube was placed in a gel box filled with the same buffer, and the DNA was eluted overnight at 50 V. Then the dialysis bag was cut, and the buffer containing DNA substrate was collected into 15 ml centrifuge tubes. 0.45 µm filters were used to remove any debris, and the DNA was concentrated by micro- concentration to about 500 µl using centricon-

100 (Amicon). The concentrate was collected into 1.5 ml Eppendorf tubes and precipitated with 1/9 volumes of NaOAc and 2.5 volumes of 100% EtOH, washed with 70% EtOH and dissolved in 50 µl TE.

3.4 Bus cell and HCT116 cell extract preparation:

Bus cells were grown into confluence on thirty 15 cm dishes each with 20 ml alpha-MEM medium with 10% FBS. HCT116 cells were grown to a confluency of 70% - 90% and then serum starved with 0.5% FBS for 4 days. On the day of the experiment, the dishes were washed with 20 ml PBS at room temperature. 3 ml of 0.25% trypsin-EDTA was added to each dish, making sure it covers all the cells. They were incubated for 5 min until the cells are detached and then 3 ml medium and serum was added. These samples were collected and pelleted in 50 ml tubes at 1500 rpm for 5 min in ultracentrifuge using SW55 rotor at room temperature. The cells were resuspended in 50 ml medium and serum and pelleted again. The pellet was again resuspended in 25 ml medium and serum and pelleted again. The pellet was resuspended in 30 ml ice-cold PBS and pelleted at 4 °C and packed cell volume (PCV) is recorded. The last process was repeated. The pelleted cells were resuspended in 5 X PCV cold hypotonic buffer containing 10 mM Tris-HCl pH 8, 1 mM EDTA, 5 mM DTT and proteinase inhibitors pepstatin 1 µg/ml, chymostatin 1 µg/ml, aprotinin 2 µg/ml, leupeptin 1 µg/ml, PMSF 1 mM. The cells were quickly pelleted. This pellet was again resuspended in 2 X PCV hypotonic buffer and inhibitors and let set on ice 20 min. 1.5 ml of this solution was put in a small dounce homogenizer each time and stroked 20 times. After it was let set for 20 min, it was transferred to cold 5 ml centrifuge and ¼ volume of the hypertonic solution (83.5 mM Tris Ph 7.5, 1.65 M KCl, 3.3 mM EDTA, 1 mM DTT) and inverted several times to mix well.

This was centrifuged at 43K for 3 hr in SW55 at 2 °C. From the top the middle layer which has cytosol was collected using a 22G needle, avoiding cloudy layer on the top. The cytoplasm thus collected was dialyzed for 3 hr in storage buffer (20 mM Tris pH 8, 0.1 M KOAC, 1 mM DTT, 0.5 mM EDTA, 20% glycerol) with inhibitors at 4 °C. The resulting solution was freezed in small aliquots (10 µl - 80 µl) at -80 °C.

3.5 End joining assays using cell extracts:

Bustel whole cell extracts which are deficient in XLF or HCT116 whole cell extracts were used for the reactions in a buffer containing 50 mM triethanolammonium acetate (pH 8), 1 mM ATP, 1 mM DTT, 50 µg/ml BSA, 1.3 mM $Mg(OAc)_2$ and dNTPs at 100 µM each.

The total reaction volume was 16 µl, with 10 µl of extract, resulting in a final protein concentration of 8 mg/ml. 200 nM of human recombinant protein XLF was substituted for some reactions. 100 ng of the substrate was added and the reaction mixed by pipetting and incubated at 37 °C for 6 hr. Samples were deproteinized by adding an End Joining Lysis buffer containing 1 mg/ml of Proteinase K for 3 hr at 56 °C. The DNA was then extracted after proteolysis and precipitation with glycoblue and ethanol after one hour. After the precipitation, all samples were dissolved in 43 µl of TE and digested with 20 units of NdeI and PstI and 5 µl of 10X CutSmart buffer (New England Biolabs) at 37 °C for 3 hr. Gel electrophoresis of the samples was done in 20% polyacrylamide sequencing gels. Then the gels were exposed to phosphor imaging screen for 1 to 2 days at -20 °C. Data were analyzed using a Typhoon 9100 imager (GE Healthcare Bio-Sciences, Pittsburgh) and Image Quant 3.1 or 5.1 software (GE Healthcare Bio-Sciences, Pittsburgh). The percentage of end joining was determined by measuring the percentage radioactivity of the joined fragments as a function of total radioactivity in the same lane.

3.6 Polyacrylamide gel electrophoresis:

For electrophoretic separation of the DNA strands, Polyacrylamide gels (20x30x0.08 cm) containing 40% acrylamide: bisacrylamide in a ratio of 20:1, 8 ml of 10XTBE and urea in a final concentration of 8.3 M were used in total volume of 80 ml. The mixture was cooled to room temperature, and 0.06 g ammonium persulfate and 45 µl of TEMED (N', N,' N', N'-tetramethylethylene diamine) were added. The gel was allowed to polymerize for 1 hour. 15 µl of samples are then loaded into the wells of the gel and electrophoresed at a constant power of 42 W until the marker reached the bottom of the gel.

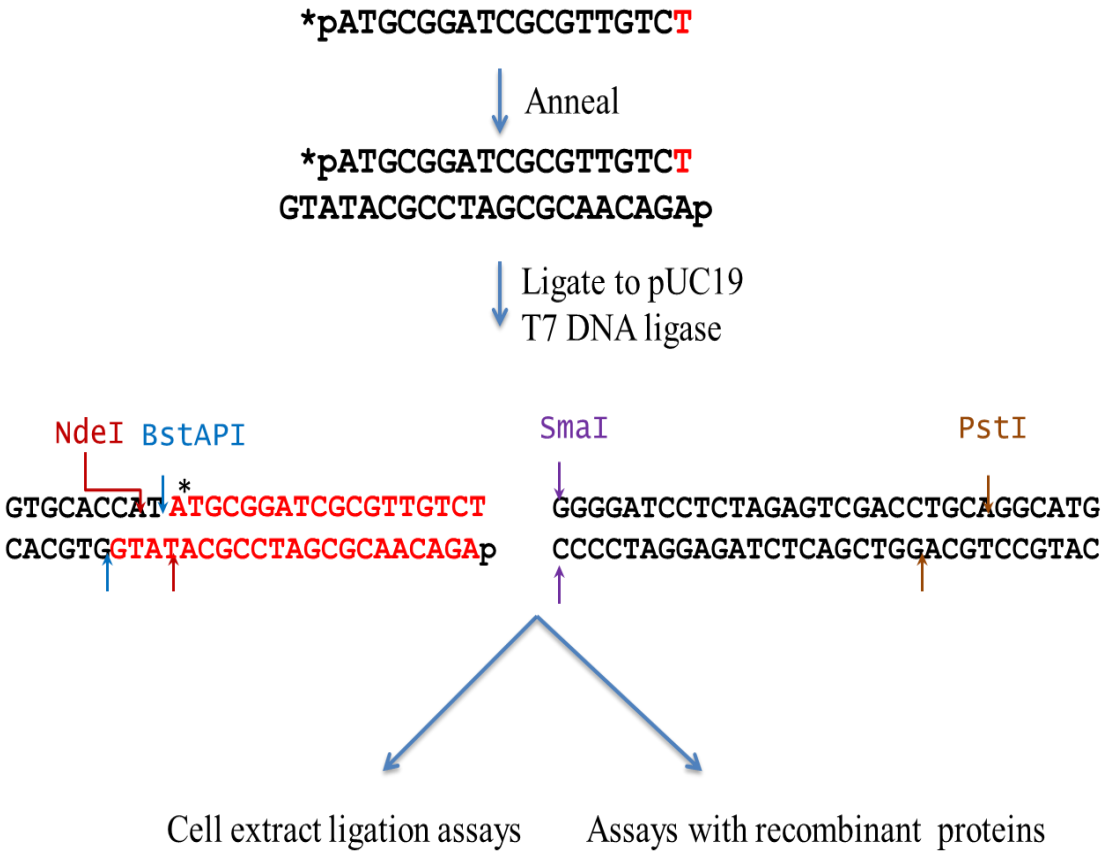

Fig. 3.1: Preparation of the substrate: The oligonucleotide with Tg was radiolabeled with P^{32} at 5′ end is annealed with a complementary strand. This was ligated to the BstAPI cut end of the pUC19 using T7 DNA Ligase. The substrate thus prepared had a head with BstAPI and NdeI restriction sites and a tail with SmaI and PstI restriction sites. This substrate was used in both cell extract ligation assay and assay with recombinant proteins.

Preliminary Data

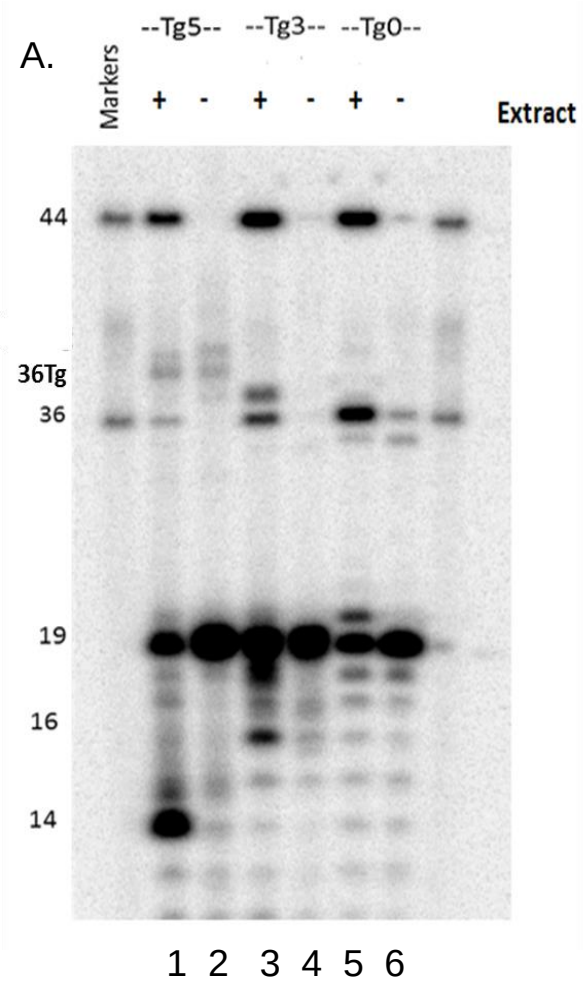

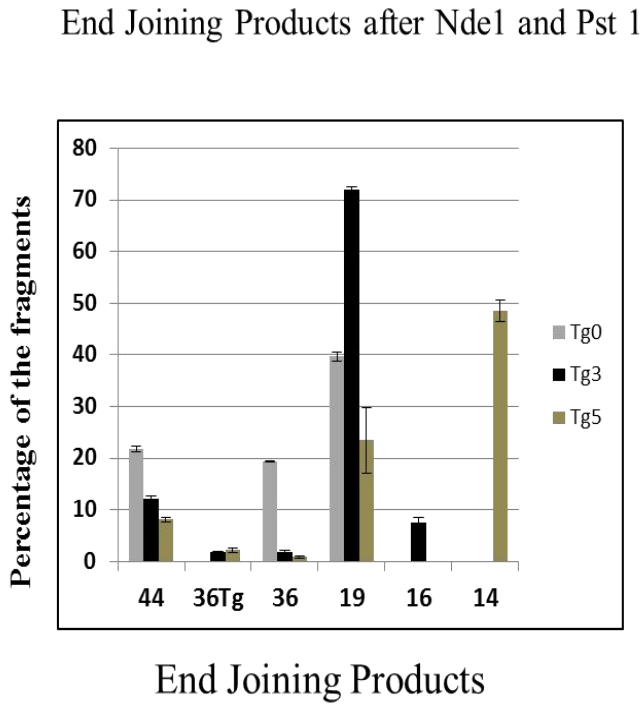

3.2 Comparison of the repair between Tg3 and Tg5: A) Autoradiograph showing the repair (joining and BER) fragments of Tg0, Tg3, and Tg5 in Bus cell extracts supplemented with XLF. B) The graph is representing the percentage of both joining and BER fragment for Tg3 (16-bp) and Tg5 (14-bp). (n = 3)

IV. Results

Double-strand breaks induced by DNA damaging agents have the propensity to turn lethal for cell survival if unrepaired or misrepaired. The complexity of composition at these breaks renders them more resistant to repair by NHEJ, which tends to ligate simple double-strand breaks spontaneously. One such structural hindrance is posed commonly by the presence of oxidized bases at or near the end of the DNA strands. Oxidized bases are a common result due to energy transfers and radiolysis during irradiation or internal metabolic processes. Since the production of these lesions in isolation is robust even during normal metabolism, there is a highly evolved Base Excision Repair (BER) pathway that executes the repair of oxidized bases, with a minor contribution from other repair pathways such as NER (David, O'Shea, & Kundu, 2007). Nonetheless, when oxidized lesions are complexed with DNA double-strand breaks, there will be an interplay between NHEJ and BER. To evaluate the interference of these lesions with NHEJ, DSB's substrate with partially complementary (–ATG and –ACA) 3′ overhangs with oxidized bases, either 8-oxo guanine (8-oxoG) as a terminal base or Thymine glycol (Tg) as a penultimate base were analyzed for end joining. These studies revealed Tg as a substantial hindrance to gap-filling and hence the end joining (R.-Z. Zhou et al., 2008b). Other studies have also shown Tg as a lethal modification in contrast to 8-oxoG which

was mutagenic (Bellon, Shikazono, Cunniffe, Lomax, & O'Neill, 2009) (Pearson, Shikazono, Thacker, & O'Neill, 2004).

To further evaluate the influence of Tg on NHEJ, blunt-ended DSB substrates were designed. These substrates were internally radiolabeled, and have Tg at different positions near one of the ends as shown in the Fig. 4.1. These blunt DSB's were tested in cell extracts and recombinant protein assays. An increase in the end-joining was observed with the increase Tg position from the double strand break (Tg3>Tg2>Tg1) (Mohammed Almohaini et al., 2016). Surprisingly, a reduced end-joining substrate with Tg placed at the fifth position was observed compared to Tg at the third position (10% vs. 14%) (Fig. 3.2 lane 1 vs. lane 3). Also, there was the appearance of an extra band corresponding to the length of either 3-nucleotides (16-bp, lane 3) for Tg3 or 5 nucleotides (14-bp, lane 1) for Tg5, lesser than the usual unjoined (19-bp) band, suggesting removal of the Tg from the substrates. Further, the intensity of this band differed vastly for these substrates, Tg3 - 7.6% vs. Tg5 - 48.5% (lane 3 vs. lane 1). Formation of this smaller fragment was almost instantaneous for Tg5 substrate.

This disparity in the end joining and the production of the smaller fragments can be explained by the attempted repair of the substrates by BER interfering with the end-joining process (Fig. 4.3). The recombinant protein assay with NHEJ core proteins confirmed this by showing an increased end joining in Tg5 substrates in comparison with Tg3 (7.2% vs. 3.3%). When the Klenow Exo- polymerase enzyme was used on the substrate incubated for either 5 min, before it was digested, there was the conversion of almost all the 14-bp fragment to 19-bp or 20-bp (due to the addition of one extra-base by the enzyme) at 5 min time point. However, substrate incubated for 6 hr showed the addition of bases

between 14-bp to 20-bp suggesting a nucleolytic degradation of the 5′ overhang of the complementary strand with time leading to the failure of the end joining of Tg5 substrate. To verify if the interference with NHEJ by BER is dependant on the position of Tg in the substrate, one of the major DNA glycosylases, hNTH1, which targets oxidized pyrimidine lesions, was tested on the Tg DSB substrates.

4.1 Recombinant protein hNTH1 activity on 3′ Tg substrates:

There are various enzymes in place to remove and repair the damaged base in base excision repair. DNA glycosylases, monofunctional and bifunctional excise the damaged base in a lesion and function specific manner. Oxidized pyrimidines are resolved by two specific enzymes: endonuclease III (EcNth) and endonuclease VIII (EcNei) in E.coli, and by their human orthologs hNTH1 and hNEIL1 (Bandaru, Sunkara, Wallace, & Bond, 2002). In the previous experiments using 3′-Tg substrates, EndonucleaseIII was successfully used to remove thymine glycol (M. Almohaini et al., 2016). Therefore, in the current experiments, we used recombinant hNTH1 protein (provided by David Pederson, University of Vermont) to assay the removal of Tg from the substrates in extract-free reactions (Fig. 4.1). Initially, hNTH1, at a concentration of 840 nM was added to the reactions containing the different Tg substrates separately to evaluate the substrate specificity. Only Tg3 and Tg5 substrates were susceptible to the removal of Tg and not Tg1 or Tg 2 substrates. In correlation with the extract assays, Tg5 was processed robustly (79.6%) releasing a product corresponding to 3′-deoxyribose phosphate (dRp)-terminated 14-bp. As expected, the Tg3 was minimally processed with 20.5% of 3′- dRp terminated 16-bp. There were small amounts of 3′-phosphate termini for both the substrates (16P and 14P). On further treatment of the substrates with TDP1 enzyme, which is capable of

cleaving various 3′-blocks (Nilsen et al ., 2012), most of the 3′-dRp-terminated termini were converted to 3′-phosphate termini.

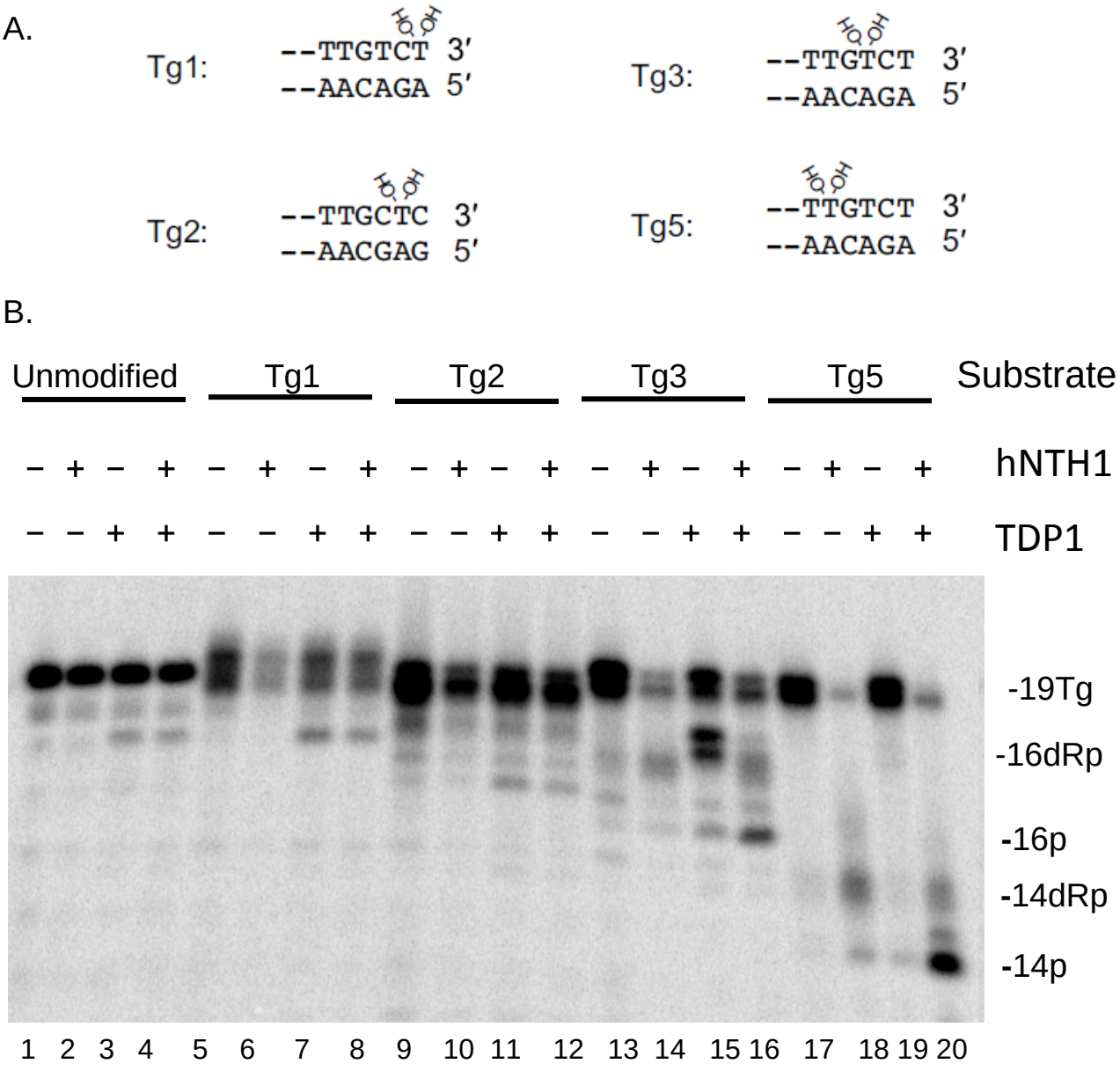

Fig. 4.1: Recombinant hNTH1-mediated processing of 3′-proximal Tg substrates: A. Illustration of the ends of different Tg substrates. B. Individual substrates were treated with 840 nM hNTH1 for 1 hr and then with 10 µM TDP1 for 1 hr before NdeI cleavage and gel electrophoresis. As observed in the above gel picture Tg5 was more susceptible to cleavage by hNTH1 than Tg3 (lane 20 vs. lane 16). Figure adapted with permission from M. Almohaini et al., 2016.

4.2 Concentration-dependent kinetics of hNTH1:

hNTH1 enzyme was titrated at different concentrations to measure the kinetics of activity as a function of concentration. When Tg3 and Tg5 were incubated in reactions with the increasing amounts of hNTH1, there was a steady and rapid increase in processing of the Tg5 substrate. Even though an increase in Tg3 processing was also observed, it was less effeciiently processed than Tg5. Percentage of removal of Tg was plotted as a function of hNTH1 concentrations in Fig. 4.2B. While the total processing of Tg3 substrate was 78 ± 1.2%, Tg3 processing was 24 ± 0.42%. These observations suggest that Tg at the fifth position is a better substrate than at the third position for the BER. Further, when TDP1 was added to the reaction, there was a visible cleavage of 3′-dRp for Tg5 substrate as shown in the leftmost lane of the Fig. 4.2A. This extensive excision of Tg5 substrate by base excision pathway in the extracts might have compromised end-joining of the substrate.

A.

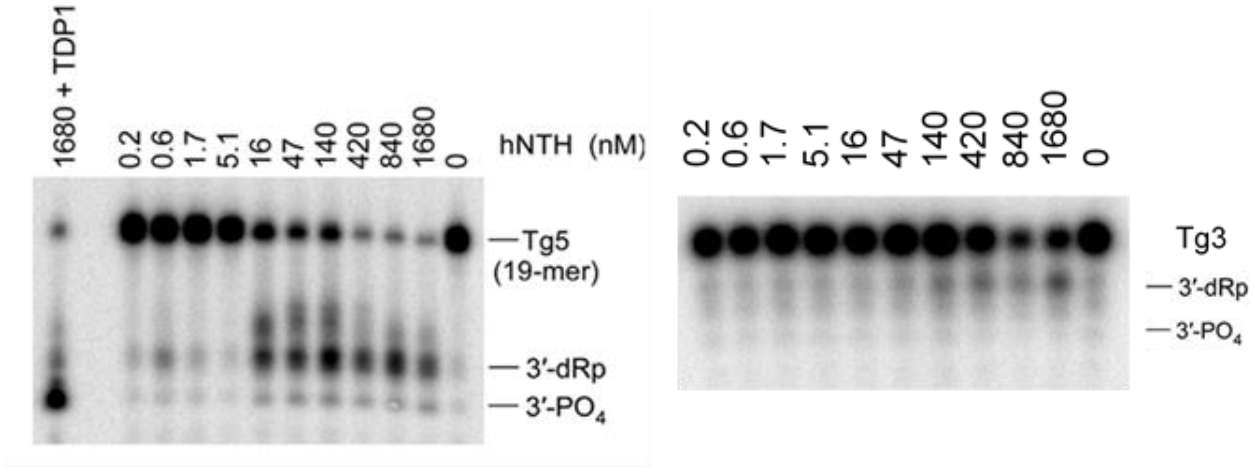

B.

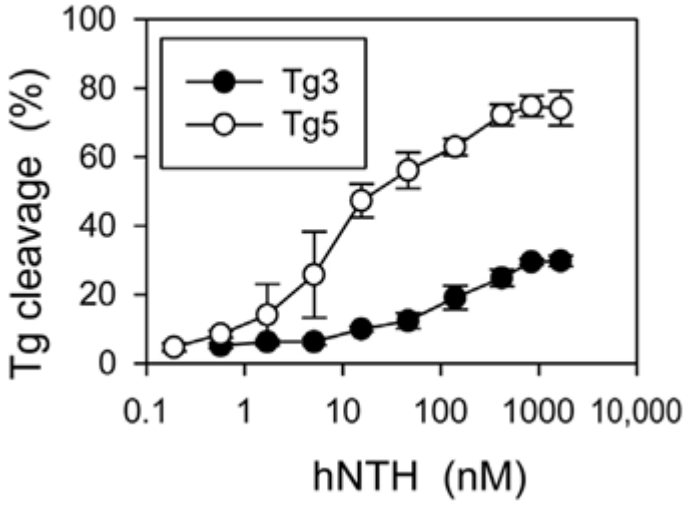

Fig. 4.2: Purified hNTH1 mediate Tg cleavage from 3′-Tg3 and 3′-Tg5 substrates: A. The Tg5 (left) and Tg3 (right) substrates were treated with the indicated concentrations of hNTH1 for 1 h, th cut with NdeI before denaturing gel electrophoresis. Additional treatment of the substrate with TDP1 removed the 3′-dRp as shown in the leftmost lane in Tg5 processing. B. Comparison of Tg cleavage for the Tg3 and Tg5 substrates as a function of hNTH1 concentrations. Figure adapted with permission from M. Almohaini et al., 2016. (n = 3)

4.3 Effect of 5′-end Tg in end-joining of blunt double-strand breaks (DSB):

Since the experiments with the substrates possessing Tg at various positions at the 3′ blunt end have given interesting results, we pursued the same experiments with substrates having Tg at the 5′ of the blunt end at either second (5′-Tg2) or a third position (5′-Tg3). Unlike the previous substrates which were labeled internally on 3′-strand, the 5′-substrates were radiolabeled at the 5′-terminal phosphate. Therefore loss of radioactivity as a result of processing in the cell extract experiments was a sign of Tg cleavage. These substrates were incubated in Bus cell extracts with (Fig. 4.3) and without XLF (Fig. 4.5) for 6 hours and processed similarly to that of 3′-Tg substrates.

Upon incubation, there was a discernable amount of end-joining for both of these substrates as evidenced by the radioactive Head-to-Tail end-joining (38-bp) fragment on the gel. This was in contrast to the absence of any end-joining for the 3′-Tg2 substrate, and was only two-fold different from the 5′-Tg3 end-joining, 7 ± 1.2% vs. 12 ± 2.7% (Fig. 4.3 B lane 5 vs. lane 7), considering its proximity to the ends. These results suggest compatibility of 5′-Tg, even when at the second position, for the Head-to-Tail end-joining as evidenced by the retained radioactivity. Further, there was no Head-to-Head end joing (36-bp) of these substrates, probably due to the strong hindrance of Tg presence at both the ends of DSB. However, there was a smaller amount of 22-25-bp end joining products (lane 5 and lane 7) for both the substrates probably due to a possible induction of resection at one of the ends owing to the presence of Tg at both the ends, with intact one end preserving the radioactive label. Nonetheless, there appears to be retention of most of the radioactivity for both the 5′-Tg substrates as seen by the similar intensity of bands collectively in both cells extract free (Fig. 4.3B lane 3, and 5) (Fig. 4.6A lanes 4 and 7)

and added samples (Fig. 4.3B lanes 4 and 6) (Fig. 4.6A lanes 5,6,7 and 9), suggesting a less removal of Tg relative to 3′-analogs.

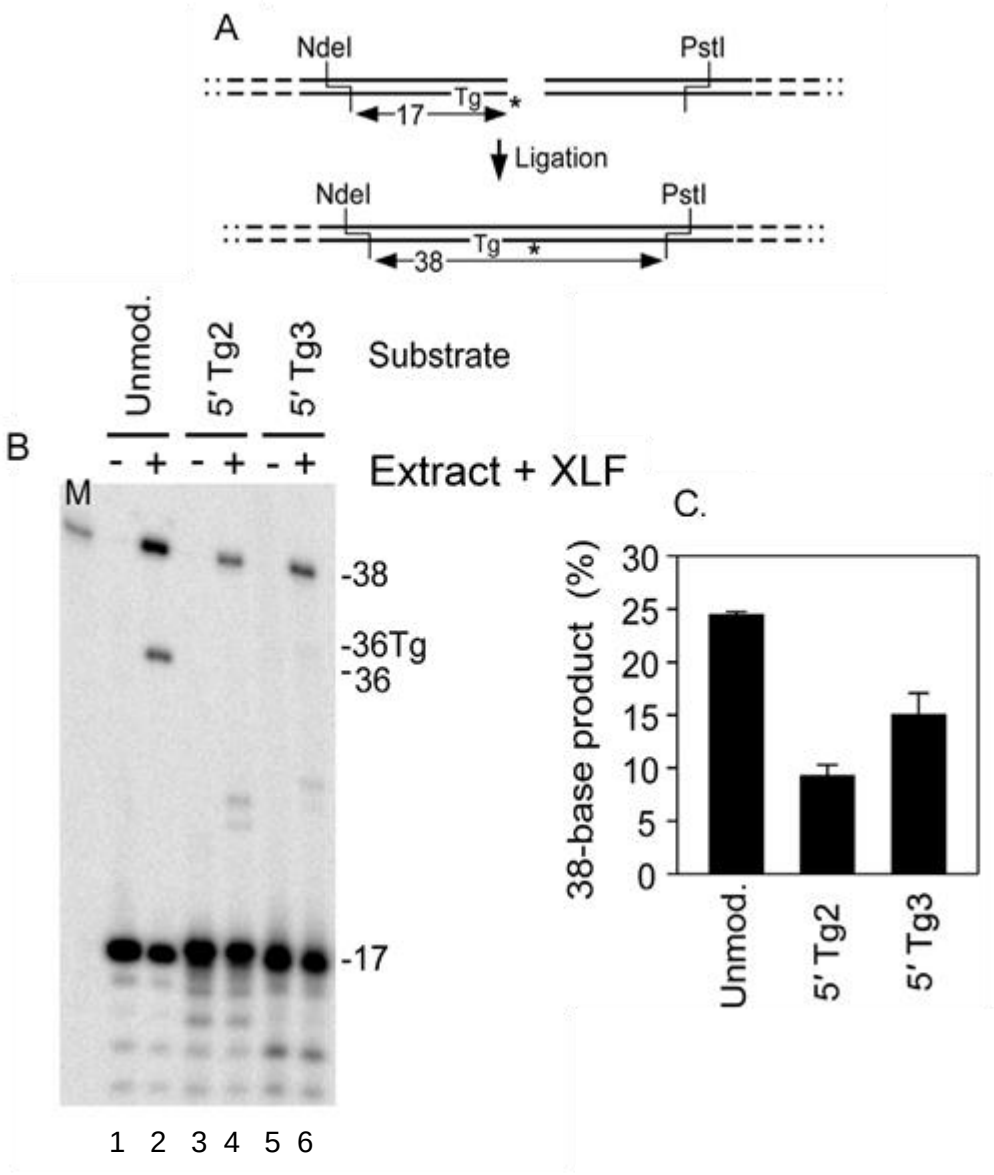

Fig. 4.3: Effect of 5′-proximal Tg on NHEJ in Bus cell extracts with XLF: Substrates with Tg as the second or third base from the 5′ terminus at the blunt labeled end were incubated for 6 h in XLF-complemented Bustel extracts. A) Illustration of the substrates and head-to-tail ligation products. B. Denaturing gel analysis of end joining products following cleavage with NdeI and PstI is expected to release 38-bp Head-to-Tail, and a 36-bp Head-to-Head end joining products. C. Plot of percentage of Head-to-Tail products observed for the substrates. Figure adapted with permission from M. Almohaini et al., 2016. (n = 3)

4.4 Susceptibility of 5′-Tg substrates to processing by recombinant hNTH1:

Similarly to the 3′-Tg substrates, the 5′-Tg substrates were treated with increasing concentrations of pure protein hNTH1. The release of radioactive fragments was monitored to measure the function of bifunctional DNA glycosylase. As observed in Fig. 4.4A, there was concentration-dependant release of radioactive fragments from both the substrates suggesting a Tg cleavage. Maximum release of radioactivity from both of these substrates by 840 nM hNTH1 was found to be similar (~60%). On comparison, excision of Tg from the 5′-Tg substrates was lesser than the 3′-Tg5 substrate but was higher than the 3′-Tg3 substrate (Tg3- ~30%, Tg5- ~80 %, and 5′-Tg2 and 5′-Tg3- ~60%). Total cleavage from both the 5′-Tg substrates is similar.

A.

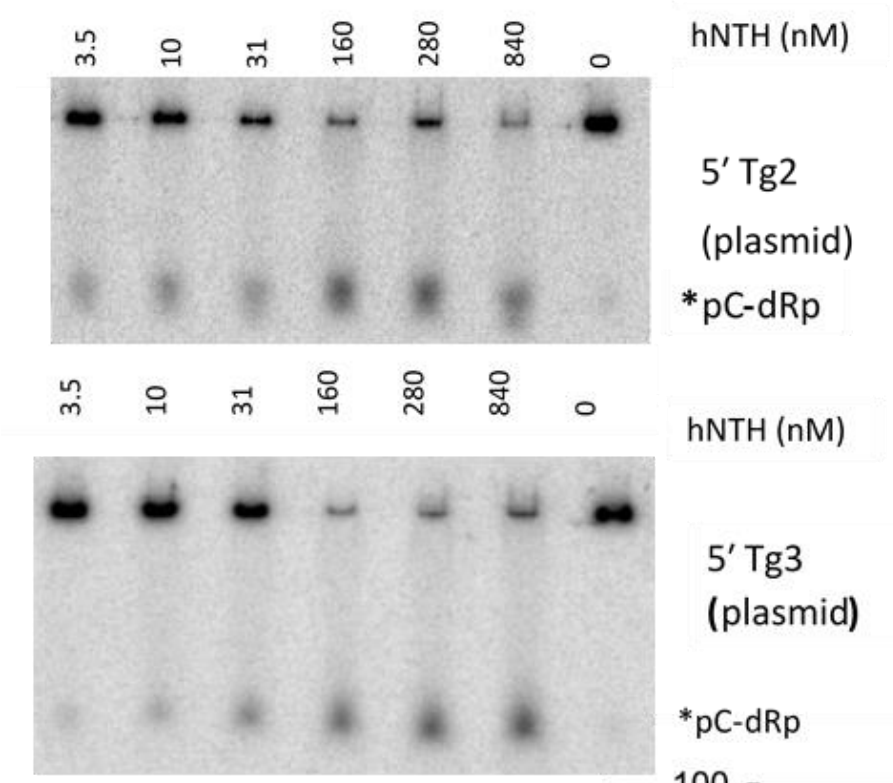

B.

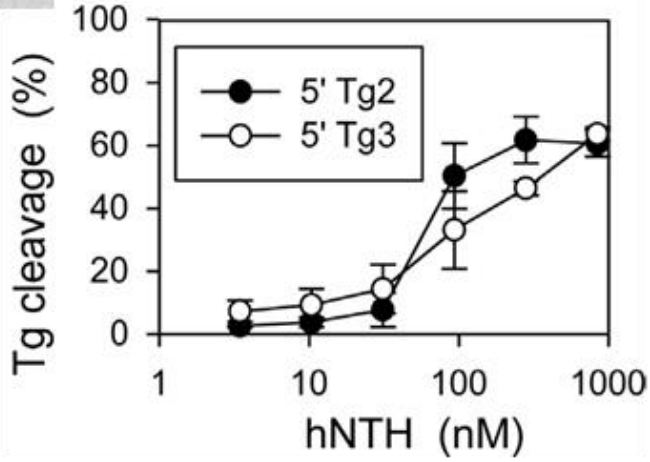

Fig. 4.4: Processing of substrates containing terminally labeled 5′-Tg to by purified hNTH1: A) The 5′-Tg2 (top) and 5′-Tg3 (bottom) substrates were treated with the indicated concentrations of hNTH for 1 hr and analyzed on a 36% nondenaturing gel for the release of the 5′-terminal nucleotide-ribose phosphate from the plasmid substrate. B) The release of the 5′-terminal 1- or 2-base fragment measured as a percentage of radioactivity released into the gel from the well and plotted as a function of NTH1 concentrations. Figure adapted with permission from M. Almohaini et al., 2016. (n = 3)

4.5 Validation of the above-observed results in cancer cell extracts:

Irradiation is one of the primary treatment modalities used to kill cancer cells, because of its capacity to cause enormous damage to cellular components, especially DNA. As with the normal cells, even cancer cells resort to repair these lesions by the retained repair pathways. To evaluate the repair of Tg lesions in cancer cells, all the above-mentioned substrates were processed in HCT116 colon carcinoma cell extracts.

4.5.1 Processing of the 3′-Tg lesions in HCT116 extracts:

The 3′-Tg substrates were incubated in HCT116 extracts for 6 hours before being proteolyzed, ethanol precipitated and treated with restriction enzymes NdeI and PstI (Fig. 4,5). Repair of the substrates in the cancer cell extracts followed a similar trend of end-joining (Tg3>Tg5>Tg2>Tg1) and BER (Tg5>Tg3), as in non-cancer fibroblast cell extracts, but with a lesser percentage end-joining compared to that of in Bus cell extracts (Fig. 4.5 vs. Fig. 3.4). There was a formation of the BER product for Tg3 (16-bp) (lane 8) and Tg5 (14-bp) (lane 10), similarly to Bus cell extracts. As with the Bus cell extracts, Tg5 is processed greater (~22%) than the Tg3 substrate (~4.8%) by BER. And also, this extensive processing by BER has reduced the Head-to-Tail end-joining of Tg5 substrates (~3%) compared to Tg3 end joining (~6%). The observed percentages Head-to-Tail end-joining for all the substrates and the BER products of Tg3 and Tg5 substrates were plotted (Fig. 4.5 B)

4.5.2 Influence of 5′-Tg on the repair of DSB's in cancer cell extracts:

Similarly, the 5′-Tg substrates (5′-Tg2 and 5′-Tg3) were incubated in HCT116 extracts alongside the Bus extracts with or without substituted XLF. As seen in the radiograph of the gel (Fig. 4.6), there was lesser end-joining of these substrates in HCT116 extracts than in Bus extracts + XLF (Fig. 4.6 lanes 4,5,6 vs. 7,8,9). There was more end joining (1.5 X) of the 5′-Tg3 compared to 5′-Tg2 substrates (Fig. 4.6 B) and corroborating the findings from Bus cell extract experiments.

These results prove that irrespective of the origin of the cell, the Tg lesions formed in the promiximity of DSB's are similarly susceptible to processing. Furthermore, the extensive processing mediated by BER can interfere with the end joining.

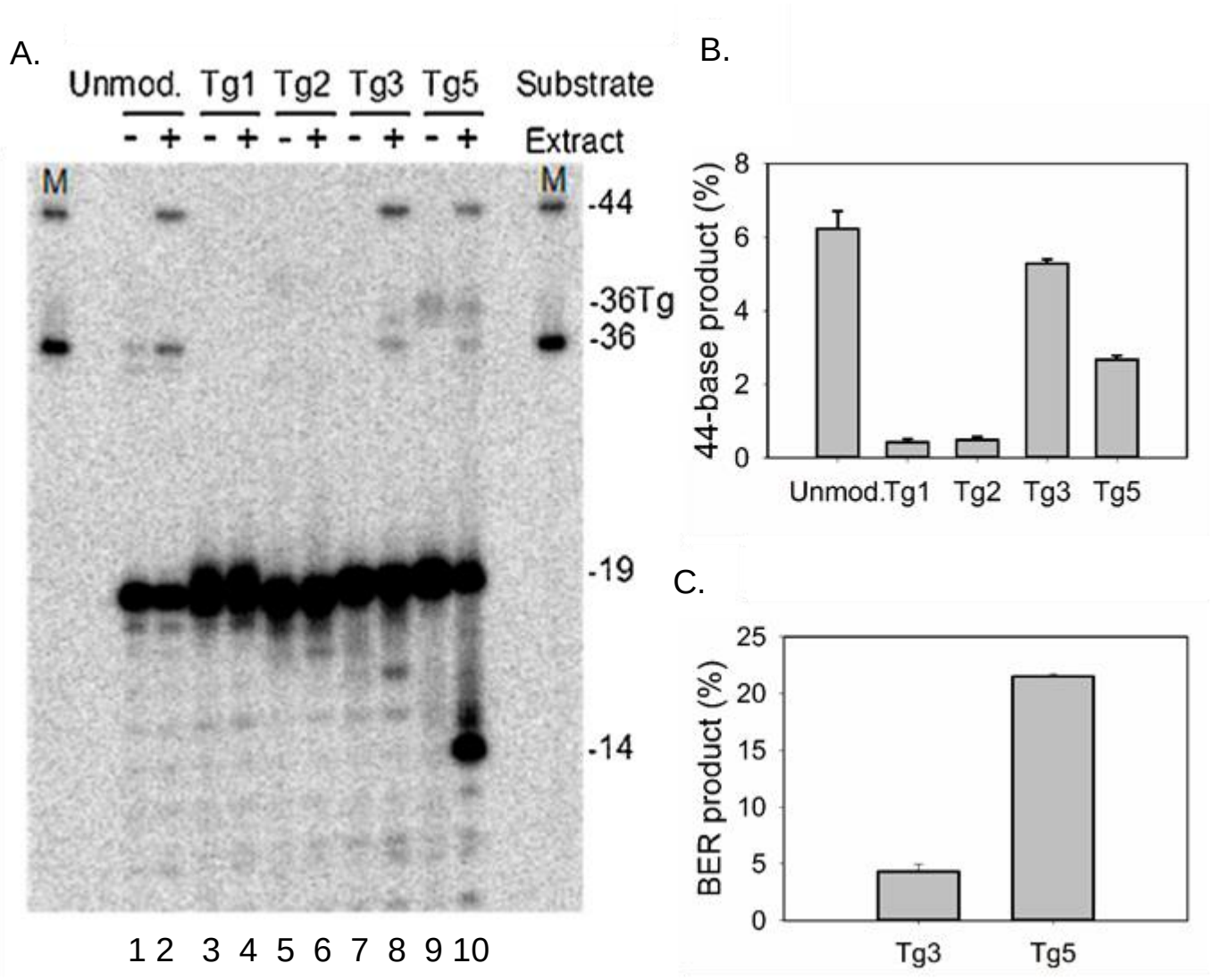

Fig. 4.5: HCT116 cell extract assays with 3′-proximal Tg substrates: A) Each of the 3′-Tg substrates were incubated for 6 hr in extracts of HCT116 cells. B) End-joining as well asTg cleavage, indication of BER were analyzed and plotted. Incresed formation of BER product is detected with less end joining for Tg5 (lane 10) compared to Tg3 (lane 8). Figure adapted with permission from M. Almohaini et al., 2016.

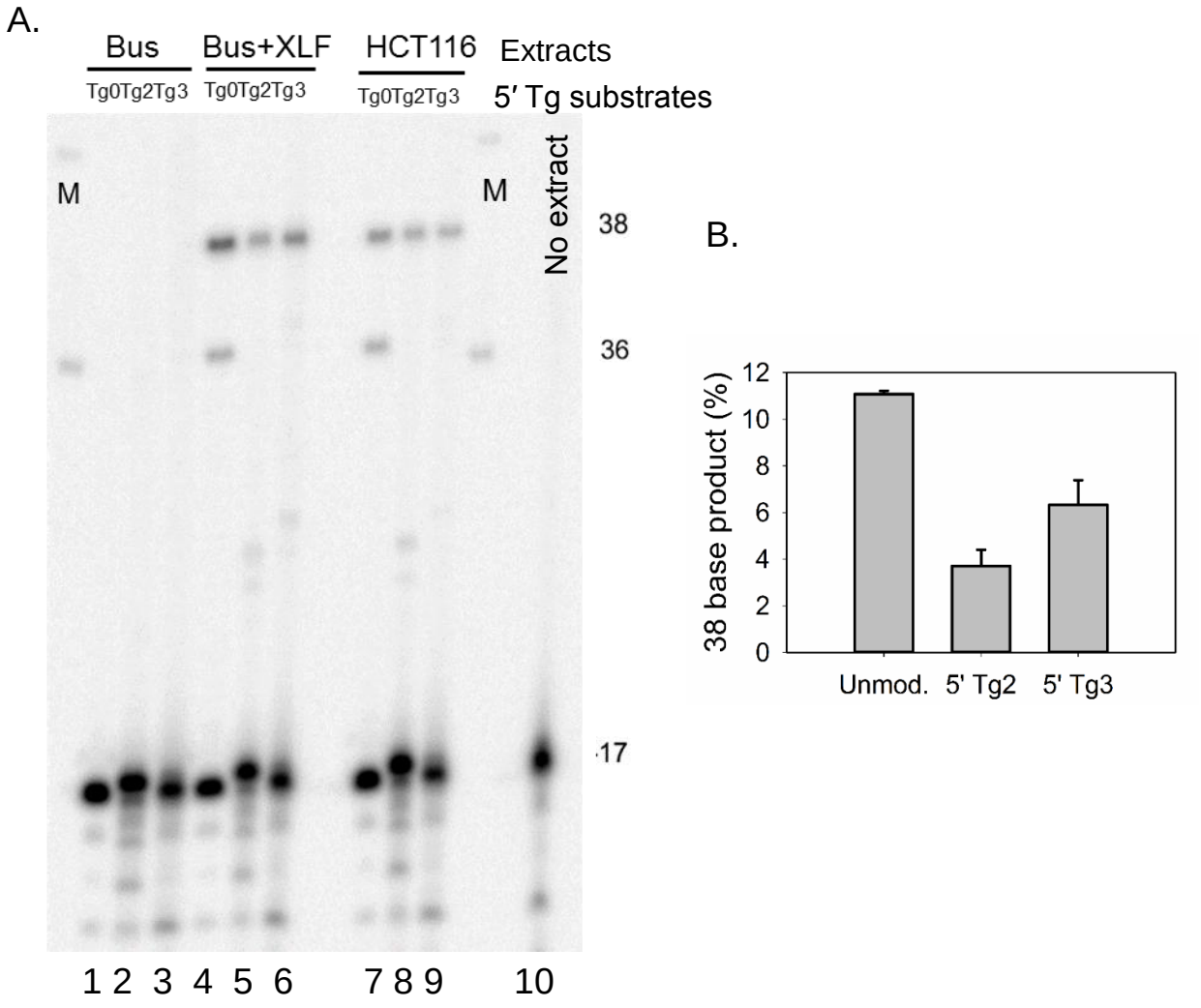

Fig. 4.6 Effect of 5′-proximal Tg on NHEJ in Bus cell extracts with XLF: A. The 5′-Tg2 and 5′-Tg3 substrates were treated with HCT116 whole cell extracts (lanes 7-9), in addition to Bus extract with (lanes 4-6), and without XLF (lanes 1-3), for 6 hours. B. The percentage of Head-to-Tail end joining was measured and plotted. (Tg0 = unmodified ends)

On the whole, repair of complex lesions, especially those involving strand breaks pose a complicated scenario requiring an interplay between multiple repair pathways to resolve the lesion to avoid lethality. It can be hypothesized that in cells there could have been end-joining of the Tg5 substrates by the resection dependant late NHEJ or alternative end-joining pathway (Alt-NHEJ) and if progressed to G2, repaired by Homologous recombination. However, in our extracts when we tried to sequence the end-joining, there was no evidence of deletions or insertions at least in the 20 samples screened. There can be two possible reasons for this. The end-joining in these samples was allowed to progress only for 6 hr and the other processes mentioned above takeover after 6-8 hr. Moreover, since the experiments were done in a cell-free extract, it might not be possible to replicate all of the processes occurring in the cells, with a limitation of the activation and availability of other factors.

V. Discussion

Oxidative lesions are one of the most common lesions due to radiation, DSB's being the lethal amongst them, more so if accompanied by a modified or complex lesion at the ends. Further, BER enzymes can convert readily repairable or bypassable lesions into lethal while processing bistranded damage clusters (Harrison, Hatahet, Purmal, & Wallace, 1998). Radiation can produce strand breaks accompanied by damaged/oxidized bases. Most commonly oxidized bases are Guanine to 8 –oxo-guanine (8 oxo-G) and Thymine to thymine glycol (Tg). Previous experiments with 8 oxo-G have suggested it to be least tolerant when placed at the DSB, at least 4 bases from a 3′end or 6 bases from a 5′end and when two 8-oxoG lesions are positioned across the break junction, ligation is severely retarded (Dobbs, Palmer, Maniou, Lomax, & O'Neill, 2008). In the current study, we wanted to research the tolerability of Thymine glycol at the blunt double-strand break. Thymine glycol (5,6-dihydro-5,6-dihydroxythymine, Tg), a prototypic pyrimidine lesion arises from reactive oxygen species attacking either thymine or methyl cytosine. Tg is a common product of endogenous metabolism, chemical oxidation, or ionizing radiation (Cathcart, Schwiers, Saul, & Ames, 1984). Unlike 8-oxo-G, the most common purine oxidative lesion which was shown to be mutagenic, Tg is a lethal lesion as it blocks the replication. Due to its non-planar structure, the base becomes extra-helical hindering the stacking of the next 5′ templating residue and inhibiting the next incoming nucleotide, effectively blocking conventional polymerase-mediated DNA replication. (Robert C.

Hayes & Leclerc, 1986). However, polκ/polζ and polθ mediate alternate pathways for promoting replication through a Tg lesion. In the polκ/polζ pathway, following the insertion of an A opposite TG, polζ would extend from the TG: A base pair. On the other hand, polθ carry out both steps of TLS, generating ~5% mutationally altered TLS products (Yoon, Roy Choudhury, Park, Prakash, & Prakash, 2014). Repair of the thymine glycol lesion can be by BER, NER and transcription-coupled repair (TCR), hNTH1 and hNEIL1 of BER playing a major role in excising Tg (Dolinnaya, Kubareva, Romanova, Trikin, & Oretskaya, 2013b).

The current study is an extension to previous observations made in the lab by Mohammed et al., 2016, positioning Tg at different lengths from the 3′ end of the blunt double-strand break and study it in the context of NHEJ. It was noted that Tg placed at the third position allowed for an efficient end-joining compared to the first and second positions. However, placing Tg at fifth position limited the end joining while producing a more evident smaller fragment of DNA corresponding to a cleaved product at the Tg. Tg is a substrate for two BER repair proteins hNTH1 and NEIL1, which removes the lesions via β-elimination or β,δ-elimination respectively. Although these proteins can backup each other, they are expressed in a tissue-specific manner (Hazra et al., 2002) (Aspinwall et al., 1997). To support our hypothesis that there is more base excision repair of Tg5 substrate hindering the end-joining, a pure recombinant NHEJ protein assay was done. In the absence of other repair factors, we evidenced an increase in the end-joining of Tg5 substrate compared to Tg3 substrate. Further, we wanted to see if Tg5 was a better substrate than Tg3 for BER by performing a recombinant protein assay with hNTH1. As expected, hNTH1 repaired Tg5 more efficiently compared to Tg3.

Next preference of positioning Tg at 5′end for BER was measured by positioning Tg at the second or third position of the blunt DSB. There appeared to be no preference in overall processing these substrates.In contrast to the internally labeled 3′ substrates, 5′ substrates are terminally labeled, and the end-joining of these substrates was evident from the detection of the band which was about 40% and 60% of the unmodified substrate end-joining for Tg2 and Tg3 respectively. Unlike 3′-Tg at a second position which allowed for minimal end-joining, 5′-Tg at second position allowed for considerate end-joining, with Tg in position.

All the above experiments were performed in Bustel fibroblast extracts which are inherently deficient in XLF, an end-joining protein, to study its role in NHEJ. To validate the observations made in these extracts and also to study the repair of Tg lesions in cancer cells which could be a result of radiotherapy, processing of Tg lesions was tested in HCT116 cell extracts. Even though the overall end joining seen in these extracts is less compared to Bus cell extracts, the profile of the repair of Tg lesions appeared to be similar. Extensive nucleolytic excision of the 5-base 5′-overhang of the complementary resulting from the BER might have limited the end-joining of the Tg5 substrates in both the extracts (Fig. 3.2 vs. Fig. 4.5). Similarly, there was appearance of the unjoined BER product of Tg3 in both the extracts. On the whole, these studies provide evidence that both BER and NHEJ function hand in hand in the repair of oxidative lesions, with BER interfering with NHEJ in a lesion dependant manner.

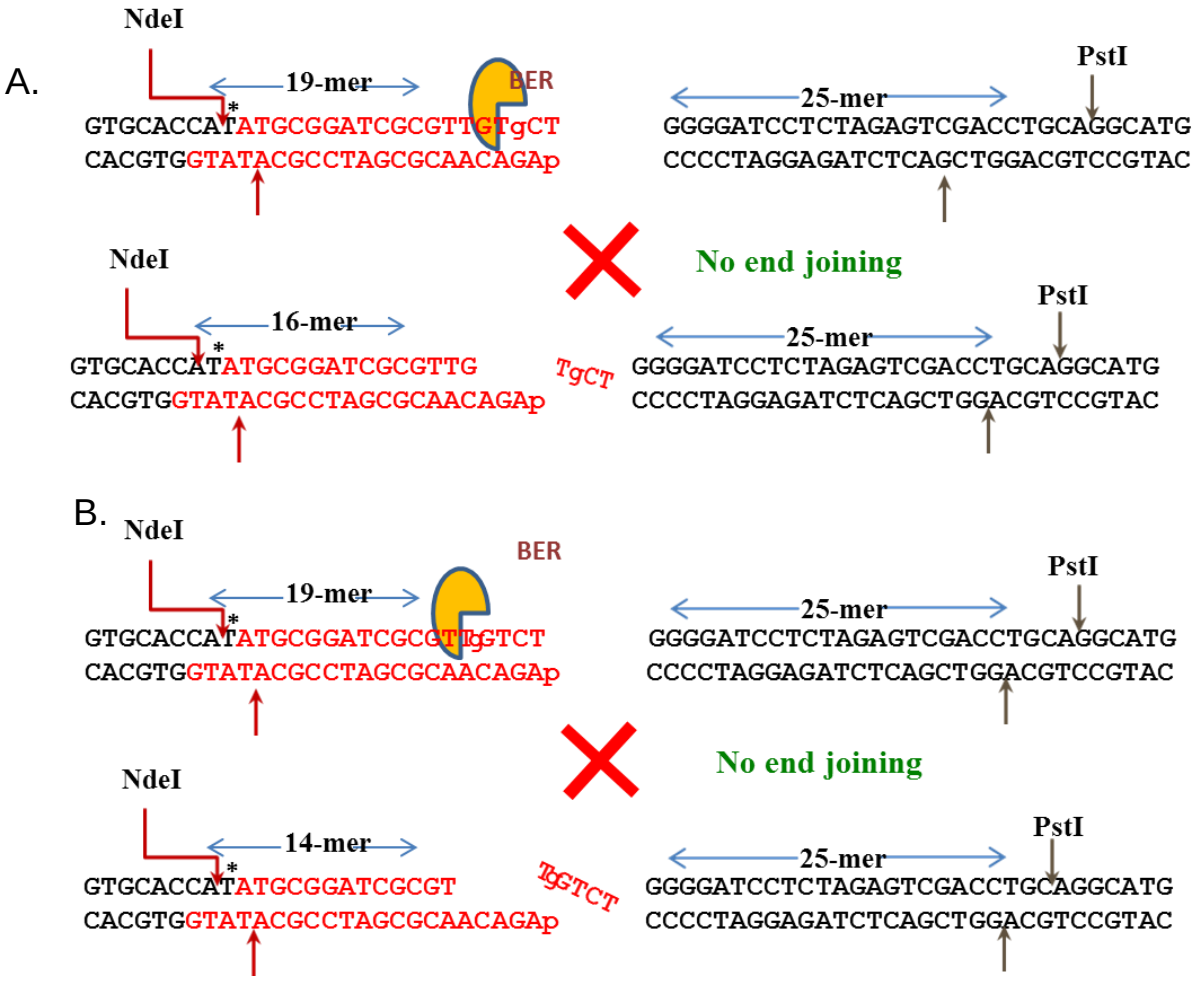

Fig. 5.1: Proposed model for the interference by BER in NHEJ : A) When base excision repair proteins recognize and remove the Tg from the third position in Tg3, instead of the 19- bp fragment 16-bp fragment was formed and there was no end joining of the fragments. B) When the Tg from the Tg5 substrate was removed, there was the formation of 14-bp fragment, and there was no end joining.

Chapter 2

RESOLUTION OF DNA 3′-PHOSPHATE ENDS IN THE ABSENCE OF PNKP AT THE FREE RADICAL-MEDIATED DNA DOUBLE-STRAND BREAKS FOR NONHOMOLOGOUS END JOINING

VI. Introduction

A feature of ionizing radiation resulting from its mode of energy deposition is a generation of a high local concentration of free radicals producing complex DNA lesions, two or more lesions within 1–2 helical turns of DNA, which may involve strand breaks. DNA strand breaks are also a consequence of DNA damage due to chemotherapy, metabolic oxidative process or during repair of the complex lesions by the repair machinery. These strand ends are rarely clean with a variety of chemical modifications and are non-compatible for re-ligation. 3′- phosphate and/or 5′- hydroxyl ended SSB's or DSB's can be a direct result of the insult or as an intermediate during processing of the base damage or overhang 3′-phosphoglycolate end by NEIL enzymes and TDP1, respectively. PNKP is a bi-functional enzyme with a DNA 5′- kinase and 3′-phosphatase function that restores the strands conventional compositions –i.e., a 3′-hydroxyl and 5′- phosphate ends.PNKP was the first gene for a DNA-specific kinase from

any organism and the second gene for a mammalian DNA 3′-phosphatase to be identified (Jilani et al., 1999) PNKP plays a crucial role in processing both single strand, and double strand breaks, enabling them to be filled in and ligated by DNA polymerases and DNA ligases, respectively. Because of its ubiquitous role in repair of the DNA, PNKP is being considered as a potential target for chemotherapy. Stable down-regulation of PNK in human cells results in hypersensitivity to a number of DNA damaging agents including ionizing radiation, camptothecin, and H2O2 and also increases the spontaneous mutation frequency (Rasouli-Nia, Karimi-Busheri, & Weinfeld, 2004). Studies have also shown that PNKP's role as a party of NHEJ is essential for the normal neurological development of the organism (Dumitrache & McKinnon, 2017) (Bras et al., 2015) (Reynolds, Walker, Gilmore, Walsh, & Caldecott, 2012). These studies showed that knockout of PNKP resulted in lethality while the mutations induced developmental delay of the CNS.

6.1 Polynucleotide kinase phosphatase

6.1.1 Structure:

The domain-mapping experiments, sequence analysis, and crystallography studies have revealed a three domain molecular structure - Kinase, Phosphatase and Fork Head Associated domains (FHA) for the PNKP protein. The phosphatase (Gly 145–Glu 336) and the kinase (Phe 340–Glu 521) catalytic domains are linked flexibly to an aminoterminal phosphoprotein-binding forkhead-associated domain (Ser 6–Ser 110) (Bernstein NK et al., 2005). This flexible organization of the FHA and catalytic domain was revealed by the trypsin digestion which releases a 40 kDa (catalytic domain) and 14 kDa FHA domain. The interdomain linker (Leu 337–Ala 339) and the C-terminal residues Gln 518–Gly 522 pack against helix 5 and the β12-α4 loop of the phosphatase prohibiting

the separation by proteolysis. The phosphatase domain which encompasses 136 to 337 residues has a structure typical of the haloacid dehalogenase (HAD) superfamily, which includes β-phosphoglucomutase (β-PGM), phosphoserine phosphatase (PSP), P-type ATPase and RNA polymerase II CTD phosphatase (Aravind, Galperin, & Koonin, 1998). Although there is low sequence similarity between these proteins, there is a conserved motif Dx(D/T)x(T/V), where the first Asp (170 in mPNK) forms the covalent phosphoaspartate intermediate. Serine or threonine (216), a lysine (259), and a pair of aspartates (288 and 309) are the other conserved residues, all of them located in the HAD α/β domain (Bernstein NK et al., 2005). Despite structural variations among the α/β domains, the active site configuration is exquisitely preserved.

The kinase domain is of 189 residues and belongs to the adenylate kinase family and consists of a 5-stranded parallel β sheet, common to GTPases and P loop kinases (Leipe, Koonin, & Aravind, 2003) (Leipe et al., 2003), and is flanked by helices on both sides. Also, there are three helices (α12, 13, and 15) which lie between the α/β sandwich and the phosphatase domain. The kinase active site is located in a long cleft and similar to other ATP binding sites, it has a conserved Walker A and B motifs. The protein-phosphoprotein interaction motif, FHA, has a high specificity for phosphothreonine (pThr) residues. Structurally, it possesses the typical β sandwich fold consisting of a 3-stranded and a 4-stranded antiparallel β sheets. The N- and C termini of the domain are located on adjacent β strands, and loops bind the phosphopeptide on the opposite side of the domain. There is a conserved motif S47RNQ50 that forms a protruding U-turn shape preceding the β5 strand, and the recognizes of phosphopeptide by a conserved Arg (Arg70) and Ser (Ser85) residues and nonconserved Arg48 residue.

Among the domains of the protein, FHA domain is poorly ordered, allowing for the flexibility of the catalytic domain.

6.1.2 Substrate specificity, recognition, and function of PNKP:

Each catalytic domain has its preference for the substrate. The kinase domain of PNKP preferentially phosphorylates the 5′ end of DNA at the nicks and small gaps (Karimi-Busheri & Weinfeld, 1997) and a duplex of at least 8 nucleotides with a 3′-overhang of ≥ three nucleotides (Bernstein et al., 2009). The kinase active site located in the deep cleft with ATP binding site on one side and the DNA substrate binding site on the other. The substrate binding site has two positively charged surfaces, one flanking the Asp 396, which acts as a general base to activate 5′-OH group in the duplex. The phosphate group, 3′ to the 5′OH end, is stabilized by Thr 423, and no contact is made with the protein by the substrate until 6-8 nucleotides on the complementary strand upstream around Arg 403, consistent with the substrate requirement. The other side of the cleft surface consists of Arg482 and Lys483 which interact with the four backbone phosphate groups of the single-stranded 3′ overhang downstream of 5′ OH strand, explaining the minimal length requirement for the 3′ overhang.The Aspartic 396 interacting with the 5′-OH group of the substrate forms general base assistance for the nucleophilic attack on the ATP γ-phosphate, with the aid of Mg2+, resulting in the phosphorylation of the 5′-end.

In contrast to the kinase domain, the phosphatase domain accepts a broad range of substrates including nicked, gaped DSB and oligonucleotides of short segments 5′ to the 3′-phosphate. The phosphate group at the active site in the conserved motif Dx(D/T)x(T/V), is stabilized by, Mg2+, Lys 259, Thr 216 and main chain NH of Leu171. There is an in-line nucleophilic attack on Asp170 producing a phospho-intermediate and

a leaving group. The release of phosphate from the phosphointermediate is catalyzed by Asp 172 which functions as a general acid by protonating the alcohol leaving the group (Bernstein et al., 2008). However, the narrow, deep active cleft can accommodate only single but not the double strand substrates. To access the phosphate group in double-stranded substrates, PNKP needs to unwind the DNA with the help of its conserved basic surface. While the Phe 184 forming “the Phe wedge,” plays a critical role in the initiation of base-pair destabilization through hydrophobic interactions with the substrate bases, Phe305, buried in the active site, could play a role in stabilizing the liberated single-strand in the catalytic conformation through stacking interactions with the 3′-terminal base. Recognition and interaction of the penultimate base are also crucial for binding and activity of the enzyme. Lys184 and β13-α6 loop (residues 300–303), away from the active site engage with the partner strand in the double-stranded substrate before destabilization, providing additional binding energy, and with the complementary undamaged strand after base-pair destabilization. This stabilization of the complementary strand is required to compensate for the unfavorable free energy associated with base-pair disruption (Coquelle, Havali-Shahriari, Bernstein, Green, & Glover, 2011). Fluorescence Spectroscopic Studies of 2AP-Modified DNA Complexes have shown that the destabilization of the double-stranded DNA substrate was maximum up to 2 terminal bases with partial destabilization up to 8 terminal bases (Coquelle, Havali-Shahriari, Bernstein, Green, & Glover, 2011). The FHA domain of the PNKP recognizes the CK-2 phosphorylated phosphothreonines on XRCC1 and XRCC4, directing PNKP towards either single strand or double strand breaks, respectively.

The phosphatase activity of the enzyme takes precedence over and has a faster catalytic rate than kinase activity (Dobson & Allinson, 2006). This precedence of phosphatase over kinase activity may be due to protecting the DNA from the most common damage induced by radiation or by bifunctional glycosylases, i.e., 3′-phosphate formed more commonly than the 5′-hydroxyl ends.Given the limited flexibility between the catalytic domains, there is a sequential repair of the DSB substrates having to possess both 3′-phosphate and 5′-hydroxyl ends. There are a preferential binding and processing of the 3′-phosphate, kinase activity being almost stoichiometrically inhibited by the 3′-phosphorylated competitor (Dobson & Allinson, 2006). There appears to be interdomain cross-talk between the two active sites since the ablation of the 3′-phosphatase activity blocks the 5′-kinase activity. Presence of a 3′-phosphate end prevents phosphorylation at the 5′-end and premature conversion to 5′-phosphate end, which would result in an abortive ligation attempt by the DNA ligases adding an adenylate group to the phosphorylated end (Ahel et al., 2006a). Further, the presence of a 5′-hydroxyl block can be theoretically bypassed by extending the 3′ hydroxyl strand and by the removal of 5 hydroxyl flap by FEN, which leaves a 5′ phosphate, allowing for the successful ligation (Dianov, Sleeth, Dianova, & Allinson, 2003).

6.1.3 Role of PNKP in strand break repair:

For ligation and extension of the of the DNA ends, 3′ hydroxyl and 5′-phosphate ends are imperative. PNKP's function as a DNA 3′-phosphatase is crucial in achieving the strand integrity. Hence, PNKP participates in repairing various SSB's/DSB's caused due to drugs such as Bleomycin, during BER, and NHEJ. Depending on the repair pathway, PNKP is seen to interact with various proteins in the repair complex. In NHEJ, PNKP is shown to

form a complex with XRCC4 in dual modes, with non-phosphorylated via FHA domain or phosphorylated (pXRCC4 via the catalytic domain (Fig.5.1) Interacting with XRCC4 alone enhanced the 5′ kinase activity on the DNA ends, only to be slightly increased by XRCC4/LigaseIV. However, interacting with pXRCC4 inhibited the activity which was reversed by the pXRCC4/LigaseIV complex (Mani et al., 2010a). Small angle X-ray scattering (SAXS) structural studies have shown that there is flexible tethering of PNKP to XRCC4 via the FHA-phosphopeptide interaction, adopting a compact conformation which allows for the dynamic interaction between the PNKP catalytic domain and the N-terminal structured region of XRCC4 and/or the LigIV BRCT domain (Aceytuno et al., 2017a). Depriving of this later interaction due to an E326K mutation in human cells reduces PNKP recruitment to sites of UV laser-induced DNA damage and is associated with a severe form of the neuro-developmental disorder termed MCSZ (Shen et al., 2010).

A.

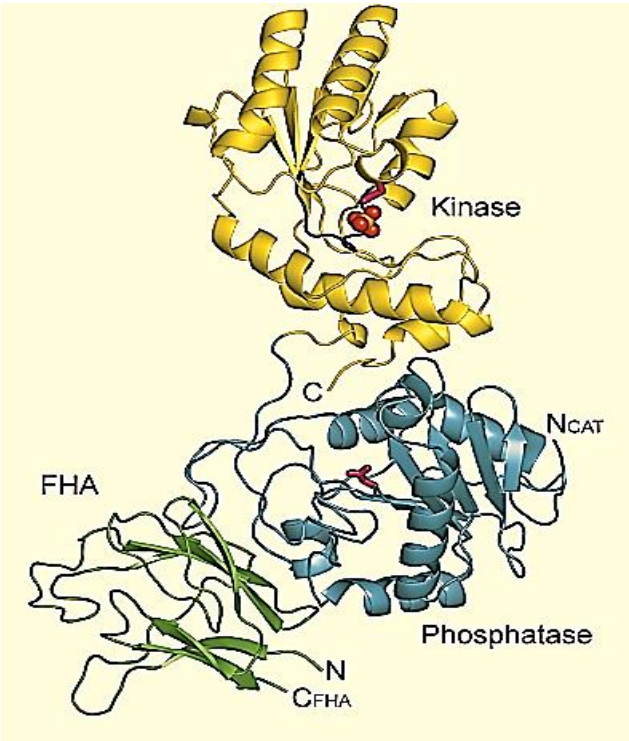

B.

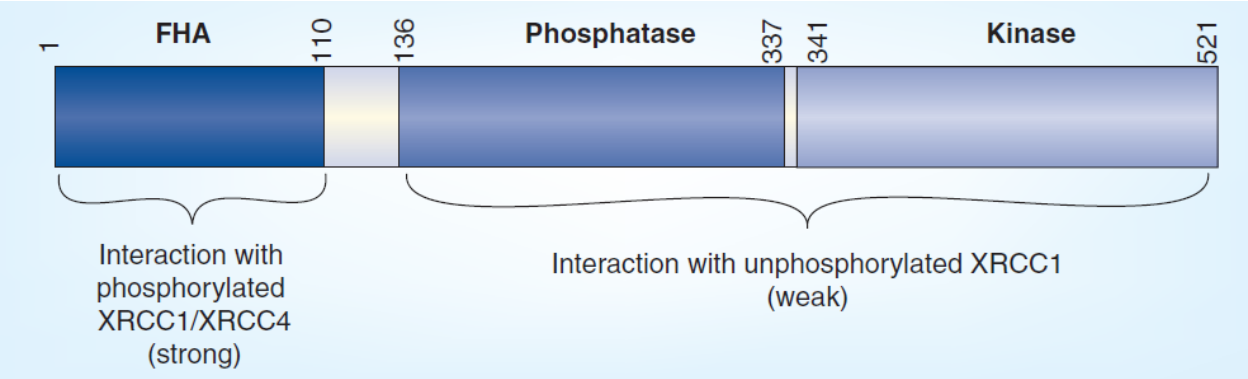

Fig. 6.1: PNKP structural representation: A. Ribbon diagram of mammalian PNKP with kinase domain represented in yellow, phosphatase in blue and FHA domain in green, with ATP binding P-loop in navy blue. Figure adapted with permission from Bernstein et al., 2005. B. Schematic representation of PNKP domains with labeled XRCC4/XRCC1 interacting regions on PNKP. Figure adapted with permission from Allison 2010.

Hypothesis

There are alternatives to Polynucleotide kinase phosphatase enzyme (PNKP) which can process DNA 3′-phosphate and 5′-hydroxyl ends in its absence

Background:

PNKP enzyme converts DNA 3′-phosphate and 5′-hydroxyl ends to 3′-hydroxyl and 5′-phosphate ends, enabling strand extension and/or ligation. . There has been no other factor identified to compensate for the loss of PNKP. However, when PNKP was knockdown or pharmacologically inhibited there was no difference in processing of the DNA 3′-phosphate ends produced by treatment of HCT116 cells with Neocarzinostatin (NCS), as detected by Ligation-mediated PCR (LM-PCR). Therefore, to further study the effects of loss of PNKP, PNKP knockout cells were used to study processing of the specific substrates, in the context of NHEJ, in the extracts. Also, we also elucidated the role of core NHEJ factors in the processing of these substrates.

6.2 Specific aims:

1: To evaluate the processing of DNA 3′-phosphate DSB substrates in wild-type and PNKP knockout extracts to determine whether there are alternative DNA 3′-phosphatases and whether they function in the context of NHEJ

2: To identify the presence of DNA 5′-kinases in the HCT116 PNKP knockout extracts

3: To determine the role of XRCC4 and XLF in processing DNA 3′-phosphate and 5′-hydroxyl substrates

VII. Material and Methods

7.1 3′-phosphate substrate

Oligonucleotides with 3′-phosphate, 3′-phosphotyrosyl ends, and 5′-hydroxyl ends are acquired from Midland labs (Texas). They were re-suspended in TE (10 mM Tris–HCl, pH 8, and 0.1 mM EDTA). 1 mCi of [γ-^{32}P] ATP was used to label 50 pmoles of the oligonucleotide, using Polynucleotide kinase (PNK) and incubated for 1 hr at 37 °C.

7.2 Preparation of pRZ56 and ligation of oligomers to the MluI cleaved pRZ56

The polylinker region of pSV56 plasmid was excised as a 625-bp PflMI/AvrII fragment, and cloned into pBR322 between the EcoRV and NheI sites (the PflMI cut was blunt-ended with T4 polymerase), to create a 5-kb pRZ56 plasmid. 76 µg of the plasmid pRZ56 DNA was linearized with 100 units of MluI (NEB) in 0.3 ml of NEB buffer 3 for 2 hr at 37 °C and was ethanol precipitated. 10 µg of the linearized plasmid was then subjected to controlled 3′ → 5′ exonucleolytic digestion with five units of T4 polymerase (NEB), 1 mM dTTP in a buffer containing 33 mM Tris-acetate pH 8, 66 mM potassium acetate, 500 µM DTT 100 µg/ml BSA at 11 °C for 2 hr. The plasmid was proteolyzed and ethanol precipitated and resuspended in 40 µl TE after drying. This procedure results in a 10-base 5′ overhang at one end and an 11-base 5′ overhang at the other due to resection at each 3′-terminal strand to the first thymine in the sequence. 5 picomoles of an unlabeled 13-mer and a 5′-^{32}P-labeled 14-mer with a 3′-phosphate, or an unlabelled 9-mer and a 5′-

^{32}P-labeled 10-mer with a 3′-phosphate or an unlabeled 13-mer and a 5′-^{32}P-labeled 14-mer with a 3′-phosphotyrosyl, each complementary to its 5′ overhangs, were successively ligated with 60 units of T4 DNA ligase, in 1X Ligase buffer in a 50 µl reaction for overnight at 16 °C to specifically labeled substrates with partially complementary (-ACG) overhangs or recessed ends. These substrates were purified on a 0.8% agarose gel, electroeluted and concentrated with an Ultracel 100k centrifugal filter.

7.3 Construction of 5′-hydroxyl substrates:

5′-CCGGGGACCTGCGTACGTGTTC and 3′-CCTGGACGCATGCAC-OH, complementary oligonucleotides were ordered from Midland Labs, Texas and re-suspended in TE (10 mM Tris–HCl, pH 8, and 0.1 mM EDTA). They were annealed in equal quantities, via heating to 80 °C followed by slow cooling to 10 °C. The duplexes generated by this annealing process resulting in 3-base 3′overhang on one end with a 5′-hydroxyl group in the complementary strand, and a 4-base 5′ overhang on the other end that is complementary to the 5′ overhang created by XmaI digestion of pUC19.

7.4 Ligation of oligomeric duplexes to the XmaI cleaved pUC19:

20 µg of the pUC19 plasmid DNA is digested with 100 units of XmaI (NEB) in 0.7 ml of NEB Cut Smart buffer for 3 hr at 37 °C. 7 µg of the cut plasmid is treated with 10 units of CIP in 2.4 µl of CutSmart buffer for 1 hr at 37 °C in a total reaction volume of in 20 µl. The linearized fragment was ethanol precipitated and was radiolabeled with 6 µl 1 mCi γATP and 3 units of T4PNK for 45 minutes in 37 °C, which was ethanol precipitated again. The precipitate was dissolved in 40 µl of TE, and to this, 20 µM, oligo duplex with 5′-hydroxyl end was ligated with 800 units of T4 ligase in 5 µl of T4 Ligase Buffer, in a total reaction

volume of 50 µl, at 16 °C overnight. The resulting substrate had two recessed 5′-hydroxyl ends and labeled on both ends.The ligation products were purified by 0.8 % agarose gel electrophoresis and Electroelution.

7.5 Electroelution of the modified substrates:

The nucleotide is electroeluted using an 11-inch segment of pretreated dialysis tubing (6,000-8,000 molecular weight) filled with the buffer composed of 20 mM Tris, pH8 and 1 mM EDTA (the elution buffer). The gel slice containing the desired DNA band was placed in the dialysis tubing, and the other end of it was knotted after removal of air bubbles. The dialysis tube was placed in a gel box filled with the same buffer, and the DNA was eluted overnight at 50 V. Then the dialysis bag was cut, and the buffer containing DNA substrate was collected into 15 ml centrifuge tubes. 0.45µm filters were used to remove any debris, and the DNA was concentrated by micro- concentration to about 500 µl using centricon-100 (Amicon). The concentrate was collected into 1.5 ml Eppendorf tubes and precipitated with 1/9 volumes of NaOAc and 2.5 volumes of 100% EtOH, washed with 70% EtOH and dissolved in 50 µl TE.

7.6 HCT 116 and HeLa cell extracts preparation:

HCT116 and HeLa, Wildtype (WT) and PNKP CRISPR knockout cells (PNKP-/-), cells were kindly provided by Dr. Weinfeld, Cross Cancer Institute, Alberta, Canada. These cells were grown to 70% - 90% confluence on 15-cm dishes each with 15 ml RPMI media with 10% FBS. Then they are serum starved for 4 days with 15 ml of .5% serum. On the day of the experiment, the dishes were washed with 20 ml PBS at room temperature. 3 ml of 0.25% trypsin-EDTA was added to each dish, making sure it covers all the cells.

They were incubated for 5 min until the cells are detached and then 3 ml medium and serum was added. These samples were collected and pelleted in 50 ml tubes at 1500 rpm for 5 min in ultracentrifuge using SW55 rotor at room temperature. The cells were resuspended in 50 ml medium and serum and pelleted again. The pellet was again resuspended in 25 ml medium and serum and pelleted again. The pellet was resuspended in 30 ml ice-cold PBS and pelleted at 4 °C and packed cell volume (PCV) was recorded. The last process was repeated again. The pelleted cells were resuspended in 5XPCV cold hypotonic buffer containing10 mM Tris-HCl pH8, 1 mM EDTA, 5 mM DTT and proteinase inhibitors pepstatin 1 µg/ml, chymostatin 1 µg/ml, aprotinin 2 µg/ml, leupeptin 1 µg/ml, PMSF 1 mM. The cells were quickly pelleted. This pellet was again resuspended in 2XPCV hypotonic buffer and inhibitors and let set on ice 20 min. 1.5 ml of this solution was put in a small dounce homogenizer each time and stroked 20 times. After it was let set for 20 min, it was transferred to cold 5 ml centrifuge and ¼ volume of the hypertonic solution (83.5 mM Tris pH 7.5, 1.65 M KCl, 3.3 mM EDTA, 1 mM DTT) and inverted several times to mix well. This was centrifuged at 43K for 3 hr in SW55 at 2 °C. From the top the middle layer which has cytosol was collected using 22G needle, avoiding cloudy layer on the top. The cytoplasm thus collected was dialyzed for 3 hr in storage buffer (20 mM Tris pH 8, 0.1 M KOAC, 1 mM DTT, 0.5 mM EDTA, 20% glycerol) with inhibitors at 4 °C. The resulting solution was frozen in small aliquots(10 µl - 80 µl) at -80 °C.

7.7 3′-phosphatase, 5′-kinase and end joining assays using cell extracts:

HCT116 Wildtype (WT) and PNKP knockout, HeLa Wildtype (WT) and PNKP knockout, Bustel whole cell extracts (with/without 200 nM recombinant XLF) and HCT116 XRCC4-

/-, were used for the reactions in a buffer containing 50 mM triethanolammonium acetate (pH8), 1 mM ATP, 1 mM dithiothreitol, 50 µg/ml BSA , 1.3 mM Mg(OAc)2 and dNTPs at 100 µM each.

The total reaction volume was 16 µl, with 10 µl or 11.5 µl of extract, resulting in a final protein concentration of 12.5 mg/ml. 20 ng of the substrate was added and the reaction mixed by pipetting and incubated at 37 °Cfor various times as mentioned. In reactions with Bus cell extracts, 200 nM XLF was added to some reactions. XRCC4 knockout extracts were substituted with either 0.6 µg of pure XRCC4/LigaseIV or 30 ng of PNKP. In some reactions, the extracts were pre-incubated for 10 min with 0.2 µl DNA-PKcs inhibitor, NU7441, dissolved in DMSO, at the indicated concentrations. After certain incubation times, samples were deproteinized by adding an End Joining Lysis buffer containing, 1% SDS, O.3 M Nacl, 20 mM Tris HCL pH 7.6, 10 mM EDTA and 1 mg/ml of Proteinase K for 3 hr at 56 °C. The DNA was then precipitated with glycoblue and ethanol for one hour. After the precipitation, all samples were dissolved in 21 µl of TE and digested with 10 units of BstXI/AvaI and TaqαI and 2.5 µl of 10X CutSmart buffer (New England Biolabs) at 37 °C for 3 hr. Gel electrophoresis of the samples was done in 20% polyacrylamide sequencing gels. Then the gels were exposed to phosphoimaging screen for 1 or 2 days at -20 °C. Data were analyzed using a Typhoon 9100 imager (GE Healthcare Bio-Sciences, Pittsburgh) and Image Quant 3.1 or 5.1 software (GE Healthcare Bio-Sciences, Pittsburgh). The percentage of 3′ phosphatase, 5′-kinase and end joining was determined by measuring the percentage radioactivity of the joined fragments as a function of total radioactivity in the same lanes

7.8 Nuclear and Cytoplasmic fractionation and Western blot:

HCT116 and Hella cell extracts fractionation was done using a kit from Bio-vision. The protein in the extracts was quantified by BCA aasay and were normalized to the same concentration. Laemmli buffer (4% SDS, 20% glycerol, and 120 mM Tis pH 6.8, 10% BME) was added to the extracts and boiled for 10 min at 90 °C. 50 µg of the protein from both the extracts were resolved on either a 10% or Any-KD Biorad SDS-Polyacrylamide gel. Pure PNKP protein, kindly provided by Dr. Weinfield was used as a positive control. PNKP in was detected by using Mouse monoclonal antibody at 1:5000, against the 1 - 140 aa epitope (initially to define the knockout status). In the later experiments, membranes were probed with either a Mouse monoclonal antibody (Santa Cruz) with an epitope of aa 379-411 (1: 500) or Rabbit polyclonal antibody (1:10,000) (Dr. Weinfeld) raised for full-length protein. All the primarry antibodies were diluted in 1%Casein in PBS, added to the membranes incubated overnigt at 4 °C, with rocking. Ater washing the blots with TBST 10 minutes x 3, the membranes were incubated in 10 ml of respective peroxidase conjugated (chemiluminiscent) secondary antibodies, recombinant anti-mouse antibody (Santa Cruz) at a concentration of 1:1000 and goat anti-rabbit (Cell-signalling) at a concentration of 1:3000, in 1% Casein in PBS, for one hour at room temperature. After washing the membranes with TBST 10 minutes x 3, ECL Thermo-scientific Fischer substrates were added to develop an X-ray or image using Biorad imager.Thermoscientific Fischer Supersignaling western blot enhancer kit was used for the antibody from Santa Cruz, to increase the sensitivity of detection. Image J was was used for the quantification of the bands.

7.9 Nuclear extract 3′-phosphatase reactions:

Nuclear extracts of HCT116 and HeLa extracts were assayed for the phosphatase activity in a reaction similar to whole cell extracts, at 2 mg/ml concentration of nuclear protein and a buffer containing 50 mM triethanolammonium acetate (pH8), 1 mM ATP, 1 mM dithiothreitol, 50 µg/ml BSA , 1.3 mM Mg(OAc)2 and dNTPs at 100 µM each. 20 ng 3′-phosphate overhang substrate was incubated in these reactions incubated at 37 °C for various times as mentioned, which were then proteolyzed, ethanol precipitated and cut with AvaI to be analyzed on a 20% PAGE.

7.10 PNKP inhibitor assay:

ST042146, a 3′ phosphatase inhibitor was dissolved in DMSO at a stock concentration of 50mM and different dilutions of 10 mM, 1 mM, .4 mM and .1 mM were made in separate tubes. They were incubated overnight at 72 °C, which darkened the drug solutions. PNKP inhibition assays were performed on either a PNKP pure protein (100ng), or 1:125 (HCT116) or 1:100 (HeLa) WT and PNKP knockout extracts diluted in PNKP storage buffer (50 mMol/L Tris-HCl (pH 7.4), 100 mMol/L NaCl, 5 mMol/L MgCl2, and 0.5 mMol/L DTT). 100ng of PNKP pure protein was added to a 20 µl reaction with 1X phosphatase buffer (50 mMol/LTris-HCl (pH 7.4), 0.01 mMol/L EDTA, 0.1 mMol/L spermidine and 2.5 mmol/L DTT). For the extract assays, the diluted whole cell extracts were added to the above phosphatase buffer in a total reaction volume of 16 µl. Before adding the 3′-phosphate substrate to these extracts, the reactions were incubated with DMSO or ST042164 to a final concentration of 20 µM or 50 µM, for 10 min at 37 °C. 20 ng of the substrate was added to each of these reactions and incubation was continued for 1 hour at 37 °C. Later the samples were proteolyzed and processed similarly as above.

7.11 Polyacrylamide gel electrophoresis:

For electrophoretic separation of the DNA strands, Polyacrylamide gels (20x30x0.08cm) containing 40% acrylamide: bisacrylamide in a ratio of 20:1, 8 ml of 10XTBE and urea in a final concentration of 8.3 M ina total volume of 80 ml, were used. The mixture was cooled to room temperature, and 0.06 g ammonium persulfate and 45 µl of TEMED (N', N,' N,' N'-tetramethylethylene diamine) were added. The gel was allowed to polymerize for 1 hour. 15 µl of samples are then loaded into the wells of the gel and electrophoresed at a constant power of 42 W until the marker reached the bottom of the gel.

7.12 Statistics:

Error bars represent standard error of the mean (SEM) for at least two independent experiments. Unpaired two-tailed t-tests and ANOVA were performed as required and the data was reported as significant if p values <0.05.

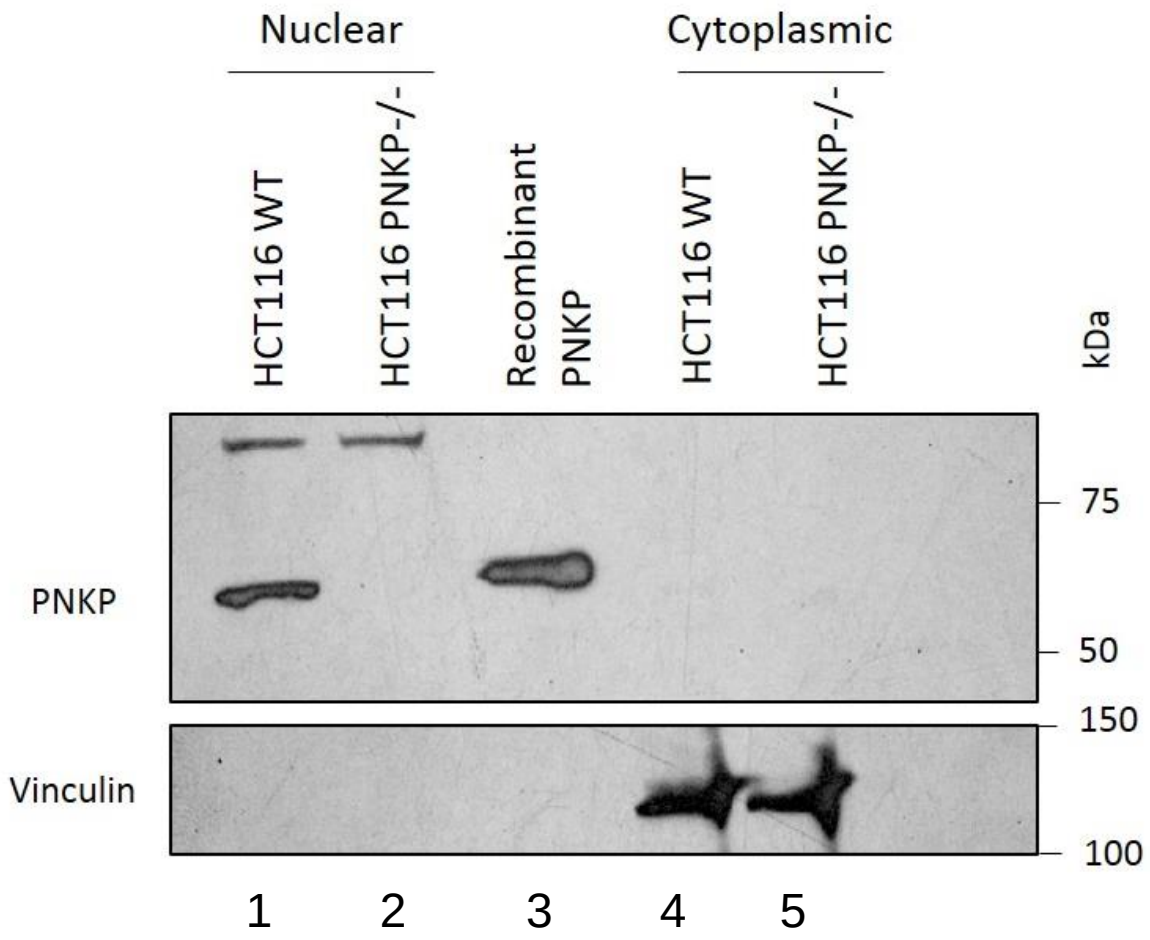

Fig. 7.1: Western Blot confirming the PNKP knockout: WT and HCT 116 cell nuclear extract and cytoplasmic extracts were fractionated using BioVision Nuclear/Cytosol Fractionation Kit and were resolved on a 10% SDS-PAGE, which was botted on to a nitrocellulose membrane, and probed a mouse monoclonal antibody targetting aa 1-140 on the N-terminal end and was detected using a secondary anti-mouse peroxidase labeled antibody. Vinculin was used as a loading marker for a cytoplasmic fraction, while the non-specific band in the nuclear extract fraction was considered as a loading control. As seen in the lane 2 from the left, there was no band corresponding to PNKP in the PNKP knockout nuclear extract

A.

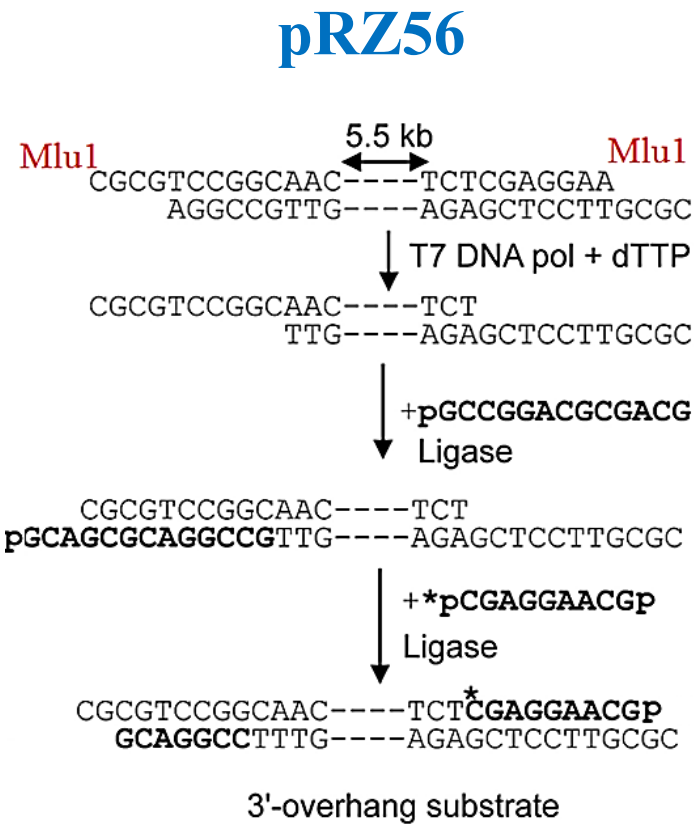

B.

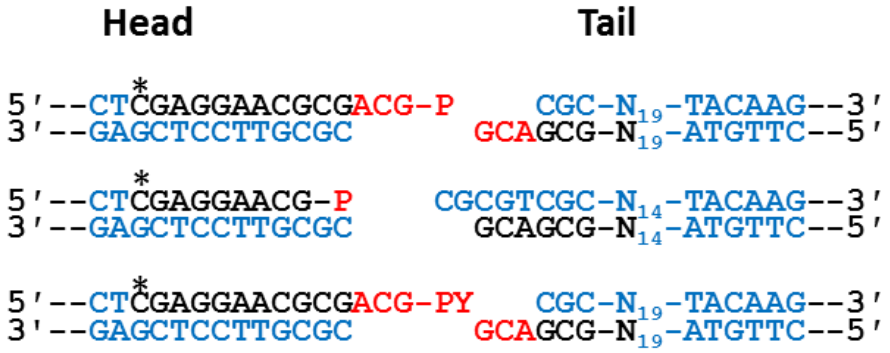

Fig. 7.2: Designing 3′-phosphate double-strand DNA break substrates: Illustration of the synthesis of a 3′-phosphate substrate by ligating different P32- labeled oligonucleotides into the MluI cut and processed pRZ6 5′ overhangs to create an internally labeled substrate (3′ overhang is shown for example). B. Three different substrates, 3-base partially complementary overhang substrate, 2-base recessed substrate with a 3′-phosphate and a 3′-base partially complementary overhang substrate with a phosphotyrosyl group are shown. For convenience, the labeled end is designated as the Head and the other end as Tail.

VIII. Results

Ionizing radiation and genotoxic agents often generate strand breaks with incompatible termini that must be processed by the repair pathways for chain extension and ligation. Some frequently occurring blocks are 3′-phosphate or 3′-phosphoglycolate ends, and more rarely, 5′-hydroxyl ends. The 3′-phosphoglycolate ends are processed by TDP1, APE1, and Artemis (Menon & Povirk, 2016). The only known and confirmed enzyme that processes 3′- phosphate and 5′-hydroxyl ends is polynucleotide kinase phosphatase (PNKP). Although its involvement in promoting cancer development is not elucidated, its role in normal neurological development has been extensively explored (Shimada, Dumitrache, Russell, & McKinnon, 2015).

Like other DNA repair factors, PNKP loss leads to disruption of neurological development resulting in diseases such as oculomotor apraxia (Bras et al., 2015). PNKP plays a crucial role in the repair of strand breaks, both single and double, thus taking part in pivotal DNA repair pathways. This ubiquitous role of PNKP along with the lack of any other identified redundant factor to replace it, makes it a very attractive target for the treatment of cancer. Many small molecule inhibitors of PNKP were identified and tested to be used as a cancer therapy sensitizers (Freschauf et al., 2009). Therefore, the current study is done to explore the presence of alternative DNA 3′-phosphatases and 5′-kinases in the cell, which might have

the capacity to compensate for PNKP loss and promote resistance to PNKP inhibition. Two basic approaches to conduct the study are to either deplete PNKP or inhibit PNKP activity.

Nevertheless, experiments with PNKP knockdown cells and the PNKP inhibitor (A12B4C3) have shown little difference in processing of the 3′-phosphate ends produced by the treatment of HCT116 cells with 5 μM neocarzinostatin (NCS) which introduces 3′-phosphate and 3′-phosphoglycolate DNA strand breaks . Hence, to completely eliminate any residual activity of PNKP, we acquired PNKP knockout cells from Dr. Weinfeld's lab. Whole cell extracts (WCE) were made from the HCT116 wild-type and the knockout cells, and and ^{32}P-Internally labeled substrates with either a 3′-phosphate end or 5′-hydroxyl end were generated to test their processing in extracts, as described in the Methods section. In addition, HCT116 XRCC4 knockout and Bustel fibroblasts (XLF deficient) WCE were made to study their role in processing of the above substrates.

In parallel, the PNKP knock-out status was confirmed using an antibody provided by Dr. Weinfeld. As shown in Fig. 6.1, there was no band corresponding to PNKP in western blots of nuclear extracts of PNKP knockout cells when a monoclonal antibody detecting N-terminal amino acids 1 - 140 was used as a probe. Furthermore, treatment with the drug NCS reduced the survival of PNKP knockout cells more than the wild-type cells. Also, the NHEJ repair foci measured as a function of the number of 53BP1 foci persisted in the knockout cells even after 8 hr, when all the foci in WT cells have disappeared. Considering the above results, we proceeded to perform in-vitro extract experiments to evaluate the removal of a phosphate from the 3′-end or phosphorylate the 5′-end, allowing for the fill-in and end-joining of a DSB.

8.1 Processing of the DNA 3′-phosphate overhang and recessed ends:

PNKP processes 3′-phosphate and 5′-hydroxyl ends at both single and double strand breaks of the DNA (Weinfeld, Mani, Abdou, Aceytuno, & Glover, 2011). In the current experiments, we wanted to explore the consequences of the loss of PNKP in processing different DSB substrates in the context of NHEJ. To assess the same, substrates with either a 3-base partially complementary 3′-overhangs or a complementary 3′-recessed ends with a 3′-phosphate on one end were incubated separately, in either WT or PNKP knockout extracts for different times.

As shown in the figure 8.1, there will be removal of 3′-phosphate from the substrates by PNKP in the wild-type extracts, thereby leading to end-joining of some strands. We wanted to observe if the same would happen in the absence of PNKP. When the conversion of the 3′-phosphate end to a 3′-hydroxyl end was measured as a function of time, when incubated in the extracts, wild-type HCT 116 cell extracts were able to remove about 50% of the 3′-phosphate in the first 5 min and convert all the 3'-phosphate into 3'-hydroxyl within 45 min of incubation, while the PNKP knockout extracts showed a delayed (10X) and incomplete (76.7 ± 1.80%, n = 4) removal even at the end of the total period of incubation (6 hr), from the substrates with partially complementary 3' overhangs (Fig. 8.2 A). Phosphate removal from the substrates with recessed 3′-ends on both sides, with 3'-phosphate on one side, was incomplete (83.6 ± 4.06%, n = 3) even in wild-type cell extract, while most of the phosphate (70.9 ± 4.38%, n = 3), was retained in PNKP knockout extracts (Fig. 8.3 A).

As the time progressed some of the ends were joined either Head-to-Tail or Head-to-Head, with a fill-in (T) reaction (Fig. 8.1 A) occuring at the partial complementary –ACGp-3′ overhangs. When this end-joining of the substrates was quantified, there was an increase

of joining observed for both the substrates with incubation time, in both WT and PNKP knockout extracts, albeit less in the knockouts. The Head-to-Tail end joining (42-bp) was 1.5 ± 0.17% (n = 4), and Head-to-Head end joining (24-bp) was 0.95 ± 0.10% (n = 4), for the overhang substrate in the WT vs 0.84% ± 0.05% and 0.56% ± 0.14%, for the knockouts. Owing to the complementarity recessed ends were joined effeciently, with a Head- to-Tail end joining (36-bp) of 3.7 ± 0.79% in WT vs. 2.75 ± 1.23% in knockout extracts (n =3) and the Head-to-Head end-joining(18-bp) was 2.5% ± 0.46% in WT vs. 0.98% in knockouts (n = 3) (Fig. 8.3 B and C). The low Head-to-Head ligation compared to Head-to-tail can be attributed to the presence of 3′-phosphates on both the ends.

When the removal of phosphate was compared, there was a disparity observed in the processing of the overhang and recessed ends even in the WT extracts. This could be explained by the reduced accessibility of the 3′-phosphate at the recessed end, as the double strand needs to be unwound to place the phosphate group in the catalytic site (Coquelle et al., 2011). This unwinding being an energy-requiring process, could have limited the phosphatase activity at the recessed end. However, retention of a substantial amount of 3′-phosphate at the recessed end indicates that PNKP is the prime DNA 3′-phosphatase at the recessed 3′- DNA ends. Adding back PNKP (100 ng) to knockout extracts resulted in a wild-type phenotype for phosphate removal from the overhang substrate. These observations suggest that in the absence of PNKP, still there is some processing of the 3′-DNA DSB ends. And the loss of activity in the knockout extracts can be attributed to loss of PNKP, since the activity could be restored on adding back recombinant PNKP (Appendix 1, Figure 1A).

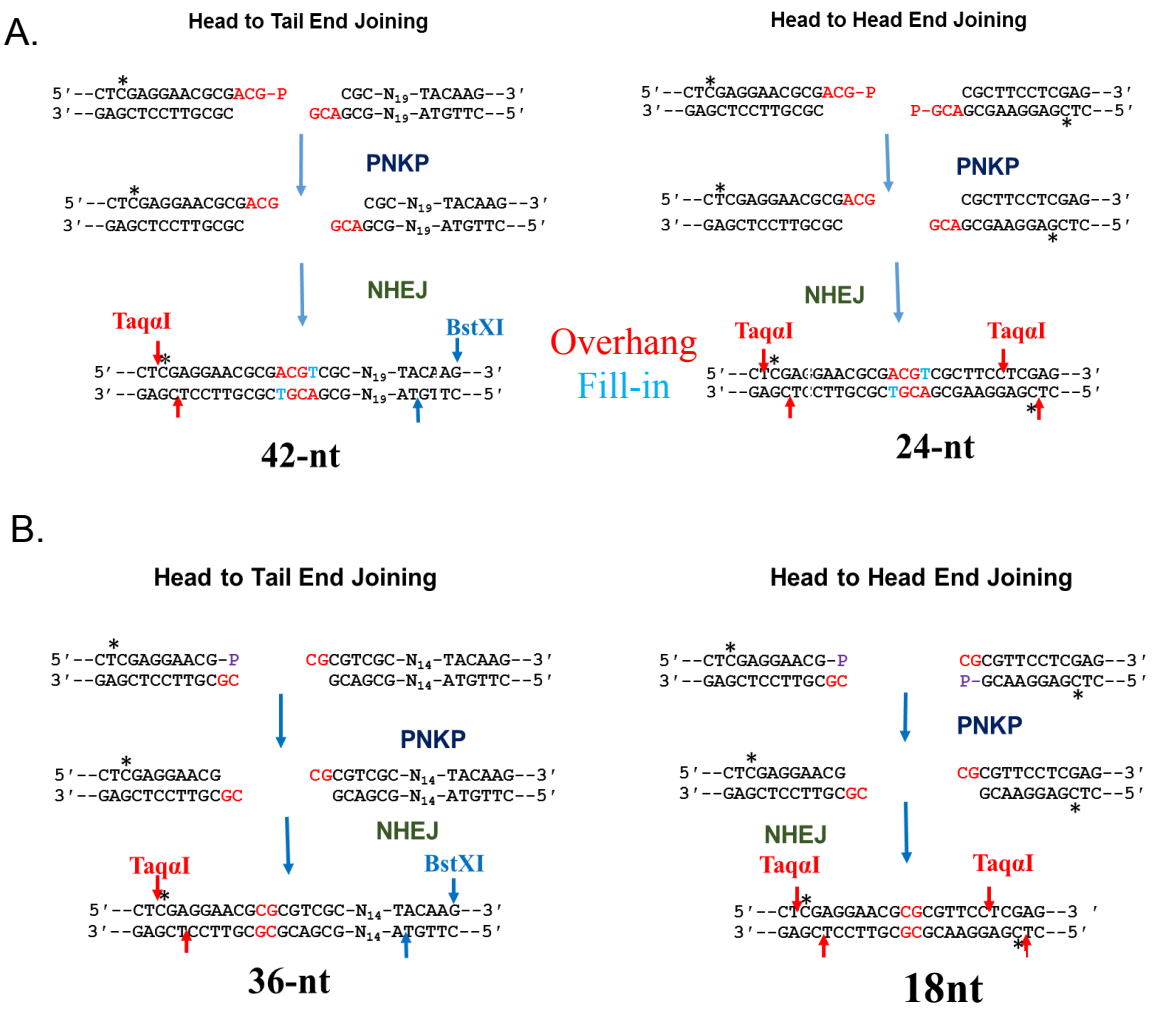

Fig. 8.1: 3′-phosphatase and Nonhomologous end joining (NHEJ) of the 3′-phosphate overhang and recessed substrates: Incubation of the 3′-phosphate substrates in the extracts results in the removal of 3′-phosphate producing a 3′-hydroxyl end which was compatible for end joining. For the partially complementary overhang substrates there will be a fill-in reaction (blue) before end joining, and on treatment with BstX1 and Taqα1, there will be the release of 42-nt and 24-nt, Head-to-Tail, and Head-to-Head end joining products, respectively(A) and a 36-nt and 18-nt, Head-to-Tail and Head-to-Head end joining products respectively, for the recessed substrate (B).

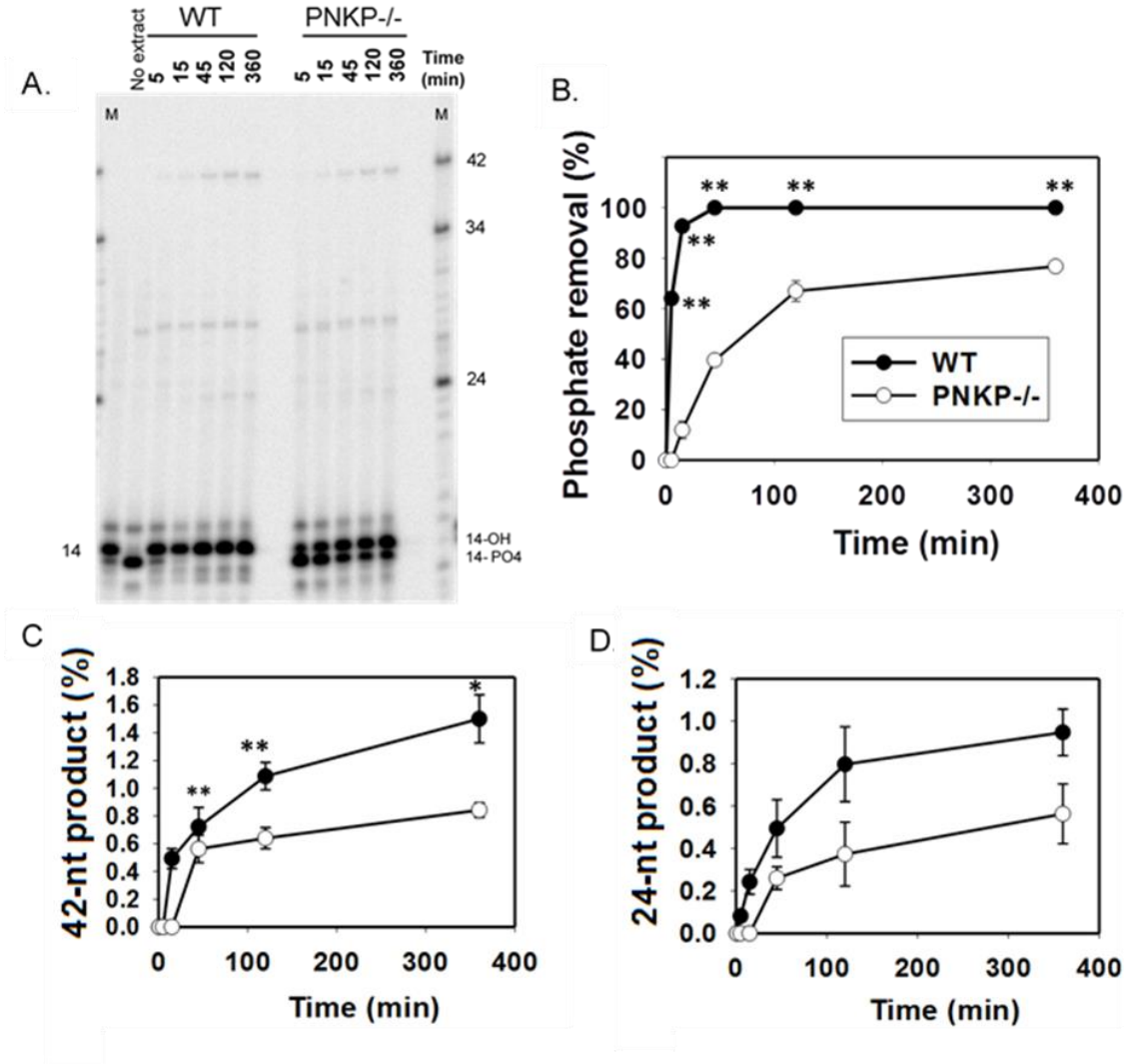

Fig. 8.2: Repair of the double strand breaks of DNA with 3′- phosphate overhang by HCT116 WT and PNKP knockout extracts: Internally ^{32}P -labeled DSB substrate with 3′-partially complementary overhang were incubated in WT and PNKP knockout extracts for different times mentioned. The samples were later proteolyzed and treated with TaqαI and BstxI, which were then run on a 20% polyacrylamide gel and exposed to a phosphoimager screen. The products of processing were visualized on a Typhoon scanner and quantified using ImageQuant 5.1. A. 3′- phosphate ends are converted into 3′- hydroxyl ends in the extracts, some of which are either Head-to-Tail or Head-to-Head end joined, running parallel to the markers (M) of the predicted size and sequence. Because of the negative charge, the unjoined fragment with the 3′-phosphate end runs faster than the one with 3′-hydroxyl end. Plots display the percentage of phosphate removal (B), and percentage of end-joining of the Head-to-Tail – 42-nt (C) and Head-to-Head - 24 end joining (D) in WT and PNKP knockout extracts (* -- $p < 0.05$, ** -- $p < 0.005$; Student t-test) (n = 4)

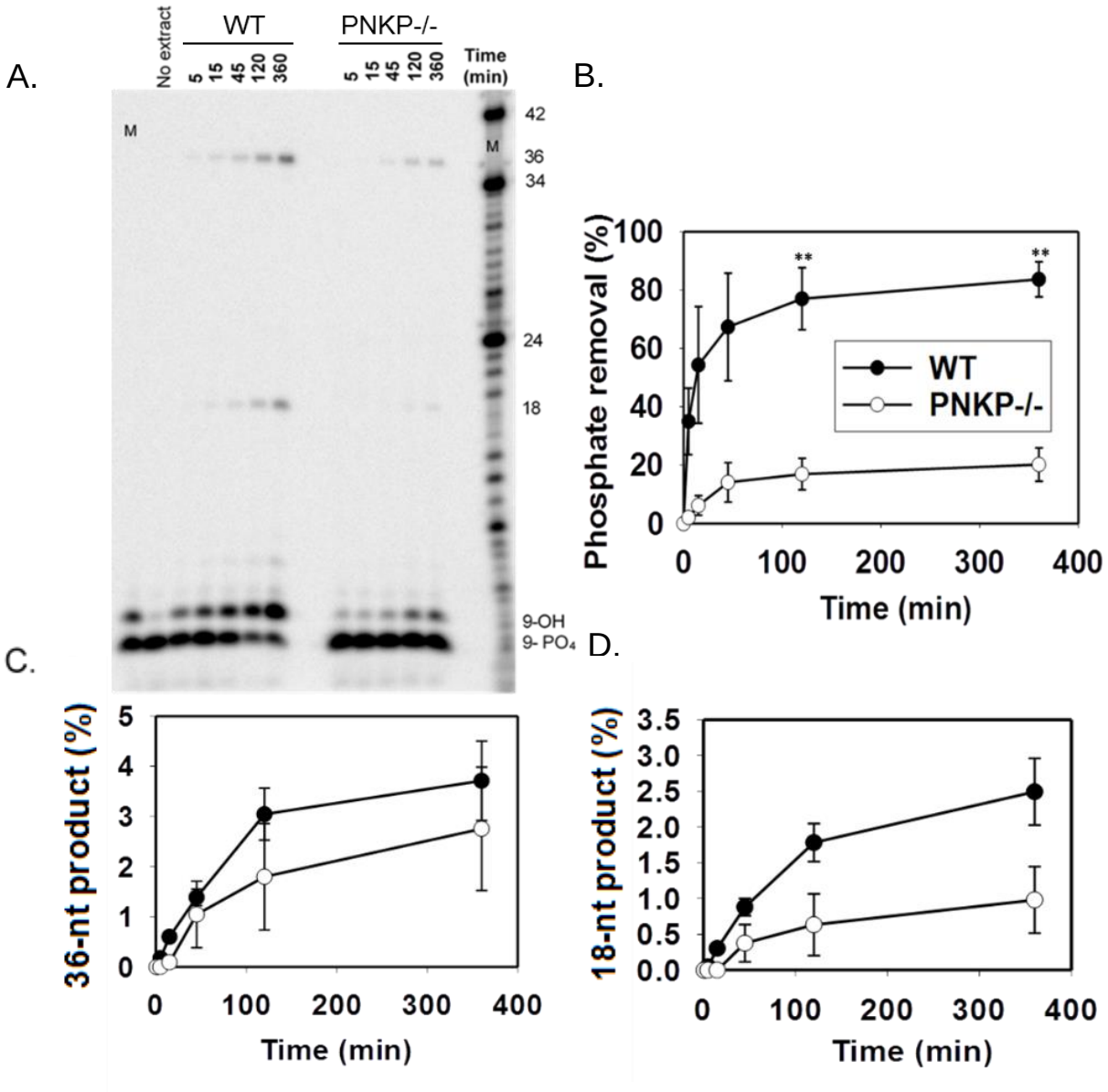

Fig. 8.3: Processing of the substrate with a recessed 3′-phosphate end at the DSB by HCT116 WT and PNKP knockout extracts: ^{32}P-labeled 3′-phosphate DSB recessed end substrates are incubated as indicated and processed similarly to overhang substrates and run on a gel (A). Plots show the increase in percentage of phosphate removal (B) and end-joining of the Head-to-Tail – 36-nt (C) and Head-to-Head – 18-nt (D), in WT and PNKP knockout extracts, as a measure with time. (** -- $p < 0.005$; Student t-test) (n = 3)

8.2 Processing of the 3′-tyrosyl substrates in PNKP knockout extracts:

PNKP is also shown to function as a processor of the intermediate 3′-phosphate DNA ends formed during processing of other complex lesions. For example, chemotherapeutic drugs such as camptothecin inhibit the re-ligation function of topoisomerase I enzyme, by inducing the formation of DNA-TOP1 protein covalent complexes at the 3′ end of the DNA (Plo et al., 2003). These complexes are further processed by peptidases to leave a shorter peptide linked via a tyrosine residue to the DNA 3′-end forming a covalent phosphoenzyme intermediate (Gottlin, Rudolph, Zhao, Matthews, & Dixon, 1998). This DNA-protein complex is resolved by TDP1 enzyme leaving a 3′-phosphate (Interthal et al., 2005). The removal of this 3′-phosphate is dependent on the enzyme PNKP (T. Zhou et al., 2009). Hence, to evaluate the processing the DNA-TOP1 complexes in the absence of PNKP, a DNA 3′-tyrosyl substrate which mimicks the ligand acted upon by TDP1 was constructed.

Similar to the above experiments, the 3′-phosphotyrosyl substrate was incubated with WT and PNKP knockout extracts. While in the WT extracts, 3′-phosphotyrosyl ends were directly converted into 3′-hydroxyl with no detectable intermediates (Fig. 8.4 A lanes 2-7), accumulation of 3′-phosphate was observed in the knockout extracts (Fig. 8.4 A lanes 7-12). This observation reiterates the requirement of PNKP for the removal of 3′-phosphate from the TDP1-processed ends and that loss of PNKP in the knockouts has prevented its conversion to 3′-hydroxyl and not compensated by any other 3′ phosphatase for its loss, at least in a part of them. The disappearance of the 3′-phosphotyrosyl is similarly incomplete in both WT and the knockouts likely due to the extracts containing insufficient TDP1 to process all the substrate (Fig. 8.4).

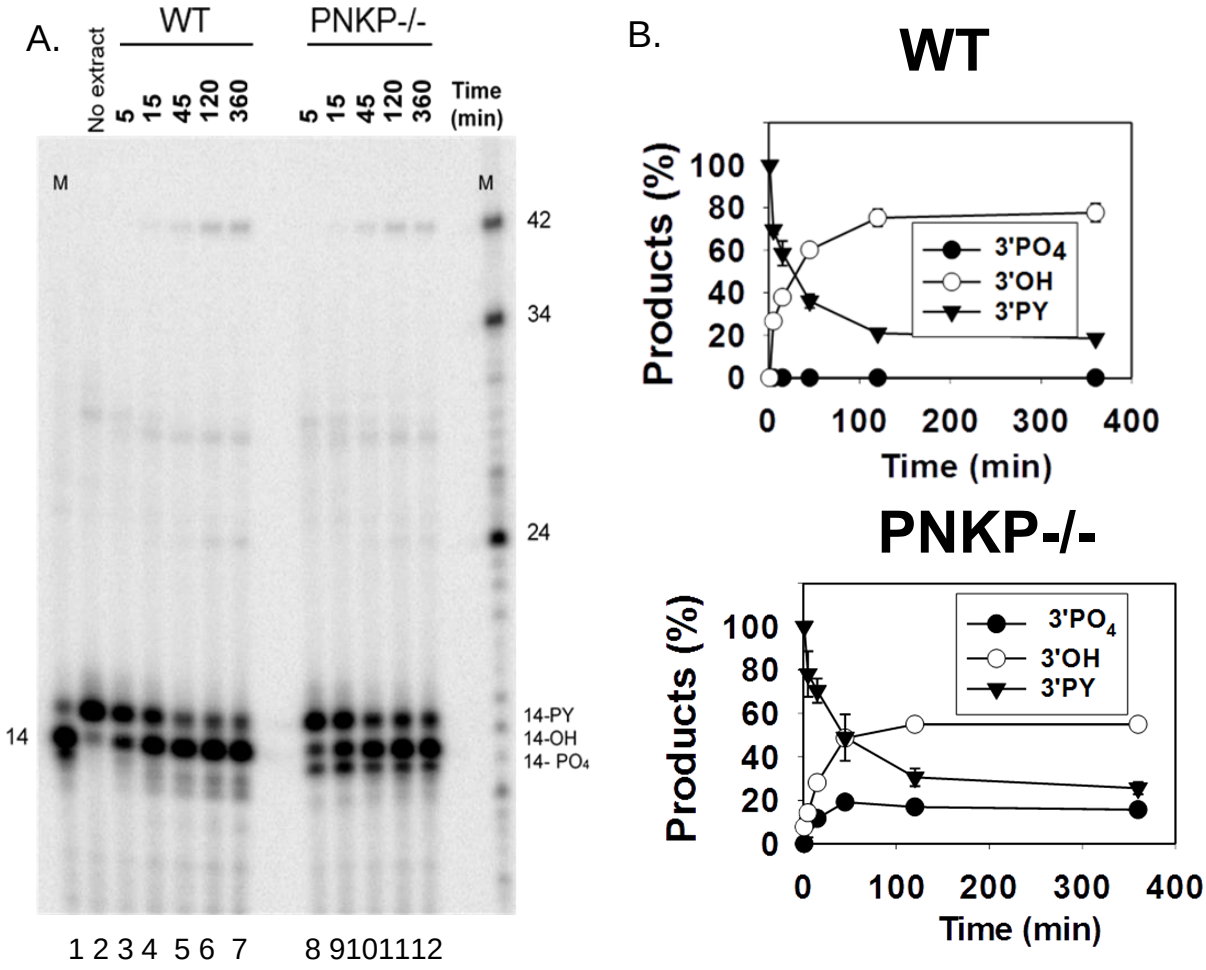

Fig. 8.4: 3′-phosphotyrosyl end processing at the DSB: DNA DSB substrate mimicking that of the substrate acted upon the TDP1 enzyme was designed by ligating a radio-labeled oligo with 3′-phosphotyrosyl end at the overhang. This substrate was incubated in the extracts for different times, processed as in Fig. 8.2, run on a gel and imaged (A), and the percentage of products formed after processing were plotted separately for HCT116 WT (upper panel) and PNKP knockout (lower) extracts (B) (n = 2). Accumulation of 3′-phosphate band was visualized in PNKP knockout extracts only.

8.3 Role of other known 3′-phosphatases in the processing the DNA double-strand breaks:

PNKP is the sole 3'-phosphatase known to be involved in the repair of DSB's by nonhomologous end joining. However, our studies using PNKP knockout extracts have demonstrated a residual 3′-phosphatase activity at the DSB's. There is an other enzyme, APE1, with a weak 3'-phosphatase activity at the SSB's in the context of BER (Chen, Herman, & Demple, 1991). Its role in the repair of DSB end-joining is yet to be elucidated. Aprataxin is another enzyme with limited evidence of 3′-phosphatase activity at the SSB's, recessed DSB's, nicked or gapped DNA (Takahashi et al., 2007). Since these two enzymes act preferably at the SSB's, it was hypothesized that end-joining of the complementary strand at the DSB leaves an SSB with the 3′-phosphate, mimiking a nick, which can be further processed by either APE-1 or Aprataxin.

To determine whether the ligation of opposite strand is promoting the repair of the 3′-phosphate end, ligation of the complementary strand was prevented. Since the ligation of 3′-ACG overhangs requires a fill-in by dTTP in both the strands (as shown in Fig. 8.1 A), substitution of ddTTP in place of dTTP was attempted to allow the fill-in reaction but prohibit the ligation. If the ligation of complementary strand instigates the repair of 3′-phosphate end at the SSB created, blocking this ligation should limit the fill-in reaction. However, when the reactions were carried out with ddTTP in the reaction, similar processing (3′-phosphate to 3′-hydroxyl) resulting in equal fill-in at the 3′- 14-nt unjoined end WT 2.73% vs PNKP -/- 2.9%, to produce 15-nt (one base extended), was observed after 6 hr of incubation (Fig. 8.4). This observation rules out the role of complementary

strand ligation in promoting the processing of the 3′-phosphate end at the DSB in PNKP knockout extracts and thus rules out the role of APE1 and Aprataxin in DSB repair, atleast at the 3′-phosphate end.

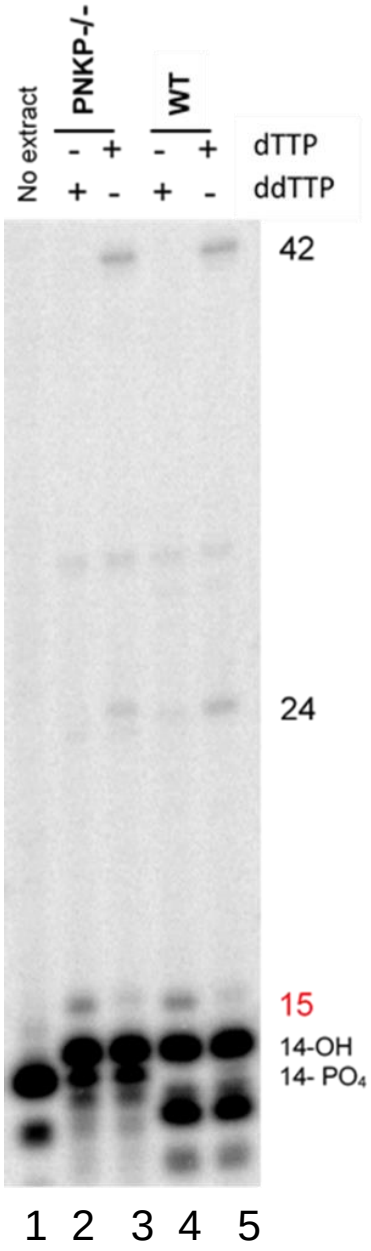

Fig. 8.5: Role of other 3′-phosphatases in the processing DNA double-strand breaks: HCT116 WT and PNKP knockout extracts were incubated with the 3′-overhang substrate in the presence of ddTTP (lane 2 and 4), to block the end-joining of both the strands after fill-in to eliminate the role of complementary strand ligation in processing the 3′-phosphate end at the DSB's. A fill-in reaction produces a band corresponding to one nucleotide higher (15) than the unjoined fragment as a result of blocking the end-joining. As expected, we could block the end joining in lane 2 and 4, however there was a prominent a nucleotide fill-in at the unjoined ends, suggesting the removal of 3′-phosphate even in PNKP knockout extracts (lane 2).

8.4 Identifying the presence of a non-conventional DNA 5′-kinase in the mammalian cells:

PNKP is the only known DNA 5′-kinase in the mammalian cell. Evidence of DNA 3′-phosphatase activity in the PNKP knockout extracts brings into question the knockout status of the cells. To verify if this activity is due to residual activity or perhaps another isoform of PNKP, we resorted to check the kinase activity on a 5′-OH substrate in these extracts.

Initially, an indirect phosphorylation assay was done with internally labeled 3′-phosphate overhang substrate treated with CIP to create a recessed 5′-hydroxyl ended substrate with a 3′-hydroxyl ends, in PNKP knockout extracts. For the DNA DSB end joining, the 5′-hydroxyl must be converted to a 5′-phosphate, and the only known converter is PNKP enzyme. However, some end-joining was observed for the substrates with the 5′-hydroxyl end suggesting that there was phosphorylation of the 5′-hydroxyl end in the absence of PNKP (Fig. 8.6 A lane 5). There was enjoining seen with the 3′-hydroxyl and 5′-phosphate ended (normal) DSB substrates (Fig. 8.6 A lane 7), as well as in 3′-phosphate and 5′-phosphate ended DSB substrates (Fig. 8.6 A lane 3), which was similar to the observation made in Fig. 8.5. However addition of ddTTP abolished the ligation for all the substrates, indirectly suffesting a fill-in occuring at all the substrates (lane 2,4 and 6).

One possible reason for this observation can be the 5′-hydroxyl strand displacement occurring after the 3′-end extension by polymerase δ/ε, and removal of the 5′-hydroxyl flap by FEN-1, simulating the long patch BER (Dobson & Allinson, 2006). For the extension of the strand to occurs, there must be a fill-in by dTTP follwed by dCTP and

dGTP in line. Hence to explore the possibility of strand displacement, experiments were done with ddGTP or ddCTP substitution in the reactions. If the strand extension occurs by incorporating one of these dideoxynucleotides at the 3′ end, a block in the ligation should be seen along with increased unjoined fragment length. However, neither of these substitutions resulted in either the ligation block or the extension of the unjoined product (Fig. 8.6 B). Hence, the end-joining must have occurred due to direct conversion of the 5′-hydroxyl end to a 5′-phosphate end by a DNA 3′-phosphatase enzyme, rather than a strand displacement followed by endonuclease (FEN-1) mediated trimming of the displaced strand. These results led us to a second possibility, presence of a non-conventional DNA 5′-kinase.

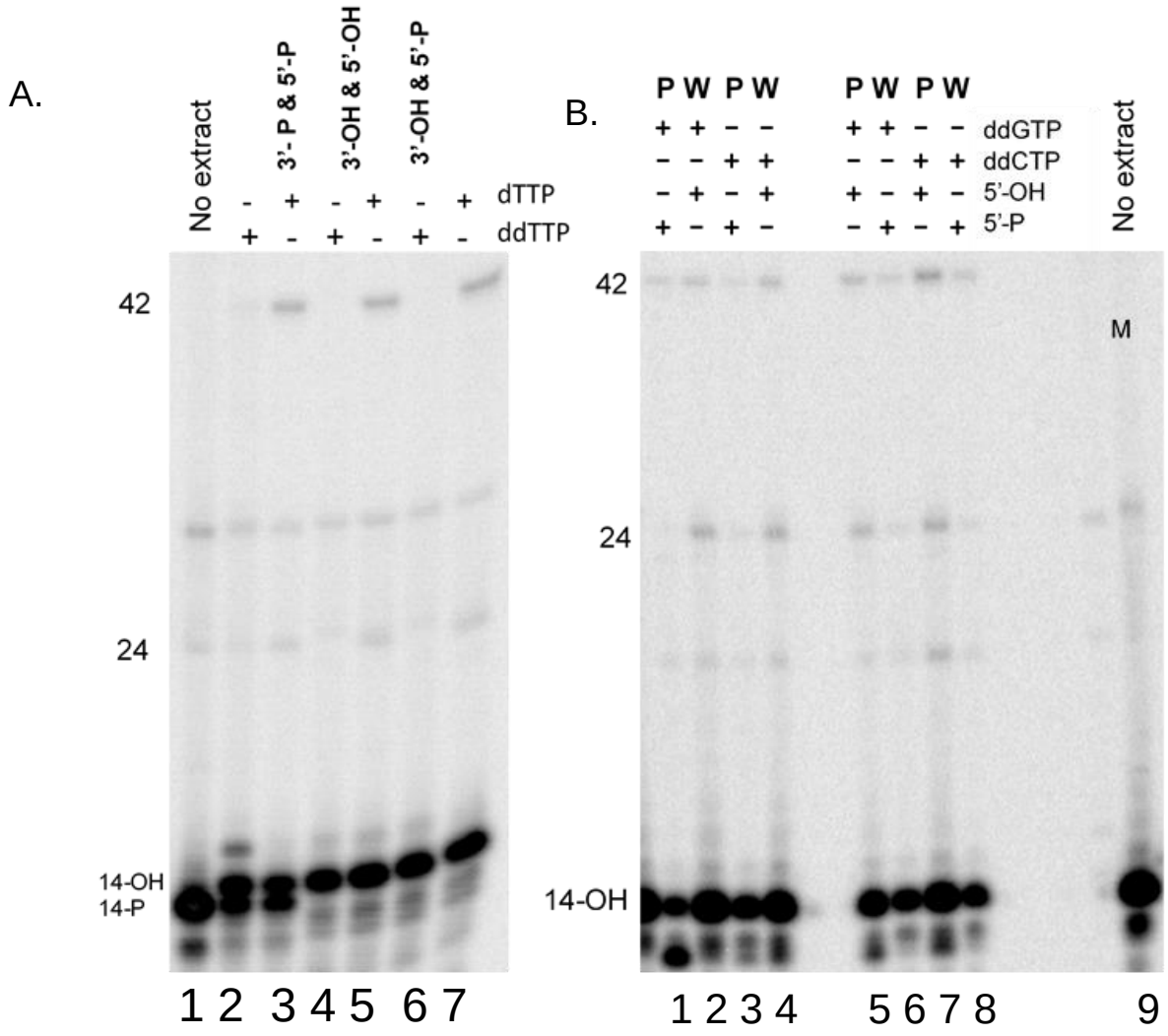

Fig. 8.6: A. Compatibility of the 5′- hydroxyl ends for the end joining: Kinase activity was screened indirectly by assesing the end joining of 3′-hydroxyl and recessed 5′-hydroxyl ends (lane 5) as compared to the end-joining of 3′-hydroxyl and recessed 5′-phosphate ends (lane 7), and 3′-phosphate and recessed 5′-phosphate ends (lane 3), all labeled on the 3′ strands, as a control, in HCT116 PNKP knockout extracts

B. Strand displacement in substrates with 5′-OH end for bypassing the blocked 5′end for strand ligation: Substrates with a 3′-hydroxyl end and either a opposite 5′-hydroxyl (lane 1,3,6 and 8) or a 5′-phosphate end (lane 2,4,5 and 7), were incubated separately in WT or knockout extracts in the presence of ddGTP (lane 1,2 5 and 6) or ddCTP (lane 3,4,7 and 8) instead of the normal counterparts, dGTP and dCTP, which would fill-in succession to dTTP at the 3′-end to initiate strand displacement of the 5′-hydroxyl end. W = HCT116 Wild-type extract, P = HCT116 PNKP knockout extract

8.5 Evaluation of DNA 5′-kinase activity in the extracts:

PNKP enzyme preferentially dephosphorylates 5′-hydroxyl termini within nicked, gapped or DSBs with single-stranded 3′ overhanging ends, compared to single-stranded 5′-termini or blunt double-stranded (Karimi-Busheri & Weinfeld, 1997). Therefore, in this assay, instead of a 3′-end-labeled substrate, a 5′-hydroxyl substrate which was internally labeled on the same strand was tested for the kinase activity in both HCT116 WT and PNKP knockout extracts. As observed in Fig. 8.7 B, incubation of the substrates in the extracts for 6 hours converts the 5′-hydroxyl to a 5′-phosphate, in both extracts albeit to a lesser extent in the knockout extracts. While 34 ± 6.7% of the 5′-hydroxyl ends were converted in WT extracts (lane 4), only 6.9 ± 1.5% were converted in PNKP knockout extracts (lane 5). Pure PNKP (30 ng) (lane 2) and T4PNK (5 U) (lane 3), were used as positive controls. The conversion of 5′-hydroxyl end observed in knockout extracts might be an indication of the presence of residual PNKP or the another yet un-known DNA 5′-kinase, which needs to be explored further.

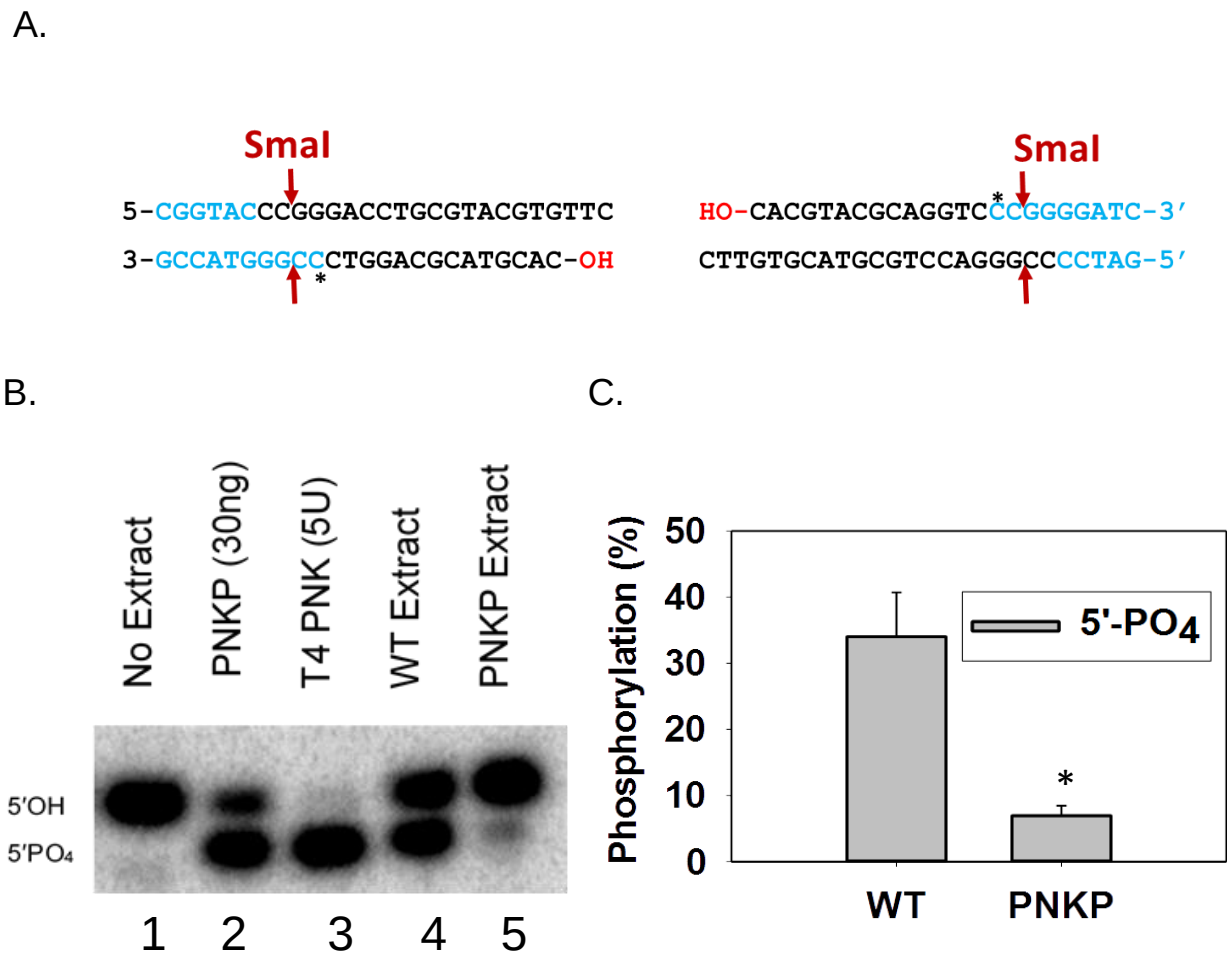

Fig. 8.7: Plasmid DNA DSB's with 5′-hydroxyl end processing: A. Illustration of 5′-hydroxyl ends of the DNA DSB substrate constructed by radiolabeling the XmaI cut 5′ ends of pUC19, on either side and ligating an oligomeric duplex with a recessed 5′-hydroxyl ends. B. These DSB substrates were treated with pure PNKP (lane 2) and T4PNK (lane 3) (1hr), WT (lane 4), and PNKP knockout extracts (lane 5) (6 hr) to observe for the conversion of a 5′-hydroxyl to 5′-phosphate. These processed substrates were cut with SmaI to be run on a gel after proteolysis. C. The percentage of phosphorylation observed at the 5′-hydroxyl ends in HCT116 WT (lane 4) and PNKP knockout extracts (lane 5) were plotted. (***** - $p < 0.05$; Student t-test) (n = 3)

8.6 Evaluating the 3′-phosphatase function observed in the extracts as a function of NHEJ:

PNKP enzyme has the propensity to act on both SSB's and DSB's in multiple repair pathways. Studies have shown that ATM and DNA-PKcs mediate phosphorylation of PNKP at serines 114 and 12 in a damage-dependent manner (Zolner et al., 2011a). This phosphorylation, although it does not influence the kinetics of PNKP accumulation, was shown to increase the turnover of PNKP at the DNA damage sites (Zolner et al., 2011b). It was also shown that the substitution of T4PNK in PNKP-immunodepleted extracts could not restore the end-joining of 5′-hydroxyl substrates implying the inaccessibility of the NHEJ protein-bound DNA to a non-specific kinase (Chappell et al., 2002). Moreover, autophosphorylation of DNA-PK complex (Ku+DNA-PKcs), is required for the internal translocation of the complex at the DSB to provide access to other processing factors to repair/restore the ends for ligation.

This access to to the DSB ends can be blocked by a DNA-PK inhibitor, which will block the autophosphorylation and thus opening up of the DNA-PK complex. In the previous experiments done in the lab with TDP1 protein to prove its role as a NHEJ factor, a DNA-PK inhibitor, NU7441, was used to block the access of the 3′-phosphoglycolate overhanging ends at the DSB's to TDP1 enzyme which processes its removal (T. Zhou et al., 2009). To assess whether the observed 3′-phosphatase activity at the DSBs in the PNKP knockout extracts is a function of NHEJ, NU7441 was used in the reactions.

Both the HCT116 WT and PNKP knockout extracts were pre-incubated with NU7441 for 10 minutes before the addition of the 3′-phosphate substrate. Significant inhibition of the phosphatase activity (Fig. 8.8), WT by 49 ± 15.58% (lane 4) and PNKP-/- by 85 ± 4.8% (lane 8) at 1 μM concentration and by 68 ± 8.1% (WT) (lane 5) and 89 ± 3.78% (PNKP-/-) (lane 9) at 10 μM concentration was seen for the overhang substrate. There was a likewise significant reduction in the removal of the recessed 3′-phosphate with 1 μM NU7441 inhibiting the phosphate removal by 62 ± 1.8% in WT (lane 4) and by 81 ± 0.5% in PNKP-/- extracts (lane 8), while addition of 10 μM NU7441 reduced the removal by 78 ± 2.1% in WT (lane 5) and by 87 ± 0.78% (lane 9) in PNKP-/- extracts.

By comparison, there was a significant decrease in the recessed end processing relative to overhang processing in the presence of NU7441 in WT extracts as seen in the plots of overhang ends and recessed ends (Fig. 8.8), signifying the major role played by PNKP in processing the recessed DNA 3′-phosphate ends, which was shown by a significant reduction in processing of these ends in PNKP knockout extracts (Fig. 8.3). Furthermore, a significant decrease in processing of the ends, even in knockout extracts, suggests that the repair factor is depending on DNA-PK function for processing the ends and hence is a part of NHEJ.

8.7 Accessibility of the 3′-phosphate ends to tissue non-specific alkaline phosphatase enzyme (CIP):

To reaffirm that the unknown DNA 3′-phosphatase in the cell is a part of NHEJ, after 10 min of preincubation of extracts with NU7441, followed by recessed 3′-phosphate substrate incubation for 10 min, 5 units of CIP (a DNA 3′ and 5′-phosphatase) was added to some reactions. CIP was added to the extracts after preincubation with the inhibitor in

order to prevent it robust phosphatase activity on the ends even before the formation of DNA-PK complex.

As evident from Fig. 8.9, in the presence of PNKP in the wild-type extracts, 85% of the 3′-phosphate ends were processed (lane 1), with a reduction in the removal of 3′-phosphate to 39.6% in PNKP knockout extract (lane 2). Addition of CIP did not enhance the phosphate removal in WT extracts (lane 3), while it enhanced the removal in the PNKP knockout extracts to 74% (lane 4). 10 μM NU7441, on the other hand could suppress the phosphatase activity in both WT and PNKP knockout extracts to 31% and 7.4%, respectively (lane 5 and 6).

However, 10 μM NU7441 does not block the 3′-phosphatase activity of CIP, 79% (vs. 85% no drug) in WT (lane 7) and 70% (vs. 74%) in PNKP knockout extract (lane 8), suggesting that DNA-PK inhibition is capable of blocking only the activity only if it is a part of NHEJ, but not the non-specific phosphatase enzyme's activity. While, PNKP and the other 3′-phosphatase enzyme in the PNKP knockout extracts depend on the phosphorylation by DNA-PK for the activity at the DSB, CIP can funtion independantly of the same, suggesting that the alternative enzyme in the knockout extracts is not a non-specific but a NHEJ factor.

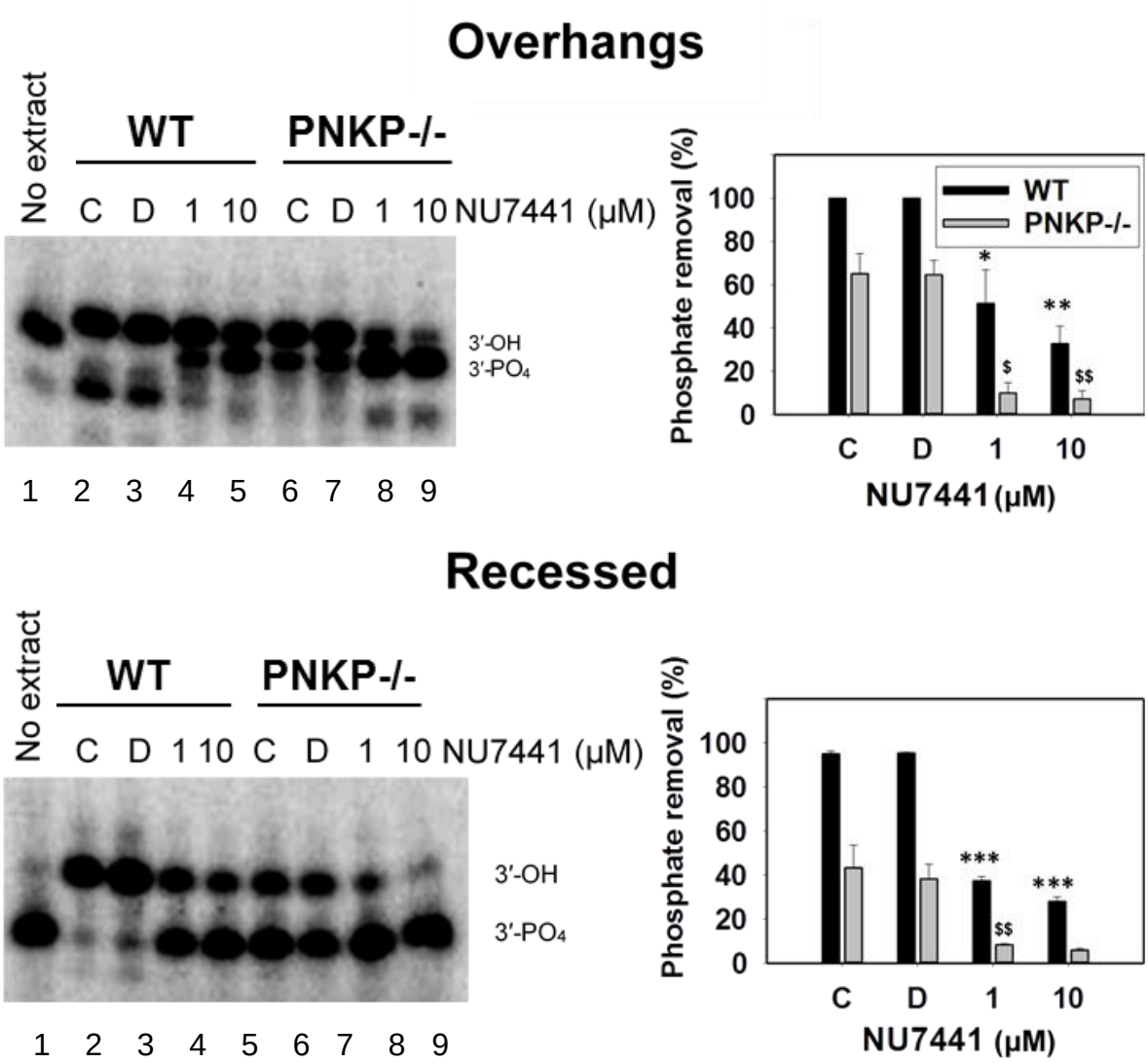

Fig. 8.8: 3′-phosphatase activity as a function of NHEJ: DNA-PKcs inhibitor, NU7441 was used to block the access of the DSB's by the enzymes that processes the 3′-phosphate ends as a part of NHEJ. NU7441 at concentrations 1 μM and 10 μM (lane 4,8, and lane 5,9, respectively) was added to both HCT116 WT and PNKP knockout extracts to test for the inhibition of processing of overhangs (upper panel) and recessed ends (lower panel), with 3′-phosphates at the DSB's. The observed level of phosphatase activity in the extracts was plotted as a percentage of phosphate removal at the mentioned concentrations of the NU7441 along with controls. Inhibition of activity was evident at both drug concentrations (lane 4,8, and lane 5,9) Statistical significance: ***** - WT VS. NU7441 treated WT, **$** - PNKP-/- VS. NU7441 treated PNKP -/- (***** , **$** - p<0.05; ****** ,**$$** - p< 0.005; ******* ,**$$$** - p<0.0005 - One way ANOVA- Dunnett test) (n = 3) (C = No drug/DMSO, D = DMSO).

How

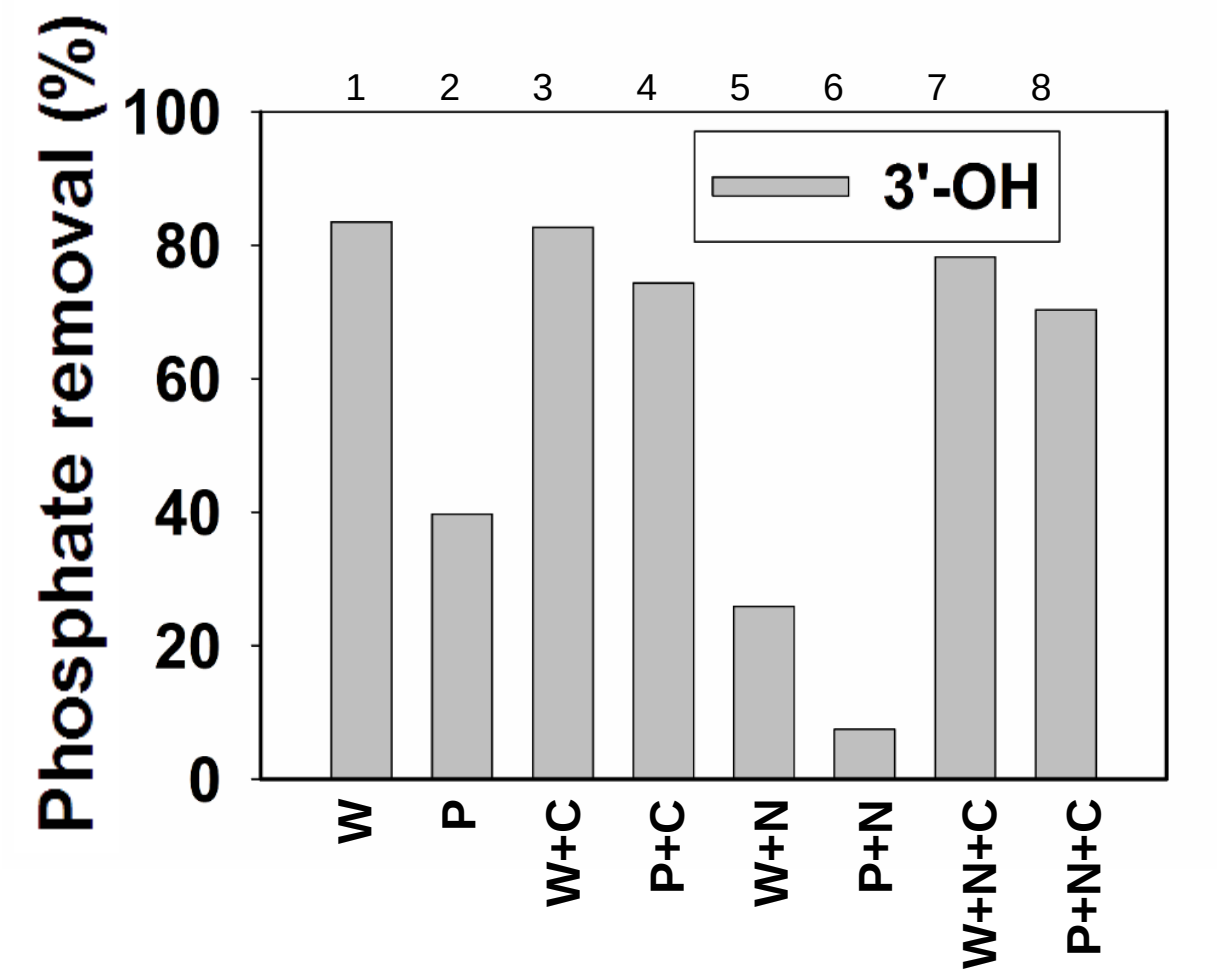

Fig. 8.9: Alkaline phosphatase activity on DNA 3′-phosphate recessed end substrates: DNA 3′-phosphate recessed end substrates were incubated with HCT 116 WT extracts (bar 1) or PNKP knockout extracts (bar 2), some of which were pretreated with 10 μM NU7441 10 min (lane 5,6,7 and 8). CIP was added to some extracts after incubation of the substrate in the NU7441 non-treated (bars 3 and 4) and the treated (bars 7 and 8) extracts after 10 min of the incubation of the substrate. The observed phosphate removal after 6 hr of incubation after addition of CIP, was plotted as a percentage for each reaction. The plot reveals the inability of the DNA-PK inhibitor to block the CIP (non-specific) activity while it is blocking the phosphatase activity in the PNKP knockouts. (W = Wild-Type; P = PNKP-/-; C = CIP; N = NU7441) (n = 1)

8.8 Sub-cellular localization of 3′phosphatase activity:

DNA phosphate ends can also be dephosphorylated by the tissue non-specific alkaline phosphatase enzyme which is membrane-bound mostly in the extracellular and cytoplasmic compartments with minimal expression in the nucleus (Hsiang, Hertzberg, Hecht, & Liu, 1985). However, this activity has no specificity for either 3′ or 5′ ends. PNKP is a nuclear enzyme and is found in small quantities in mitochondria. Depletion of nuclear PNKP with shRNA was shown to deplete mtPNKP (Tahbaz, Subedi, & Weinfeld, 2012). Experiments performed in whole cell extracts revealed a 3′-phosphatase activity even in the absence of PNKP.

To compartmentalize the observed 3′-phosphatase activity in the knockout extracts, nuclear/cytosolic fractionation was made using BioVision kit. Overhang 3′-phosphate substrates were incubated for different times as shown in Fig. 8.10 A. Similar to the whole cell extracts, there was 3′-phosphatase activity (80 ± 0.12%) in the PNKP knockout nuclear extracts after 120 min incubation (Fig. 8.10 A lane 7). This suggests that the suspected DNA 3′- phosphatase enzyme acting at the DSB is present in the nucleus. Also, there was digestion of the DNA seen on incubation of the overhang substrates for 120 min in both the extracts, suggesting possible exonucleolytic digestion of the converted 3′ hydroxyl ends. The digestion of the processed ends is probably due to a lack of protection of these ends which would be present in whole cell extracts.

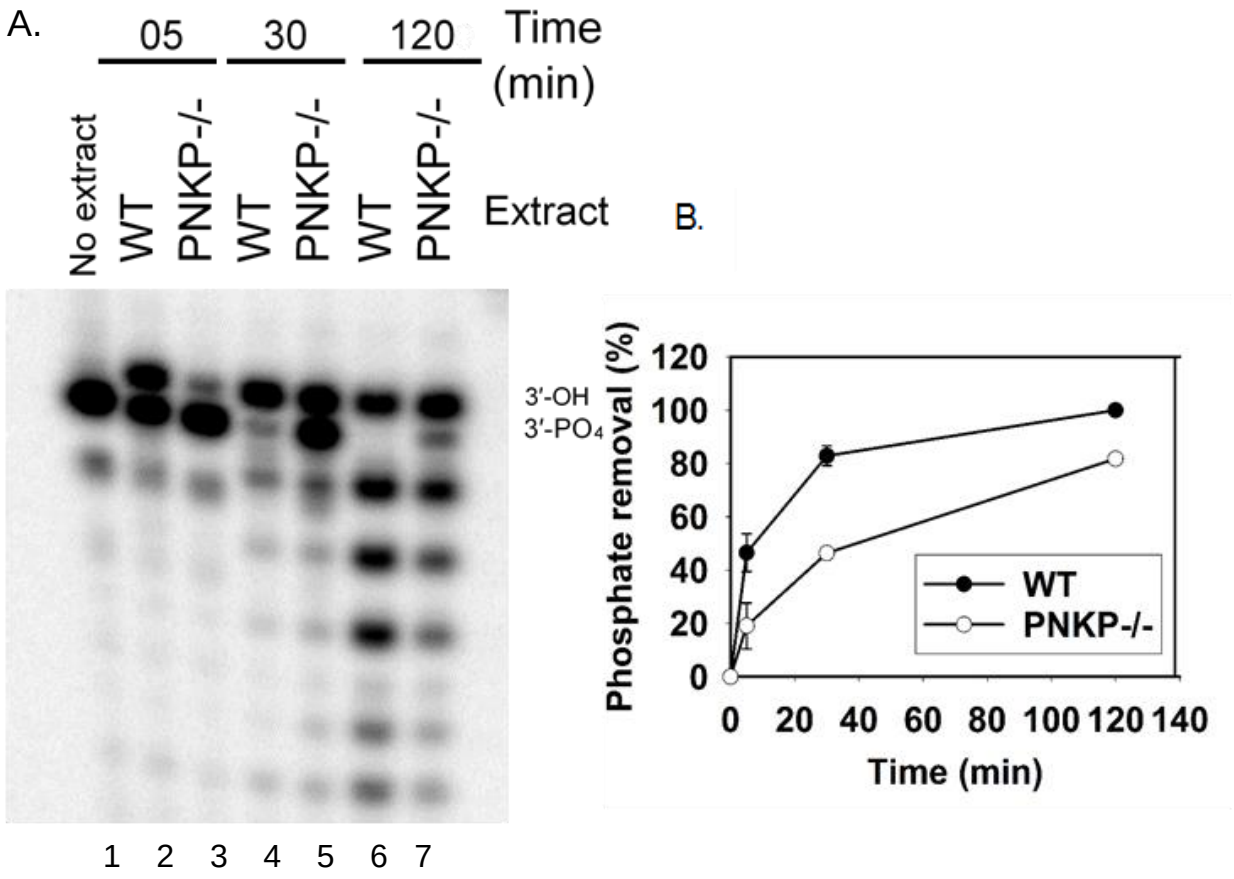

Fig. 8.10: Detection of 3′ phosphatase activity in the nuclear extracts: A. Overhang 3′-phosphate substrates were incubated in the HCT116 WT or PNKP-/- extracts for 5, 30 and 120 min, processed and run on the gel. B. Observed removal of phosphate in both the extracts was plotted as a percentage of time. Phosphatase activity was evident in the PNKP knockout nuclear extracts (lane 3, 5 and 7). (n = 2)

8.9 Assessing the role of XRCC4 in DNA kinase and phosphatase activities:

DNA-PK, a core NHEJ factor was shown to influence the DNA 3′-phosphatase activity in the above experiments. Numerous studies on the role of XRCC4, another core NHEJ factor, interacting with and influencing the function of PNKP, have revealed complex interactions (Aceytuno et al., 2017b) (Chappell et al., 2002) (Mani et al., 2010a). As with the other accessory repair proteins, PNKP also interacts with the scaffold formed by XLF and XRCC4/LigaseIV complex. PNKP interaction with XRCC4 is by dual modes, with phosphorylated (pXRCC4) and non-phosphorylated form (XRCC4) (Fig. 6.1 B). Interacting with XRCC4 or pXRCC4/LigaseIV is shown to increase PNKP turnover at the 5′-hydroxyl ends after phosphorylation, and the lack of XRCC4 has reduce the kinase activity (Mani et al., 2010b). Phosphatase activity of PNKP was shown to be predominant over kinase activity (Dobson & Allinson, 2006). Nevertheless, not much work has been done regarding the effect of XRCC4 on the DNA 3′-phosphatase activity of PNKP.

By adding HCT116 XRCC4 knockout extracts to the DNA 3′-hydroxyl and 5′-phosphate substrates, we attempted to define XRCC4's role in PNKP activity. The observed activity in these extracts was compared to the activity in HCT116 WT extracts (lane 1), HCT116 PNKP knockout extracts (lane 2), and to the activity restored after the addition of pure protein 0.6 µg of XRCC4 (lane 4) or pure 30 ng of PNKP to the XRCC4 knockout extracts. As observed in the Fig. 8.11, the absence of XRCC4 in the extracts has reduced the phosphatase by 47 ± 6.1% and kinase activity by 40 ± 1.4% as compared to the wild-type extracts (lane 3). There was no end-joining observed in either the WT or PNKP knockout extracts since the incubation period was only one hour for 3′-phosphate substrates and due to incompatible ends in 5′-hydroxyl substrates, incubated for 5 hours.

Adding back 0.6 µg XRCC4/LigaseIV protein not only enhanced the 5′-kinase (58 ± 10%) and 3′-phosphatase activities (92 ± 7.4%), but also strongly promoted end-joining for both the substrates (lane 4). This suggests that even at the physiological concentrations of PNKP present in the extracts, it requires XRCC4 for the enhancement of the catalytic activity. Adding 30 ng of pure PNKP, there was an obvious (37 ± 8.3%) increase in the 3′-phosphatase activity (similar to WT) and around 3.8 ± 0.25% increase in the 5′-kinase activity (still somewhat less than WT) in XRCC4-/- extracts (lane 5). This further proves that while the added PNKP can act on the available 3′-phosphate ends, XRCC4 is required to reduce its affinity at the phosphorylated ends, and therefore absence of XRCC4 in the knockouts attenuates the turnover of the added PNKP, limiting the kinase activity. End joining of the non-complementary ends of hydroxyl substrates proves the ability of XRCC4/Ligase IV to promote ligation such ends. And also, since the experiment with both the substrates is performed in parallel using the same extracts, the difference in potency of the DNA 3′-phosphatase activity vs. 5′-kinase activity of PNKP is clearly seen for all the extracts and protein additions. As reported, the phosphatase activity (1 hr incubation) is predominant over kinase activity (5 hr incubation)..

A.

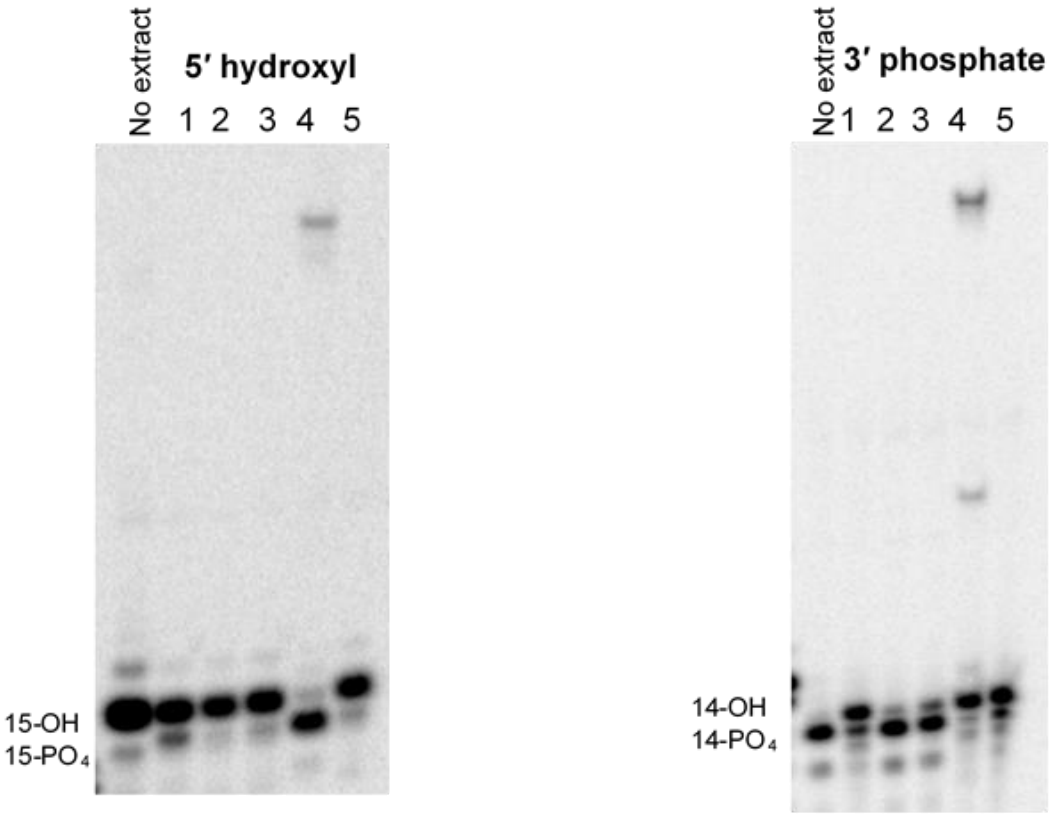

B.

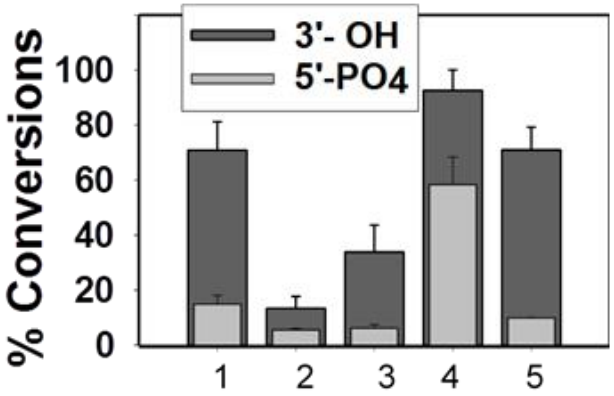

Fig. 8.11: XRCC4/LigaseIV enhances PNKP activity: HCT116 XRCC4 knockout cell extracts were used to assess the DNA 3′-phosphatase (1hr incubation), and 5′-kinase activities (5 hr incubation), using respective substrates. Recombinant proteins, 0.6 µg of XRCC4/LigaseIV and 100 ng of PNKP were added to these extracts, separately. A. Gel images of the products resulting from processing of 3′-phosphate (right panel) and 5′-hydroxyl (left panel) substrates B. Percentage of conversions of each substrate ends is plotted. While the lack of XRCC4 reduced the activities (lane 3), adding back XRCC4 to the knockout increased the activities, and promoted end joining (lane 4), while the added PNKP stimulated phosphatase activity only (lane 5). 1. Wild-type, 2. PNKP knockout, 3. XRCC4 knockout, 4. XRCC4 knockout+recombinant XRCC4, 5. XRCC4 knockout + pure PNKP. (n = 3)

8.10 Role of XLF in processing the 3′-phosphate or 5′-hydroxyl ended DNA DSB's:

Previous studies evaluating the role of XRCC4 in PNKP function have shown either a non-phosphorylated XRCC4 or an XRCC4/LigIV complex, independent of Thr-233 phosphorylation status increases the turnover of PNKP at the 5′-phosphorylated ends of DNA DSB's (Mani et al., 2010). XRCC4 interacts with XLF creating a helical filament of alternating XRCC4 and XLF dimers, thus stabilizing DNA end synapsis (Wu et al., 2011). XLF is shown to promote the re-adenylation of DNA Ligase IV, thus reactivating its active site, independent of its interaction with XRCC4 (Roy et al., 2015).

Based on this evidence, an attempt was made to study XLF's role in phosphatase and kinase activities in Bustel fibroblast extracts (deficient in XLF). 3′-phosphate DNA DSB substrates and 5′-hydroxyl DNA DSB substrates were employed to evaluate the phosphatase and kinase activities respectively. Upon incubation for 6 hr in Bus extracts with and without complementation of XLF, an increase in the kinase activity by 30.7 ± 3.2% was observed on XLF substitution (Fig. 8.12 lane 9) with no discernable change in phosphatase activity on both overhang (lane 2 and 3) and recessed 3′-phosphate substrates (lane 5 and 6), suggesting a possible influence of XLF in processing the 5′-hydroxyl at DSB's by PNKP, by increasing its turnover similar to XRCC4. End joining of phosphate substrates has occurred in the presence of XLF (lane 3 and 6), which could not occur in its absence (lane 2 and 5), reinstating the requirement of XLF for the ligation of a DSB, especially in extracts. However, owing to the non-complementarity of the ends, there was no end joining of 5′-hydroxyl substrates.

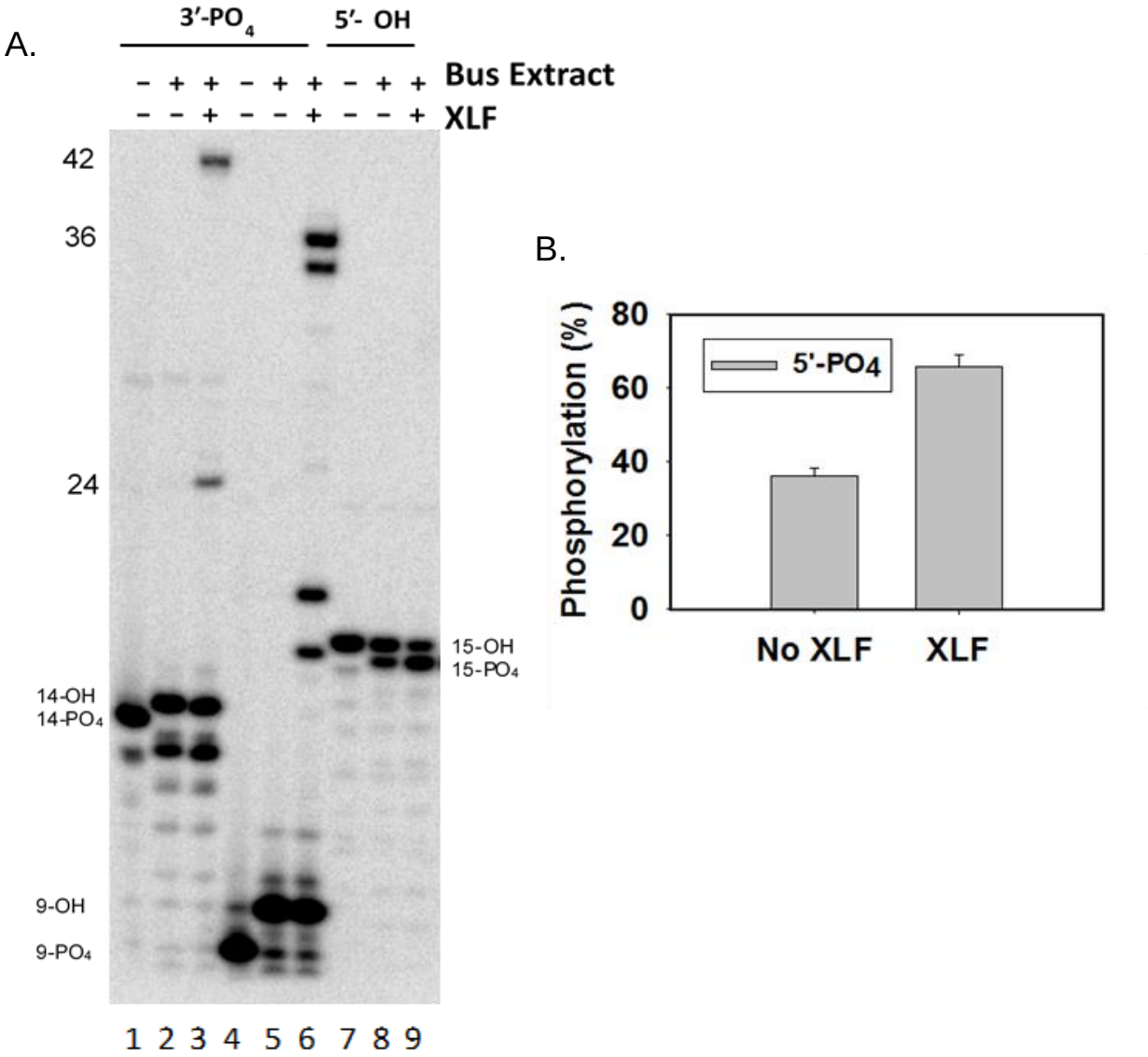

Fig. 8.12: Effect of XLF on the phosphatase and kinase activity: Substrates with 3′-phosphate (overhang (lane 1,2 and 3) or recessed (lane 4,5 and 6)) or 5′-hydroxyl ends (lane 7,8 and 9, at the DSB's were incubated in Bus extract with (lane 3,6,9)/without XLF(lane 2,5 and 8) for 6 hr, and the phosphatase and kinase activities were assessed by measuring the conversion of the 3′-phosphate ends to 3′-hydroxyl ends and 5′-hydroxyl ends to 5′-phosphate ends. B. The observed kinase activity in the presence and absence of XLF was plotted as percentage. As observed on the gel there was no difference in the presence and of XLF in phosphatatase activity (lane 2 vs. lane 3 and lane 5 vs. lane 6). However, kinase activity was stimulated by PNKP (lane 8 vs. lane9). There was promotion of end joining for both the 3′-phosphate substrates (lanes 3 and 6). (n = 3)

Results from all the above experiments led to two speculations. One possibility is that there could be either residual PNKP due to insufficient knockout or the presence of an isoform of PNKP. Literature reveals that there is another isoform of PNKP which is 40 amino acids shorter at the aminoterminal FHA region where the first 1-50 aminoacids MGEVEAPGRLWLESPPGGAPPIFLPSDGQALVLGRGPLTQVTDRKCSRTQ are replaced by MQILTPPLQSS (GCID:GC19M049861). However, CRISPR mediated targetting of Exon3 would knock out both the isoforms. The other possibility is the presence of alternative DNA 3′-phosphatases and 5′-kinases.

8.11 Detection of PNKP by Western Blot using alternative antibodies:

The only confirmation to this point regarding the knockout status of the HCT116 cells is the western blot analysis done by using a mouse monoclonal antibody targeting an epitope of aa 1-140 of PNKP which detects the FHA domain of PNKP. PNKP interacts with XRCC4 via the FHA domain (pXRCC4) and the catalytic domain (XRCC4) at the DSBs (Mani et al., 2010b). Lack of detection of the FHA domain leaves a possible presence of catalytic domain (phosphatase and kinase) which might be responsible for the observed activity in the extracts.

Western blot experiments were repeated using Rabbit anti-PNKP polyclonal antibody (full-length epitope) and a mouse anti-PNKP monoclonal antibody which detects C-terminal aa 379-411, for verifying the presence or absence of the catalytic domain of PNKP (Fig. 8.13 A and B). Surprisingly, there was a band detection with both the antibodies (Fig. 8.13 lane 5 (left and right panels)). For PNKP knockout in these cells, CRISPR was targeted Exon 3 (Appendix II), resulting in deletion and rearrangement in Allele 1 and an in-frame insertion and two site mutation in Allele 2. While the first allele

targetting should eliminate the expression of the protein, the insertion in the second allele targetting appeared to allow for expression of a full-length protein. However, the observed band (lane 5, right panel) appeared slightly lower in the gel than the full-length protein, which is not consistent with an in-frame insertion. This observation suggests a possible presence of a truncated PNKP, although its contribution to the activity seen in the knockout extracts requires further elucidation.

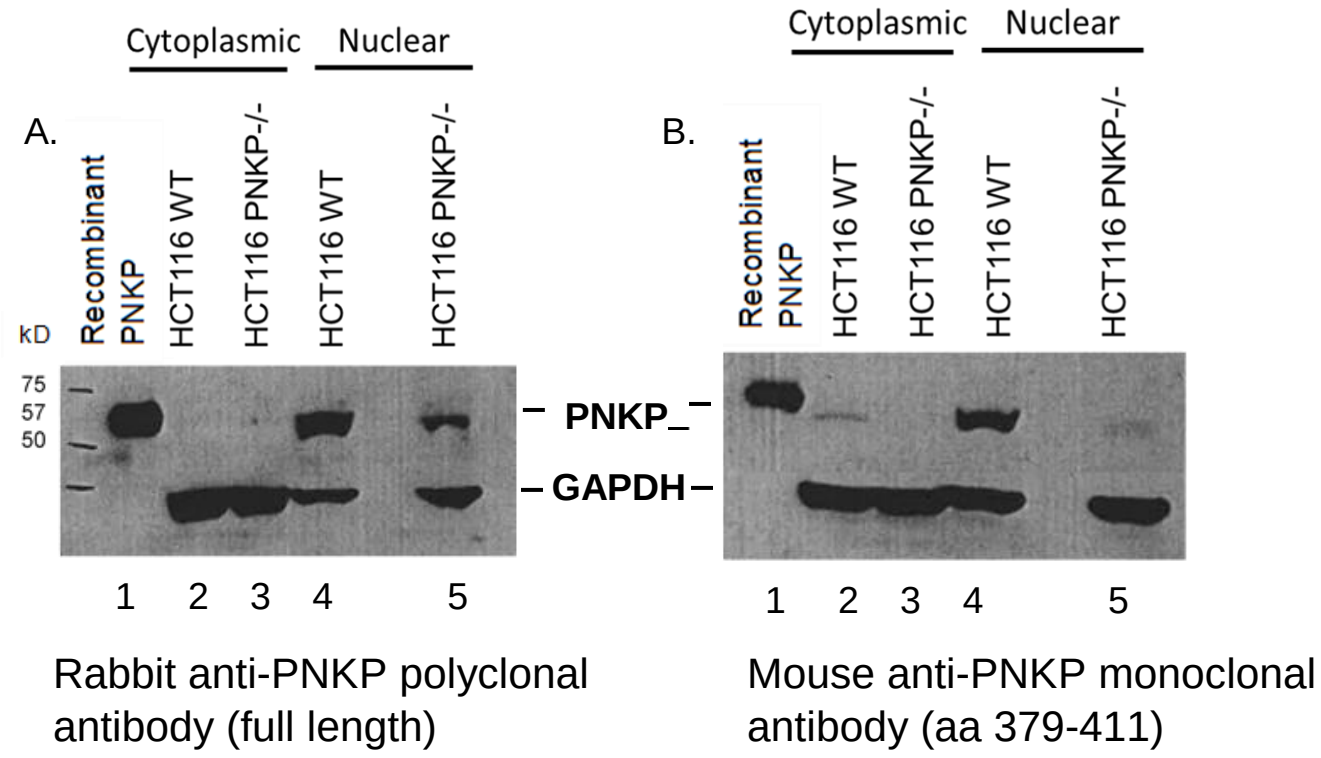

Fig. 8.13: PNKP detection in the knockout extracts by Western blot: HCT116 WT and PNKP knockout cytoplasmic and nuclear extracts extracts (50 µg) were resolved on 10% SDS-PAGE. After transfer to 0.45 µm nitrocellulose the blotted bands were immunodetected with either a rabbit anti-PNKP polyclonal antibody (whole protein epitope) (A) and mouse anti-PNKP monoclonal antibody (Mab) (aa 379-411 epitope) (B) and subsequently visualized with peroxidase labeled rabbit anti-rabbit IgG (A) or anti-mouse IgG (B) antibodies. Band detected in the WT nuclear extracts (lane 4) is migrating with the recombinant protein (lane 1). There is a band detected in lane 5 (PNKP knockout nuclear) of both the blots with the band in the right panel running faster than the WT. GAPDH was used as a loading control. For both the blots, Lane1: Recombinant hPNKP, Lane 2: HCT116 WT cytoplasmic extract, Lane 3: HCT116 PNKP knockout cytoplasmic extract, Lane 4: HCT116 WT nuclear extract, Lane 5: HCT116 PNKP knockout nuclear extract, kD: kilo Dalton – molecular weight of the protein.

8.12 Dilutional analysis of the detected PNKP:

The appearance of this band was not be predicted by DNA sequencing of the knockout but could not be attributed to the PNKP isoform which is approximately 4 kD less than the conventional PNKP. We quantified the band detected in knockout extracts as a fraction of that detected in wild-type extracts by the mouse Mab.

Starting with 2 mg/ml, priteins contained in increasing dilutions of HCT116 wild-type nuclear extracts were resolved on AnyKD gel along with the 2 mg/ml of PNKP knockout nuclear extract. The sensitivity of detection of PNKP was increased by using SuperSignal™ Western Blot Enhancer kit. After transfer to 0.45 µm nitrocellulose membrane, the blot was incubated with antigen pretreatment solution for 10 min before blocking, followed by incubation with the mouse Mab (aa 379-411) in the primary antibody diluent provided in the kit. These blot treatments resulted in a clear enhancement of the bands with less background. The intensity of the bands detected on the blots was measured using ImageJ software. As seen in the Fig. 8.14, the band detected in PNKP knockout extract appeared to be running as a doublet (lane 8). When quantified and interpolated to the dilutions of the HCT116 WT nuclear extracts on a log scale; it was found to be approximately $1/13^{th}$ of the level found in WT nuclear extracts.

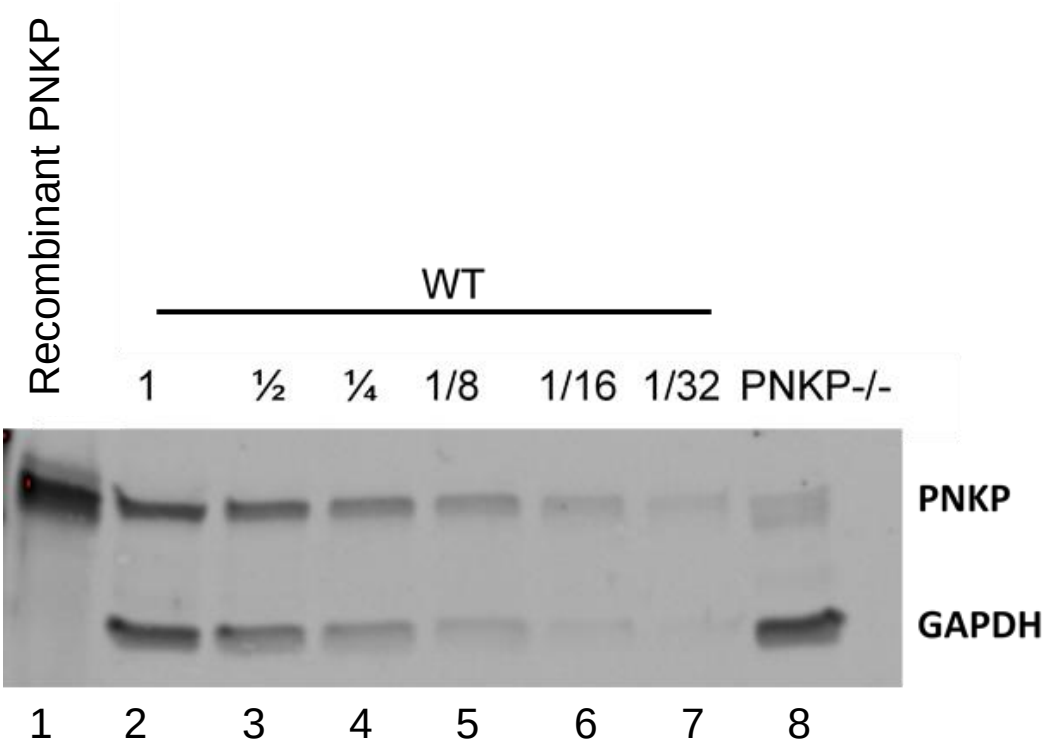

Fig. 8.14: Dilutional analysis of PNKP in the knockout nuclear extracts: Increasing dilutions of the HCT116 WT nuclear extract (Lanes 2 to 7) along with the PNKP knockout extract (lane 8) were resolved on AnyKD gel, transferred on to to 0.45 µm nitrocellulose membrane was treated with SuperSignal™ antigen pretreatment solution for 10 min before being blocked. The mouse anti-PNKP Mab (aa 379-411), was diluted in the SuperSignal™ primary antibody diluent for overnight incubation of the blot which was subsequently visualized with peroxidase labeled anti-mouse IgG. Image J software was used to quantify the band intensities which were plotted to derive the intensity of the band detected in the PNKP knoctouts as a fraction of WT intensities. GAPDH was used as a loading control. The band detected in lane 8 (PNKP knockout) appears to be running like a doublet and its intensity was approximately 1/13th of the WT undiluted extract. Lane 1: Recombinant PNKP, Lane 2-7: Increasing dilutions of HCT116 WT nuclear extract, Lane 8: HCT116 PNKP knockout nuclear extract.

8.13 Western blots on HeLa extracts:

Due to the possibility of the band detected by PNKP antibody in the HCT116 PNKP knockouts to be functional PNKP, we have also obtained HeLa PNKP Knockout cells from Dr. Weinfeld along with CRISPR controls to repeat the phosphatase and kinase assays. The gene sequencing data (Appendix II) and the western blot provided by his laboratory suggested a clean knockout of all the three allelles of PNKP. Western blot analysis of the cytoplasmic and nuclear extracts of the cells was done using the rabbit anti-PNKP polyclonal antibody (full-length epitope) and a mouse anti-PNKP Mab (379-411).

As shown in the Fig. 8.15, after probing with peroxidase tagged specific secondary antibodies, there was a faint band (lane 5) detected with the polyclonal antibody after 5 min exposure, without any band detection mouse monoclonal antibody (lane 5) even after 30 min exposure to X-ray screen. This lack of band detection suggested a clean knockout of PNKP in the HeLa extracts. These extracts were used to corroborate the findings obtained for processing the 3′-phosphate and 5′-hydroxyl ends in HCT116 PNKP knockout extracts.

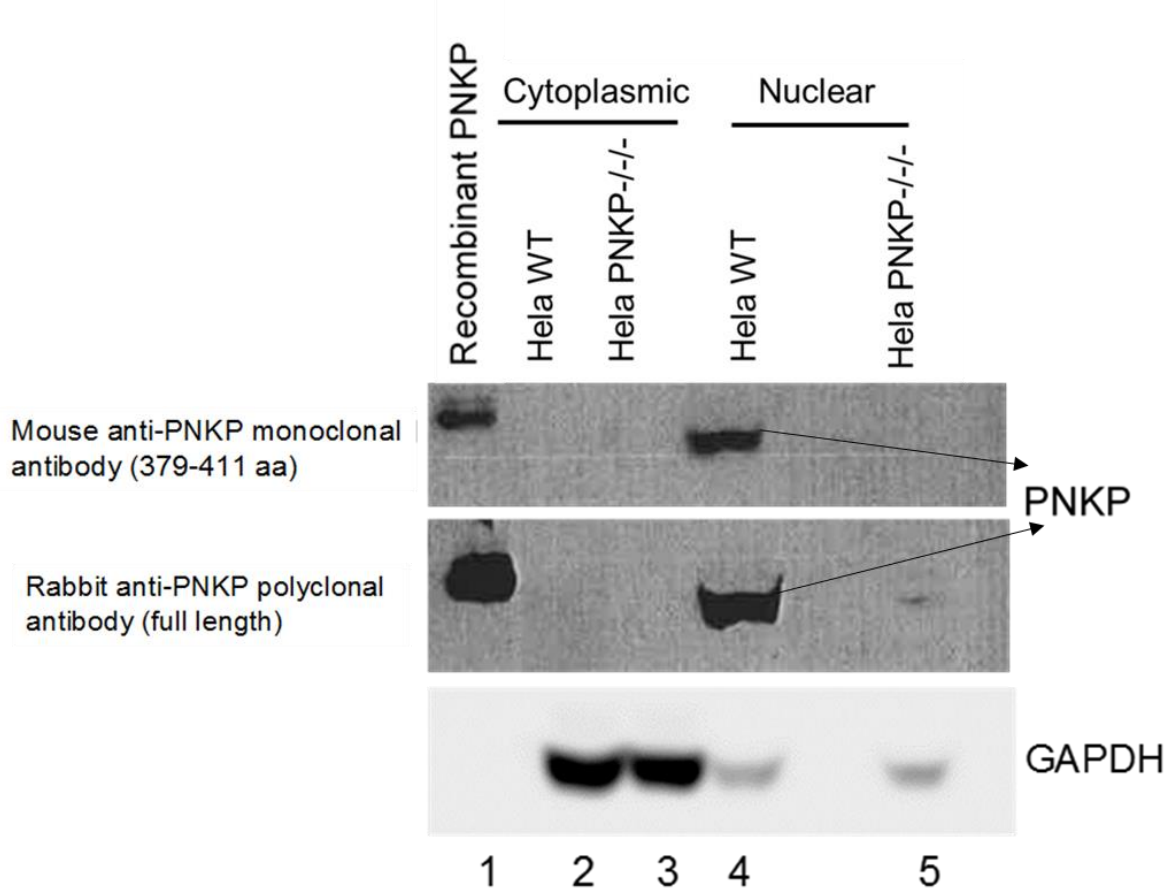

Fig. 8.15: PNKP knockout status verification on Western blot: HeLa WT and PNKP knockout extracts were resolved on 10% SDS-PAGE and transferred on to to 0.45 µm nitrocellulose membrane, which was treated with mouse anti-PNKP Mab targeting aa 379-411 (top panel), rabbit anti-PNKP antibody (full-length) (middle panel) and detected with peroxidase labeled specific secondary IgG. While the lane 5 in the top panel was clean even after 30 min exposure, a faint band was detected anti-rabbit secondary (lane 5) after 5 min exposure to X-ray. GAPDH control was detected with Alexa Flour 680 labeled anti-mouse IgG (bottom panel).

8.14 Experiments in HeLa Extracts:

To substantiate the findings made in the HCT116 knockout extracts and to rule out that the band detected in the HCT116 PNKP knockout extracts (Fig. 8.13 lane 5 (right panel) and Fig. 8.14 lane 7) is contributing to the activity seen in those extracts, HeLa PNKP knockout extracts which were confirmed to lack any PNKP by the same antibodies that detected its presence in HCT116 knockouts, were used to study the DNA 3′-phosphatase and 5′-kinase activities. As with the above experiments in HCT116 extracts, the 3′ –phosphate and 5′-hydroxyl substrates were incubated in the wild-type and PNKP knockout whole cell extracts for various times.

These experiments have revealed similar processing of the 3′-phosphate recessed end, WT- 88.27 ± 1.68% vs. PNKP-/- - 33.0 ± 1.85%, with the retention of some 3′-phosphate even in wild-type extracts (Fig. 8.17), as in HCT116 extracts (Fig. 8.3). Moreover, 53.3 ± 11.2% of 3′-phosphate was removed from the 3′ overhang substrates in the HeLa PNKP knockout extracts with complete removal in the WT (Fig. 8.16). Also, DNA-PK inhibitor NU7441 blocked the removal of 3′-phosphate in both WT and PNKP knockout extracts, for either substrate. 1 μM NU7441 reduced the phosphate removal from the overhang substrate by 49% in WT and 56% PNKP-/- extracts from the overhang substrate (Fig. 8.16 lane 3 and 6), while 10 μM reduced 68% in WT and 57.1% in PNKP-/- extracts (Fig. 8.16 lane 4 and 7).

On the other hand, 1 μM NU7441 reduced the phosphate removal by 48.6 ± 2.4% in WT and 35 ± 0.8% in PNKP -/- (Fig. 8.17 lane 4 and 8), and 10 μM reduced it by

68 ± 1.71% in WT and 38.4 ± 0.44% in PNKP-/-, from the recessed substrate (Fig. 8.17 lane 5 and 9).Total Inhibition in the HeLa WT extracts was lower than HCT116 extracts due to the increased activity of PNKP owing to the presence of more amount of PNKP in the extracts as detected in the Western blot analysis of 50 µg of WT extracts.

In addition, when assesed for DNA 5′-kinase activity in HeLa PNKP knockout extracts, 9.6 ± 1.91% (Fig. 8.18 lane 5) of the 5′ phosphate ends were formed compared to 44.5 ± 1.1% (lane 4) in the wild-type extracts after 4 hr incubation. DNA 3′-phosphatase activity was found in the nuclear fraction of both the WT and knockout extracts with the total removal and digestion of the substrate in WT extract and retention of 78 ± 0.34% (Fig. 8.19 lane 7) of the 3′-phosphate in the knockout extracts with little obvious digestion of the substrate.

Since the above results of phosphatase assay (Fig. 8.16 and 8.17) and of kinase assay (Fig. 8.18) have shown processing very similar to that of processing occuring in HCT116 PNKP knockout extracts, it is likely though not certain that 3′-phosphatase and 5′-kinase activities in the HCT116 PNKP knockout extracts is also due to alternative 3′-phosphatases and 5′-kinases, rather than to the minute amount of the truncated PNKP detected in that extract by Western blot. DNA-PK inhibition (Fig. 8.16 and 8.17 B,D), suggest the phosphatase activity found in the knockouts to be a part of NHEJ similar to HCT116 knockout extracts (Fig. 8.8). However, there is a wide disparity detected in the 3′-phosphatase activity between HCT116 and HeLa nuclear extracts. While 80 ± 0.12% (Fig. 8.10) 3′-phosphate ends were processed in HCT116 extracts, only 22 ± 0.34% (Fig. 8.19) 3′-phosphate ends were processed in HeLa. On the whole, these observations suggest the presence of alternatives to the enzyme PNKP.

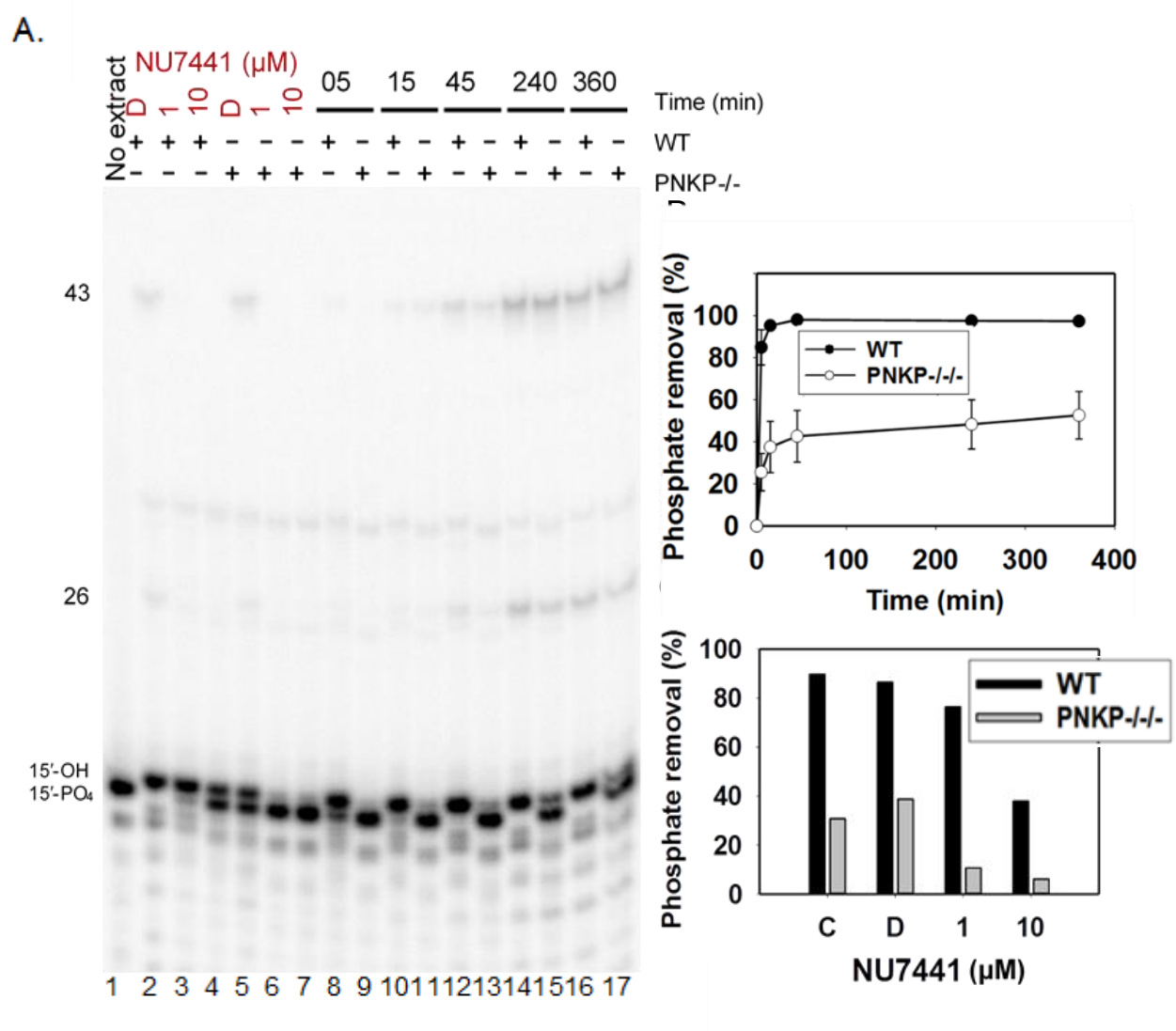

Fig. 8.16: Effect of PNKP knockout on processing the 3′-phosphate ends of overhangs at the DSB's and susceptibility to DNA-PKcs inhibition: A. Internally radio-labeled 3′-phosphate ended overhang substrate was incubated in HeLa WT, and PNKP-/-/- extracts for different times as indicated, was proteolyzed and cut with BstXI and AvaI and run on a gel. B and C. Percentage of phosphate removal as a function of time was measured and plotted for both the extracts. For samples with DNA-PKcs inhibitor NU7441 (lane 3,4,6 and 7), the extracts were incubated with NU7441 for 10 min before the addition of substrate, then incubated for additional 4 hours. Released bands are one base longer than those for TaqαI cut DNA. There was a reduction in total processing in the knockouts (lane 17) compared to WT (lane 16). Presence of NU7441 inhibited the 3′-

phosphatase activity, including in the knockouts (lane 3,4,6 and 7) (C = No DMSO/Drug, D = DMSO control) (B. n = 3, C. n = 1)

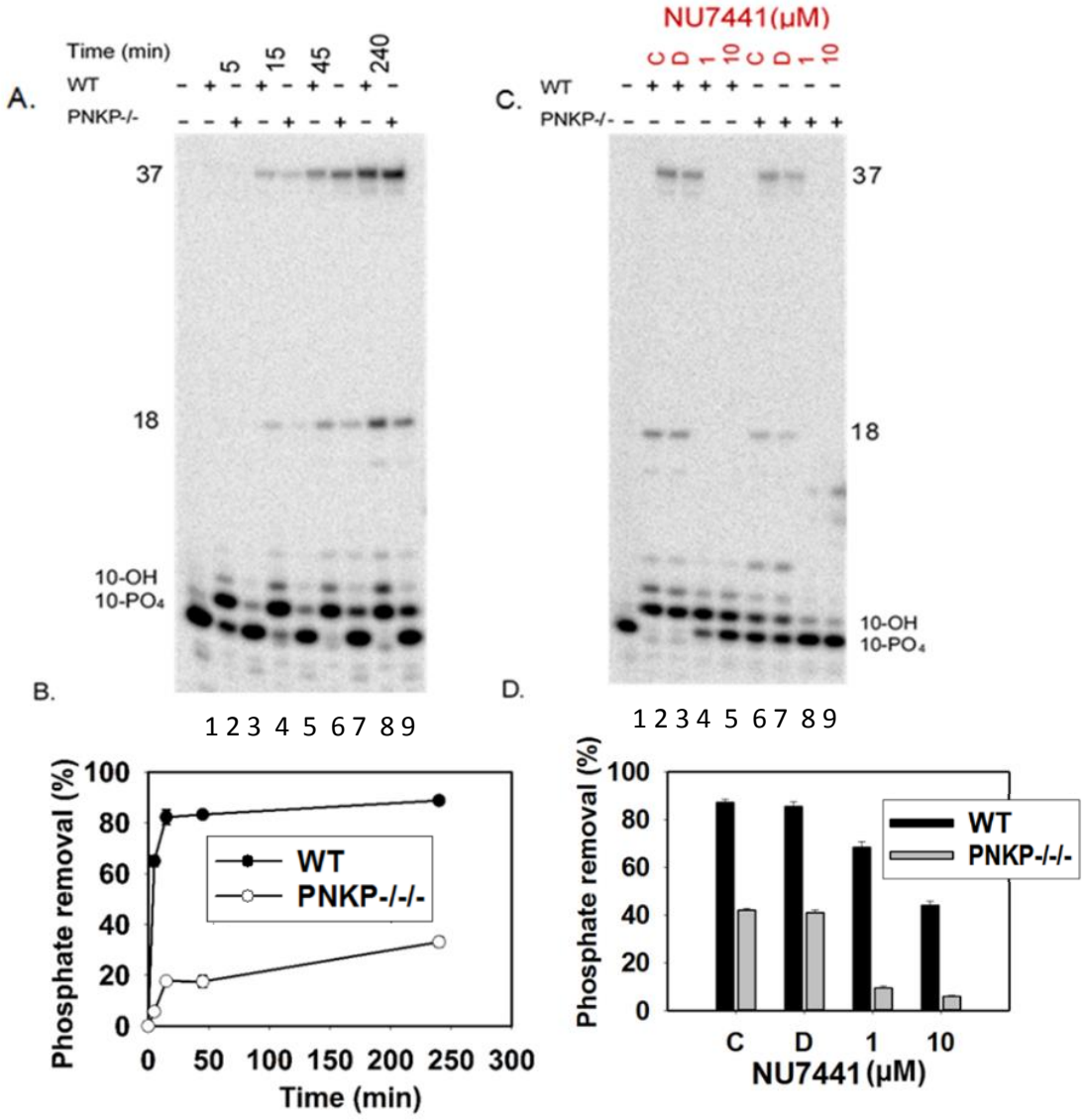

Fig. 8.17: Effect of PNKP knockout on processing the 3′-phosphate ends of recessed end at the DSB's and susceptibility to DNA-PKcs inhibition: A) Internally radio-labeled 3′ strand with a 3′-phosphate at the recessed end was incubated in HeLa WT and PNKP-/-/- extracts for different times as indicated, then were processed similar to overhang substrates and run on a gel. B. Percentage of phosphate removal as a function of time was measured and plotted for both the extracts. C. For samples with DNA-PKcs inhibitor (NU7441), the extracts were incubated with NU7441 (lane 4,5,8 and 9) for 10 min before the addition of substrate, which were then incubated for 4 hours and

the observations were plotted (D). 3′-phosphate processing was incomplete in knockout extracts (A. lane 9) compared to the wild-type extracts (A. lane 8). NU7441 inhibited the3′-phosphatase activity in both the extracts (B. lane 4,5,8 and 9). (C = No DMSO/Drug, D = DMSO control) (n = 2)

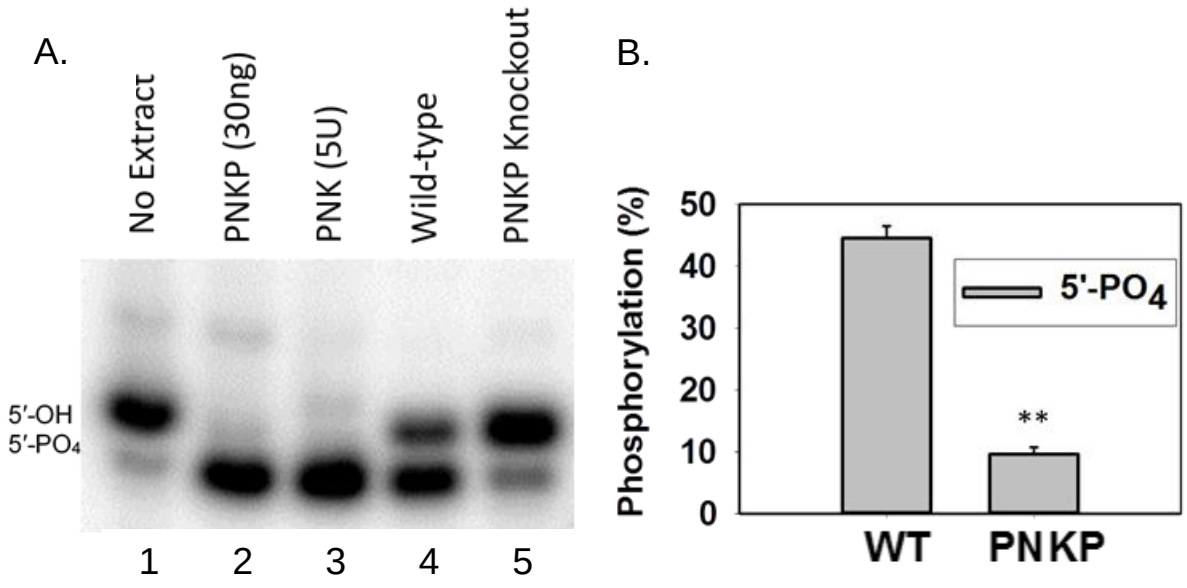

Fig. 8.18: Effect of PNKP knockout on the kinase activity on 5′-hydroxyl substrates: Substrates with 5′-hydroxyl substrates labeled on the 5′-strand, were incubated with the pure PNKP (lane 2) and T4PNK (lane 3) for 1hr , HeLa WT (lane 4) and PNKP-/- (lane 5) extracts for 4 hr, proteolyzed, cut with SmaI and run on a gel. A. Gel picture of the migrating 5′-OH (above) and 5′-PO_4 (below) at all treatments. B. The formation of 5′-phosphate was measured as a percentage and plotted for the extracts (lane 4 and 5).

(****** - $p < 0.005$; Student t test) (n = 3)

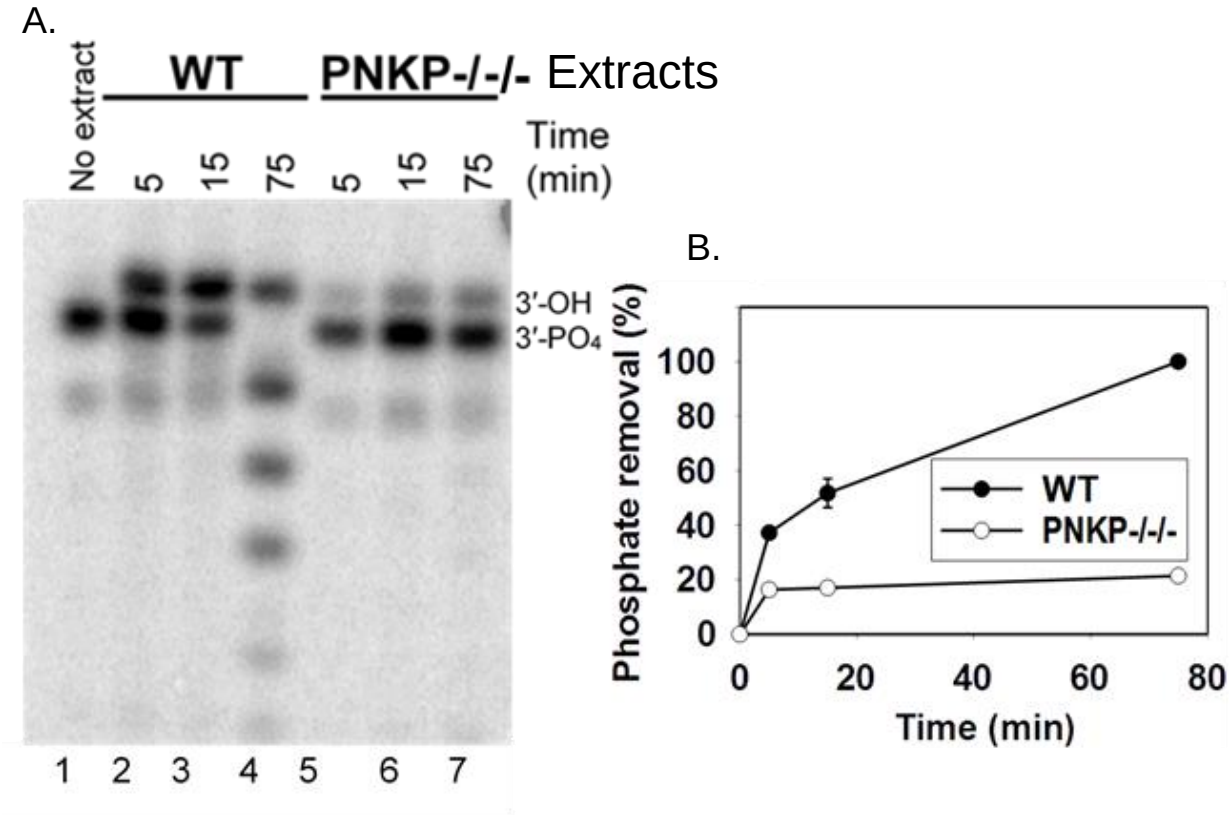

Fig. 8.19: 3′-phosphatase activity in HeLa Nuclear extracts: 3′-phosphate overhang substrate was incubated in the WT (lane 2,3 and 4) and PNKP knockout (lane 5,6 and 7) nuclear extracts made by nuclear/cytoplasmic fractionation, for the indicated times, proteolyzed, cut with AvaI and was run on a 20% gel (A). Observed phosphate removal was plotted as a percentage for both WT and PNKP knockout extracts. Reduction of the removal of 3′-phosphate from the knockout extracts can be clearly depicted from the gel (lane 7) compared to WT (lane 4) and from the plot (B).

8.15 Pharmacological inhibition of DNA 3′-phosphatase activity:

To test whether the 3′-phosphatase activity was attributable to the suspected residual PNKP protein detected by western blot in PNKP knockout extracts, PNKP inhibitor, ST042146, was used to pharmacologically inhibit the phosphatase activity of the PNKP, and thereby reveal the activity of any other DNA 3′-phosphatase acting in the context of NHEJ.

To evaluate the PNKP inhibition, 100 ng of recombinant PNKP was preincubated for 10 min with different concentrations ST042164 dissolved in DMSO, before adding the 3′-phosphate overhang substrate. As seen from Fig. 8.20, after 1 hr of incubation DMSO appears to significantly inhibit the phosphatase activity (lane 3), increasing the fraction of 3′-phosphate remaining from essentially zero to 33% . However, ST042164 was seen to increasingly inhibit the activity of the enzyme with increasing concentrations (lane 4-6). 50 μM concentration of the drug was shown to inhibit most (3.9%, lane 6) of the 3′-phosphatase activity.

Since we observed no inhibition on DNA 3′-phosphatase in the whole cell extracts even at higher concentrations (200 μM) of ST042164, we tried to simulate the conditions in which the drug was shown to be effective during its characterization. The extracts were diluted (1:125) in a storage buffer similar to the one in which PNKP was stored and the phosphatase buffer was used in the reaction (as described in Methods 7.10), to assess inhibition of 3′-phosphatase activity in the extracts. After 10 min of preincubation in the extracts, the 3′-phosphate overhang substrate was added to the

diluted extracts. At concentrations of 20μM and 50μM of ST042164, there was a 48 ± 1.1% and 56 ± 0.72% of reduction in the DNA 3′-phosphatase activity in the diluted HCT116 WT extracts after 1 hr incubation (Fig. 8.21 lane 4 and 5), but only about 12.5 ± 2.3% reduction of the activity in the diluted HCT116 PNKP knockout extracts at both concentrations of the drug even after 3 hr incubation (Fig. 8.21 lane 8 and 9). The inability of the drug to curb the phosphatase activity in the PNKP knockout extracts propones the activity of another factor with a similar function to PNKP, at least the 3′ phosphatase. Also, the presence of the drug inhibited the digestion of the substrate in both extracts, suggesting a lower conversion to 3′-hydroxyl ends, which are better substrates for the exonucleases. Experiments repeated with diluted HeLa extracts gave similar results with the drug highly inhibiting the phosphatase activity in WT extracts but not in the PNKP knockout extracts.

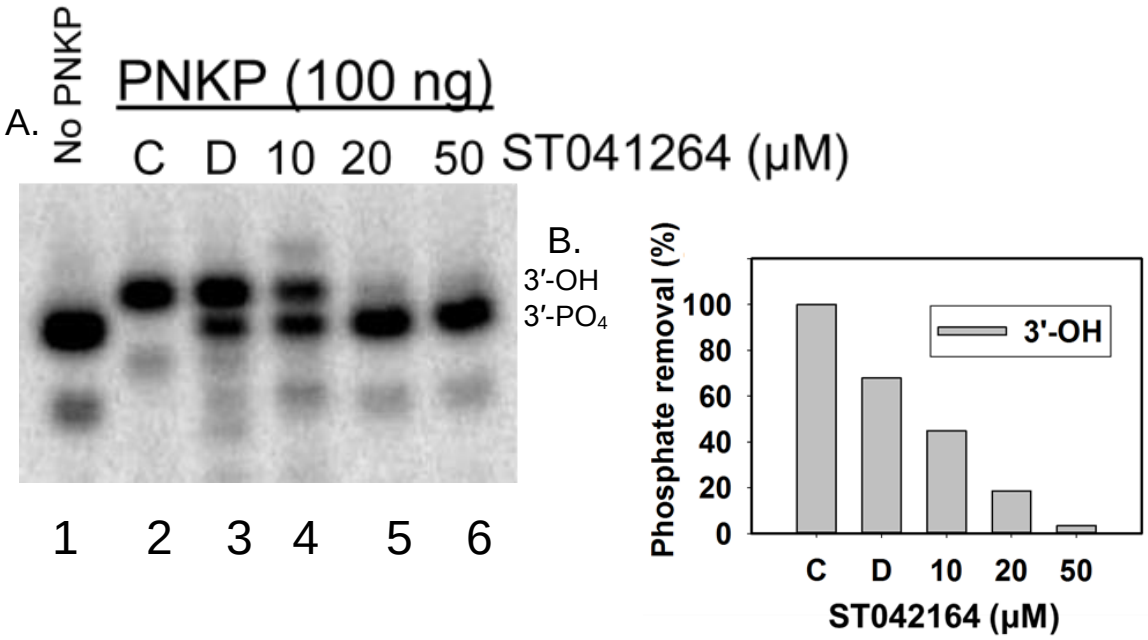

Fig. 8.20: ST042164-mediated inhibition of DNA 3′-phosphatase activity of recombinant PNKP: A. Recombinant PNKP (100 ng) was pretreated in the reactions with either DMSO (lane 3) or different concentrations of the inhibitor ST042164 (lanes 4-6), before adding the 3′-phosphate overhang substrate to the reactions. After adding the substrate, these reactions were further incubated for 1 hr**.** The reactions were deproteinized, then DNA was cut with AvaI and the products were run on a gel. B. Percentage of phosphate removal by PNKP was plotted for different reactions. As seen from the gel and the plot there was nearly complete inhibition of phosphate removal from the 3′-phosphate ends by ST042164. (C = No drug/DMSO control, D = DMSO control) (n = 1)

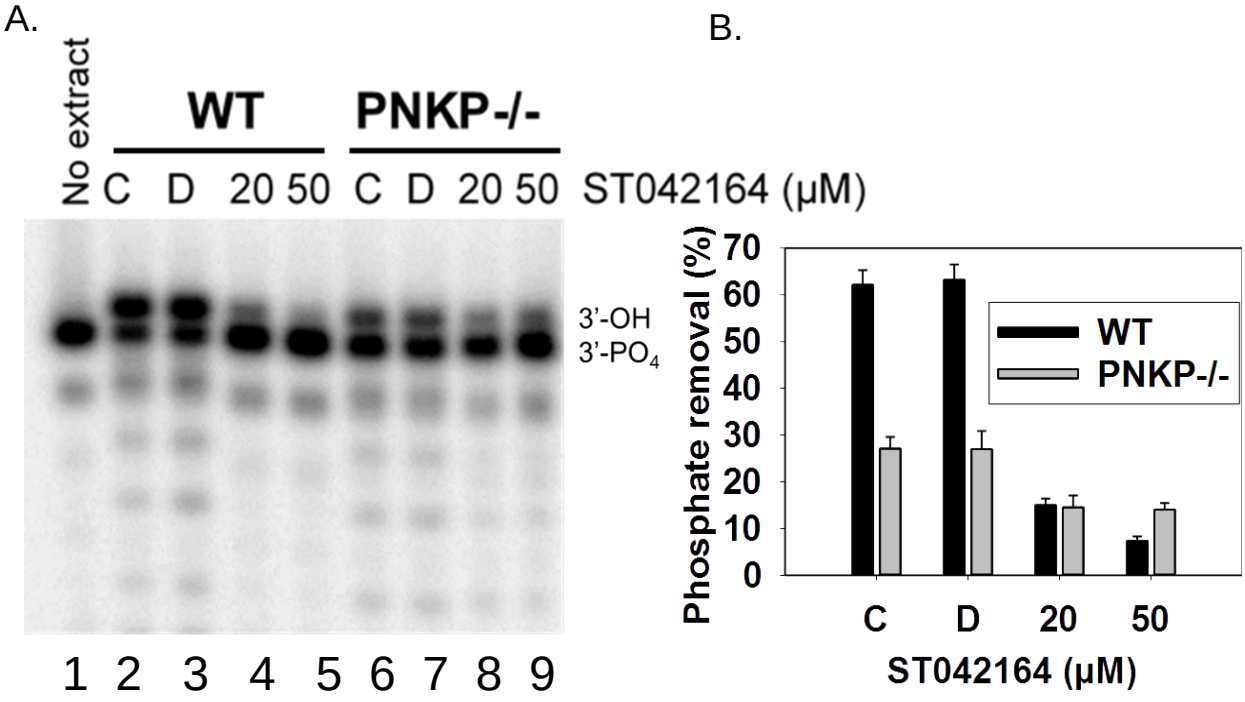

Fig. 8.21: ST042164-mediated inhibition of DNA 3′ phosphatase activity: A. Diluted HCT116 WT and PNKP knockout extracts were incubated with the defined concentrations of the heated drug for 10 min before addition of a 3′-phosphate overhang substrate. After proteolysis and AvaI treatments, products released were run on the gel. B. Image of the plot displays the percentage of phosphate removal in both the extracts in the absence and presence of ST042164 at the indicated concentrations. Reduction in phosphate removal was seen at both the concentrations of the drug (A. lane 4,5,8 and 9) for both the extracts with a much smaller inhibition in PNKP knockout extracts (A. lane 8 and 9) (C = No DMSO/Drug, D = DMSO control) (n = 2).

IX Discussion

DNA is one of the four major biomolecules in a cell, encoding genetic information which is faithfully carried across generations. Though initially thought to be a stable molecule by the discoverers, Watson and Crick, many have since shown that DNA is readily susceptible to chemical modifications by external and internal stress factors. These alterations if not repaired efficiently can result in numerous unwanted consequences such as aging (Hoeijmakers, 2009), cancer (Loeb & Harris, 2008) (Paz-Elizur et al., 2008) and neurological development disorders (McKinnon, 2009). A battery of robust DNA repair pathways have evolved to counter cytotoxic and mutational damage in a cell, functioning in a lesion-specific manner to ensure genomic stability.

Many studies have shown that defects in the DNA damage response and repair pathways are a double-edged sword, either leading to the development of tumors or rendering them resistant to cancer chemotherapy and radiotherapy whose primary goal is to kill cancer cells mostly by inducing DNA damage (Hosoya & Miyagawa, 2014). Thus, DNA response/repair factors have become potential therapeutic targets in the the recent years (Hosoya & Miyagawa, 2014) (Zhu, Hu, Hu, & Liu, 2009) (Bhattacharjee & Nandi, 2017). In every repair pathway, there are a plethora of enzymatic activities such as nucleases, helicases, polymerases, topoisomerases, recombinases, ligases,

glycosylases, demethylases, kinases, and phosphatases modifying the damaged DNA in a regulated fashion (Ciccia & Elledge, 2010a).

One such enzyme, Polynucleotide kinase phosphatase (PNKP), a bifunctional enzyme with DNA 5′-kinase and 3′-phosphatase activities, is required to modify ends of a DNA break before ligation. Occurrence of 3′- phosphate termini at the DNA breaks is common and can arise from a number of sources including reactive oxygen species, Tdp1 processing of stalled topoisomerase I complexes generated by the drug camptothecin (Yang et al., 1996) and as intermediates in a sub-pathway of base excision repair of oxidative base damage (Wiederhold et al., 2004). Nonetheless, occurrence of the 5′-hydroxyl termini is rare, being produced due to strand scission, e.g. ionising radiation (Coquerelle, Bopp, Kessler, & Hagen, 1973) camptothecin treatment, (Hsiang, Hertzberg, Hecht, & Liu, 1985) or by DNase II action. PNKP plays a crucial role in the repair of the complex double strand and single strand breaks induced by oxidative factors or repair-intermediates produced during their resolution. Like any other DNA repair factor, PNKP mutations have been identified as an etiology for neurological disorders (Dumitrache & McKinnon, 2017). Moreover, its involvement in various repair pathways made it an attractive target for chemotherapy of cancer (Allinson, 2010).

There is a considerable evidence regarding the participation of PNKP enzyme in NHEJ, one of the two major DSBR pathways (Chappell, Hanakahi, Karimi-Busheri, Weinfeld, & West, 2002b) (Chappell et al., 2002b), with accumulation of double-strand breaks in mouse models of PNKP deficiency (Shimada, Dumitrache, Russell, & McKinnon, 2015). However, no other factor has yet been identified to take over the role of PNKP in the repair of the 3′-phosphate and 5′-hydroxyl lesions at DSBs. An attempt

was made in our lab to screen for any such factor either by knocking down PNKP in HCT116 or treatment with a PNKP inhibitor, A12B4C3. None of these approaches were able to produce a distinction in the repair of 3′-phosphates DNA ends resulting from NCS treatment, as evidenced by screening the formation of 3′-hydroxyl ends by Ligation-mediated PCR (LMPCR). Therefore, for our current study, we employed CRISPR mediated PNKP knockout cells to ensure a complete loss of PNKP activity. Initially, HCT116 cells with PNKP knockout were acquired from Dr. Weinfeld's lab, and the knockout status was verified with the in-house mouse anti-PNKP monoclonal antibody raised against the N-terminal aa 1-140 peptide of the human PNKP enzyme. Survival and 53-bp1 repair foci (marker for NHEJ) assays done after NCS treatment of wild-type and PNKP knockout cells. There was a reduced survival and persistence of the repair foci in knockout cells.

Further, we proceeded to evaluate the specific enzymatic activities of PNKP, i.e., DNA 3′-phosphatase and 5′-kinase functions, in the absence of PNKP. To determine the same, specific radiolabeled DSB substrates were constructed with either a 3′-phosphate, 3′-phosphotyrosine or 5′-hydroxyl ends and cell-free whole cell extracts of HCT116 WT and PNKP knockout cells to process these substrates. Substrates with a 3′-phosphate end have either a partial complementary overhang or a complementary recessed end. Even in the absence of PNKP, removal of ~80% of the 3′-phosphate was seen for the overhang substrates. However, there was a severe limitation (~24%) in the processing of the recessed ends. Electrophoretic mobility shift assays done to characterize the DNA substrates have shown recessed end substrate to be a better binder than the overhangs (Havali-Shahriari, Weinfeld, & Glover, 2017). Surprisingly our experiments have shown

incomplete removal of 3′-phosphate from the recessed ends (Fig. 8.3). Structural studies of PNKP have demonstrated a narrow and deep active site cleft which could accommodate single but not double-stranded substrates (Coquelle, Havali-Shahriari, Bernstein, Green, & Glover, 2011b). The minimal substrate required for the catalysis in the phosphatase domain is a single-stranded three-nucleotide 3′-phosphorylated DNA (Bernstein et al., 2005). Destabilization of the double strand must occur to place the 3′-phosphate end of one strand in the narrow 3′-phosphatase cleft. Therefore, it can be hypothesized that the 3′-phosphate from the 3′-end with a 3 base overhang was easily accessible and hence the removal was rapid and complete, while the destabilization energy spent in accessing the 3′-phosphate at the recessed end, likely limited the catalytic activity on the substrate. Further, evaluation of processing of 3′-phosphotyrosyl substrates in the extracts revealed an accumulation of 3′-phosphates in the knockout extracts but not in the WT extracts, suggesting a deficiency of PNKP in the extracts.

APE1, an important constituent enzyme of BER is known to resolve various 3′ end blocks at SSB's, including 3′–phosphatases (M. Li, Wilson, & III, 2014). However, the 3′-PG and 3′-phosphate removal activities of APE1 are ∼70-fold lower than the endonuclease activity and it acts efficiently only at the recessed end of a double-strand break, at least for 3′-phosphoglycolates. It can be hypothesized that in the absence of PNKP, APE1 can take over the 3′-phosphatase function. Another enzyme Aprataxin is shown to repair DNA single-strand breaks with damaged 3′-phosphate and 3′-phosphoglycolate ends (Takahashi et al., 2007). On the other hand, Aprataxin also has an FHA domain similar to PNKP and interacts with CK2- phosphorylated XRRC4 similarly to PNKP, in a mutually exclusive manner (Ahel et al., 2006b). Hence, there can be a

competition between the two proteins in binding to XRCC4. One possible deciding factor for the interaction is the DNA substrate specificity. However, the primary function of Aprataxin is to resolve the adenylated 5'- ends of the DNA due to abortive ligation mediated by Ligase IV. In wild-type extracts, spontaneous activity of PNKP renders the ends ligatable almost immediately. Nonetheless, lack of PNKP in the knockout extracts results in the persistence of the 3′-phosphate at breaks, and if accompanied by 5'-phosphate at the other end, there will be accumulation of 5'-AMP (adenyl) ends due to abortive ligation. This accumulation along with the lack of the competitive PNKP might enhance the amount of Aprataxin binding with pXRCC4 at the non-ligated break. This increased presence of Aprataxin at the break might result in the dephosphorylation of the 3′-ends. However, APE1 and Aprataxin were shown to possess 3′-phosphatase activity at the SSB's. Experiments done to block the ligation of the opposite strand which can create a suitable substrate for APE1 and Aprataxin did not inhibit the repair of the damaged strands, limiting the evidence of their involvement in the repair of DSBs in PNKP knockout extracts. Recombinant protein assays with APE1 and Aprataxin, with and without core NHEJ recombinant proteins, using DSB substrates might reveal the function of these proteins.

All the above 3′-phosphate substrates had a 5′-phosphate end enabling the end joining at the 3′-hydroxyl ends. Though the presence of a 5′-hydroxyl end is not necessary for the extension of the DNA strand at 3′ end, ligation of the stand does. Any block at the 5′ end can be successfully overcome by strand displacement. Our substrates possessing 5′-OH ends, labeled on the 3′-end displayed end joining in the PNKP knockout extracts without any evidence of strand displacement (Fig. 8.6 B). This finding was an

indirect measure of the kinase function in the PNKP knockout extracts. Direct evidence of the kinase activity in the knockout extracts was obtained by incubating 5′-OH substrates labeled on the same strand. The observed total kinase activity in the extracts was less than the phosphatase activity (Fig. 8.6).

Before deducing the presence of other repair factors that might function similarly to PNKP, western blot experiments with antibodies that recognize different epitopes on the PNKP, were done to assess the possibility of the presence of residual PNKP or any other isoforms of PNKP. Unfortunately, these blots have disclosed a band running close to PNKP. The intensity of this band was almost 1/13th of of the band intensity at the same concentration of the protein in WT (Fig. 8.12). Meanwhile, HeLa PNKP knockout cells were obtained, and after confirming a clean knockout, DNA 3′ phosphatase and direct 5′-kinase assays were repeated, reproducing very similar results as in HCT116 PNKP knockout extracts. Although, ST042164, PNKP inhibitor obtained from Dr. Weinfeld's laboratory, inhibited the 100 ng pure PNKP's 3′-phosphatase activity at 10 μM concentration (Fig. 8.20), there was no effect was seen in the extracts even at 200 μM concentration. However, when used in 1: 125 diluted extracts, marked inhibition was visible in WT extracts but not in PNKP knockout extracts (Fig. 8.21). These findings gave a positive indication of the presence and activity of other DNA 3′-phosphatases in the cell.

Since the 3′-phosphatase activity was observed at the DSB's, we wanted to evaluate if this function is a part of NHEJ. During NHEJ, autophosphorylation of the DNA DSB bound DNA-PK complex is required for the accessibility of the ends to the end processing proteins which take part in NHEJ. By blocking the autophosphorylation of DNA-PK by the inhibitor, NU7441, this access can be limited. In both the extracts, the

phosphatase activity observed appeared to be a function of NHEJ as revealed by the DNA-PK inhibitor NU7441 treatment (Fig. 8.8). Moreover, availability of the DNA substrate ends for 3′-phosphate end processing to a non-specific phosphatase (CIP) even in the presence of NU7441 validates the above statement (Fig. 8.9). A cytoplasmic protein phosphatase enzyme, DUSP 27, (Friedberg et al., 2007) was believed to dephosphorylate DNA 3′ ends as it was identified to have a synthetic lethality with PNKP loss. Also, Alkaline phosphatase is a membrane-bound and cytoplasmic enzyme that can non-specifically dephosphorylate either 3′ or 5′ ends. However, the nuclear extracts retained the 3′ phosphatase activity even in PNKP knockout extracts, suggesting a nuclear presence of the unknown enzyme (Fig. 8.10 and 8.19).

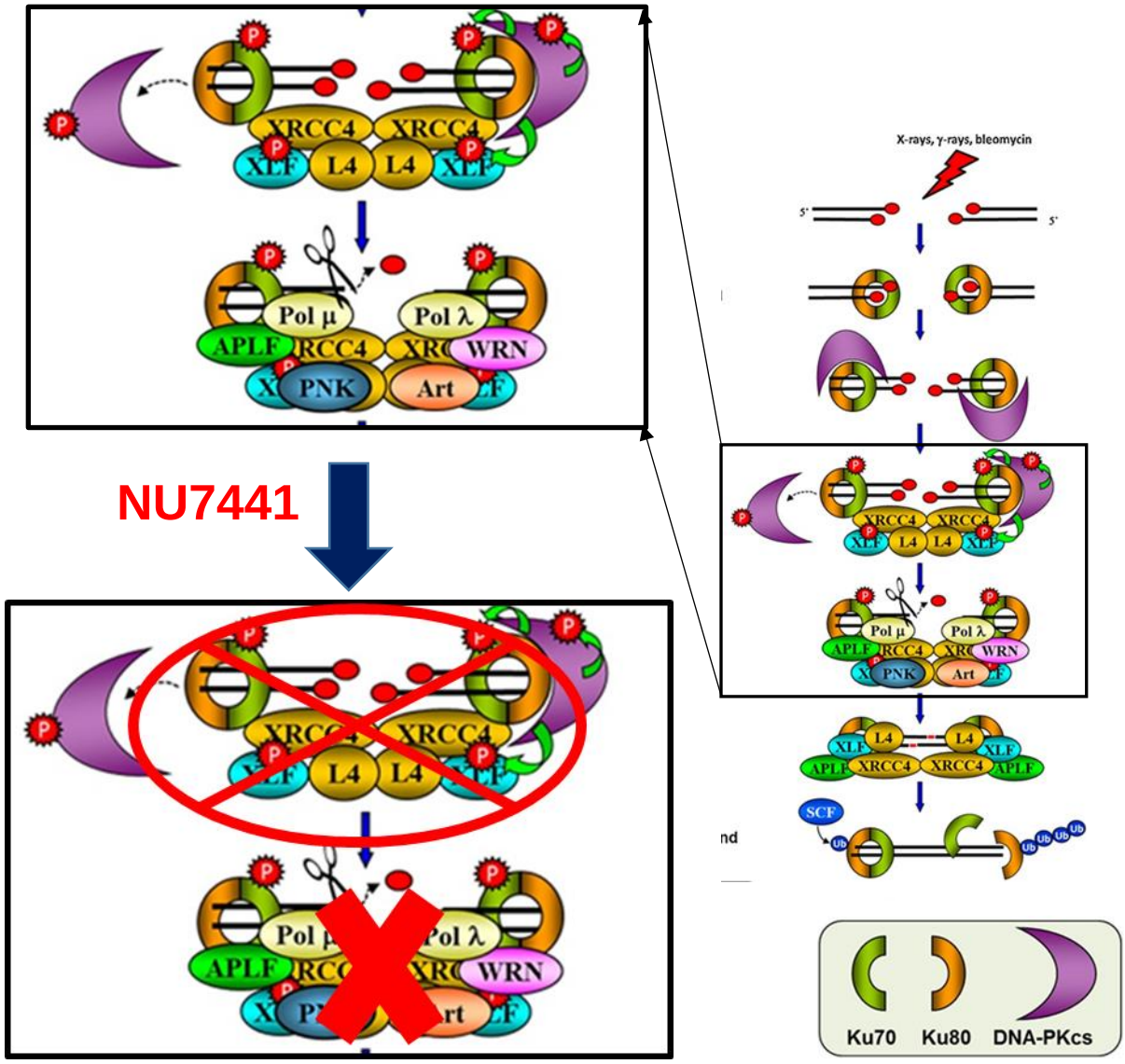

Fig. 9.1: Role of DNA-PK in NHEJ and DNA DSB processing: Formation of DNA-PK complex (Ku + DNA-PKcs) at the DSBs activates the kinase function on DNA-PKcs resulting in a series of phosphorylation events which moves the complex away from the ends and allowing for the accumulation of XLF-XRCC4-Ligase IV (ligation complex), at the DSBs. Accessory repair factors accumulate on the scaffold of this ligation complex to process the damaged ends and render them ligatable. By using a DNA-PK inhibitor, NU7441, which blocks the kinase active site, all the phosphorylation events are blocked thereby inhibiting the accumulation of either ligase complex or accessory factors. Thus, PNKP or its alternative DNA 3′-phosphatase and 5′-kinase enzyme(s) (if it is a part of NHEJ process), cannot function efficiently in the presence of NU7441. In our experiment the DNA 3′-phosphatase and 5′-kinase enzyme(s) appeared to be a part of NHEJ as the function was blocked in the presence of NU7441 (Fig. 8.10 and 8.19).

The NHEJ mediated repair of the double strand break requires more than 15 factors including the core and accessory factors to form complexes and resolve the complex strand breaks. Among the core proteins, XRCC4 is thought to be a central scaffold that coordinates handoff of DNA repair intermediates between various DNA repair enzymes (Aceytuno et al., 2017a). PNKP is shown to interact with both non-phosphorylated (XRCC4) and phosphorylated XRCC4 (pXRCC4), the latter being strong. However, this interaction with pXRCC4 reduces the PNKP activity requiring DNA Ligase IV in reversing the inhibitory effect of pXRCC4 on the turnover of the PNKP at the 5′-phosphate ends. Structural studies have shown that XRCC4 forms a 1:2:1 PNKP: pXRCC4: Ligase IV complex. XRCC4 and XLF homodimer proteins interact head to head forming long helical protein filaments to facilitate DNA double-strand break repair. (Mahaney, Hammel, Meek, Tainer, & Lees-Miller, 2013).

Further, the weak interaction between the PNKP catalytic domain and XRCC4–Ligase IV, seem suitable to position PNKP to gain access to DNA within the XRCC4-XLF filament (Aceytuno et al., 2017a). Based on these interacting studies, we wanted to explore the role of XRCC4 and XLF in the activity of PNKP in XRCC4 knockout HCT116 and Bus cell (deficient in XLF) extracts, respectively. Many studies reported the influence of XRCC4 on the kinase activity of the PNKP, with limited data on the phosphatase function. When both the activities were assayed, as expected, there was reduction observed for both the activities of PNKP in XRCC4 knockout extracts, only to be increased after complementation of the protein with an exuberant end joining of both the substrates (Fig. 8.11). Even though an increase, in the end joining of the partially complementary 3′-

phosphate substrates is conceivable, there was end joining of 5′-hydroxyl substrates with no complementarity in the overhang. This end joining appeared as a diffuse band, proposing a small resection at these ends (Fig. 8.11). This observation once again illustrates the ability of XRCC4 to promote ligation at the incompatible ends (Pannunzio, Watanabe, & Lieber, 2017). The inability of the added pure protein PNKP to restore the kinase activity in the absence of XRCC4 might be due to the reduced turnover of the PNKP after DNA 5′ phosphorylation (Mani et al., 2010b).This increased affinity of any protein to its processed substrate is to protect the DNA ends until passed on to next enzyme in the repair pathway (Hsiang et al., 1985). Further, there was no effect of XLF deficiency on the phosphatase activity in the Bus cell extracts, but the kinase activity was almost reduced to half, suggesting a role for XLF in influencing the processing of the 5′-hydroxyl ends. As expected, presence end joining was evident only in the presence of XLF, for the 3′-phosphate substrates which have a complementarity in the overhangs. However, XLF was not able to join the non-complementary ends of the 5′-hydroxyl substrates.

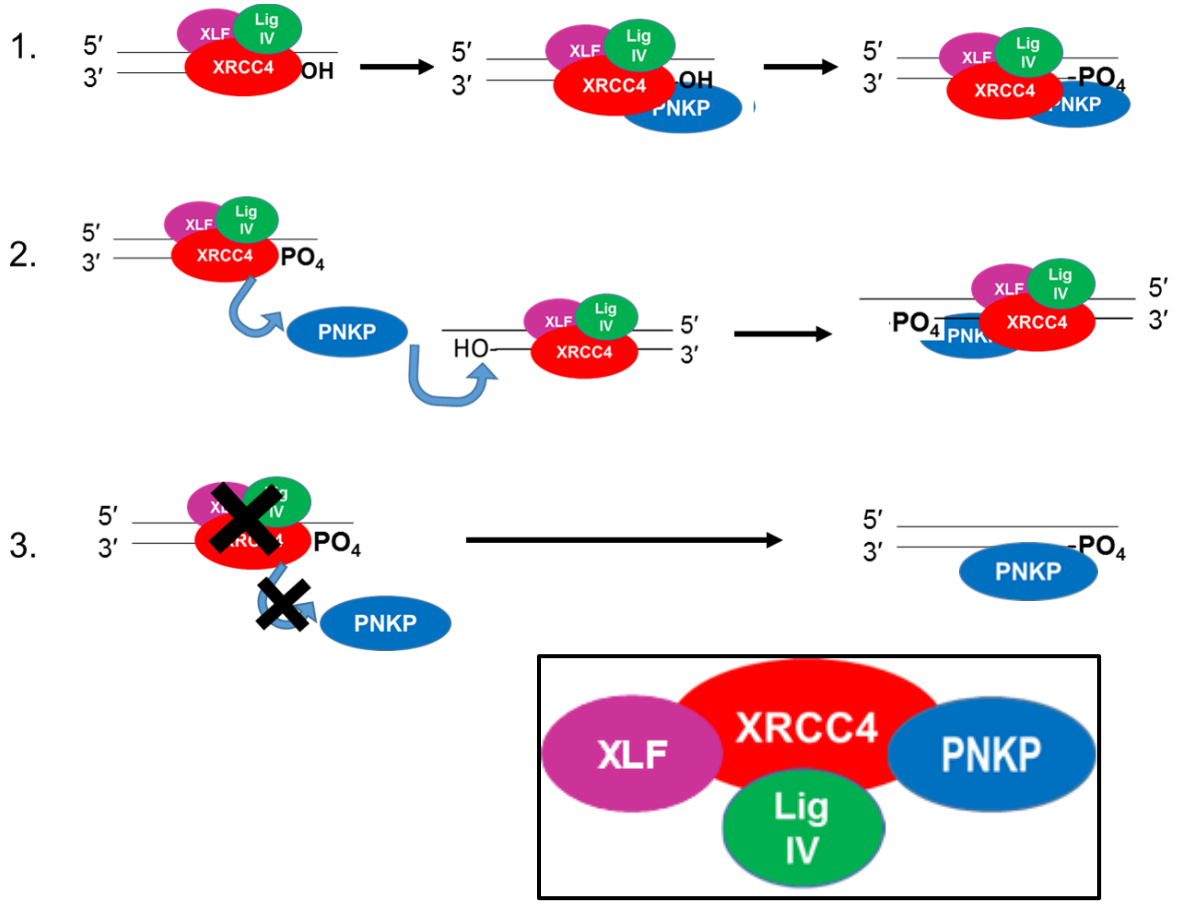

Fig. 9.2: Role of XLF-XRCC4-Ligase IV complex in influencing PNKP activity: 1. XLF-XRCC4-Ligase IV complex forms heterofilaments at the DSBs (for convenience single complex is depicted). PNKP accumulates on the scaffold of XLF-XRCC4-Ligase IV complex at the DSB for processing the DNA 5′-hydroxyl ends (also 3′-phosphate ends) and phosphorylates 5′-OH ends. 2. XRCC4-Ligase IV complex is required for the turnover of PNKP at the 5′-phosphorylated ends for reducing the affinity of PNKP to these processed ends, so that it can act on other 5′-OH ends. Hence, an increase in kinase activity (and phosphatase activity) was detected on adding back XRRC4/Ligase IV complex to XRCC4 knockout extracts (Fig. 8.11). However, in our experiments XLF has also enhanced the kinase activity (Fig 8.12), thus it is hypothesized that the XLF-XRCC4-Ligase IV complex increases the turnover of PNKP and in the absence of this complex, though PNKP can process the 5′-OH ends, remains bound to its substrates thereby limiting its activity on other substrates. XLF-XRCC4-Ligase IV complex is depicted in the box below.

Ligation-mediated PCR experiments (LMPCR) done in the lab to visualize the processing of DNA 3′-phosphate ends created by treatment of cells with the non-protein chromophore of Neocarzinostatin (NCS-C), have shown very rapid and similar 3′-dephosphorylation in both wild-type and PNKP knockout HCT116 cells at 37 °C. However, at 22 °C, there was a distinct delay in 3′-dephosphorylation of DSBs in PNKP knockout cells, with 8-fold fewer 3′-hydroxyl DSB termini than in wild-type cells 5 min after NCS-C addition and a 2 fold fewer at the 40 min time point at 22 °C. HeLa cells on the other hand showed a reduction of processing of 3′-phosphate with 3-fold fewer 3′-hydroxyl DSB termini at 5 and 15 min after treatment in PNKP knockout cells at 37 °C, although by 40 min, processing was similar to wild-type. At 22 °C there were fewer 3′-hydroxyl termini at least by 2-fold at all times with a 4-fold reduction at 40 min. These in-vivo 3′-phosphatase assays, while they confirm a partial deficiency in 3′-dephosphorylation in PNKP knockout cells, also suggest the presence of an alternative DNA 3′ phosphatase enzyme(s) which can process the 3′-phosphate ends in the absence of PNKP, and show that it is active in cells and not only extracts.

The disparity found in the DNA 3′-phosphatase activity detected in the extracts and cells from the survival assays (decreased survival of the knockout cells despite the repair seen in our 3′-phosphatase assays), can be explained by the creation of other lesions such as SSB's and 3′ phosphoglycolates by NCS, which in most cases require PNKP, delaying or interfering with the complete DNA repair, surmounting to cell death. Presence of the 53BP1 foci even after a long time suggests unrepaired DSB's, with some of the DSB's going into a delayed repair in G1, (resection dependent NHEJ or

Alt-NHEJ) which can lead to chromosomal translocations (Jeggo & Löbrich, 2017), or repaired by HR in G2 (as the cells are non-synchronized).

Resistence to chemotherapy is seen as major problem in developing new tartgets, especially the cell DNA damage response and repair factors. An enormous amount of redundancy in these factors and the ability of the cancer cells to hijack various pathways for the survival, poses a problem for a generalized targetting of the cancers. Hence, before considering a factor as a desired target, it is imperative to rule out redundancy. In the current scenario, PNKP appears to be a lucrative target due its crucial role in various repair pathways. However, as with any other factor, PNKP function might be duplicated by a redundant factor, whose function might not have been overtly obvious in PNKP's presence. Though lack of PNKP resulted in increased damage to cells, cancer cells could utilise PNKP's alternative for the survival. Hence, it would be wise to identify these alternative 3′-phosphatase factors and develop pharmacogial agents to block their activity in order to tackle future cancer therapy resistance.

X Conclusion

Repair of complex lesions at the double strand breaks requires processing of the ends by accessory factors. The nature of these lesions can be a deciding factor for the choice of repair pathway/repair factor that will act upon these lesions. From the Thymine glycol (Tg) study, we found that the Tg positioned at the fifth position is a better substrate than Tg at third position for the BER repair protein, hNTH1, precluding the availability of these ends for Non-homologous end joining. Similarly, from the PNKP experiment, we found that the 3′-phosphate at an overhang is better removed by the enzyme PNKP, than the one at the recessed end. However, PNKP seemed to be the pivotal enzyme processing the recessed 3′ ends.

Observations made in HCT116 and HeLa PNKP knockout extracts and cells suggest the presence of an alternative enzyme(s) to PNKP, although, these enzymes play a limited role in the absence of PNKP as seen by the survival assays. However, the presence of minute amounts of PNKP must be ruled out by trying to immuno-deplete the residual PNKP in the knockout extracts. Also, a recombinant ApeI which has a weak 3′ phosphatase activity, or Aprataxin can be tested either alone or in combination with other NHEJ proteins such as XRCC4-Ligase IV to disclose their activity in the context of NHEJ, in the absence of PNKP. Further, possibility that the increase lethality of the PNKP knockout cells following treatment with NCS is due to increased DSB mis-joining resulting

in lethal chromosome aberrations, can be investigated by FISH experiments to detect chromosomal translocations. Also, by column separation of proteins in the PNKP knockout extracts, different fractions can be tested for the presence of the DNA 3′-phosphatase and 5′-kinase functions. After multiple column preparations (e.g. size-exclusion, ion-exchange, and DNA affinity), the alternative DNA 3′-phosphatase(s) and 5′-kinase(s) might be isolated and identified by mass spectrometry.

Appendix I

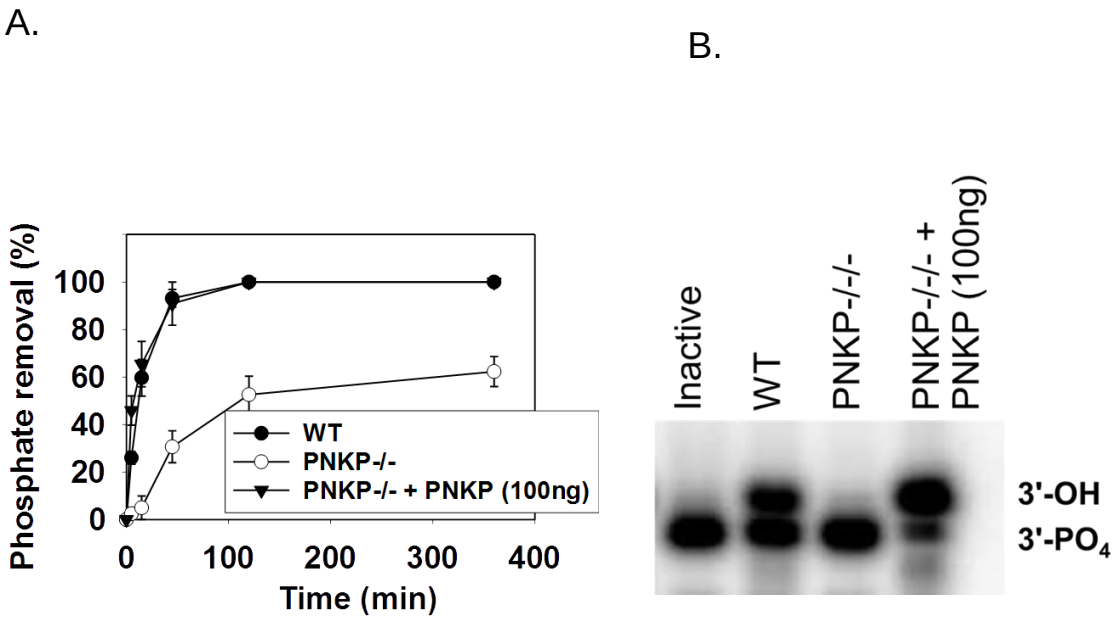

Figure 1: Restoration of DNA 3′-phosphatase activity by recombinant PNKP: To determine the loss of 3′-phosphatase activity in knockout extracts is due to lack of PNKP**,** recombinant protein (100 ng) was added to the Hct116 and HeLa PNKP knockout extracts and incubated for different times. A) Plot derived from the observed percentage of restoration of 3′-phosphatase activity on one base 3′-over hang substrate with time, in HCT116 extracts. B) Gel image allowing the restoration of 3′-phosphatase activity by PNKP addition on 3-base 3′-phosphate overhang substrate in HeLa knockout extracts. The incubation time for all the reactions was 90 sec. As seen from the plot and gel, there was restoration of the activity similar to activity seen in wild-type extracts.

Appendix II

Human HCT116 PNK gene knock out Confirmation by DNA sequencing

Alignment of CRISPR clone 3-14 with PNK Exon 3 sequences (WT)

65 nucleotide were deleted and 10 nucleotide were rearranged in Allele 1; 78 nucleotide were inserted and 2 separate nucleotides were mutated in Allele 2

```
E3-14-1         CTGGGAGTTAACCCCTCAACTACCGGGACCCAGGAGTTGAAGCCGGGGTTGGAGGGCTCT
E3-14-2         CTGGGAGTTAACCCCTCAACTACCGGGACCCAGGAGTTGAAGCCGGGGTTGGAGGGCTCT
PNK-Exon3       CTGGGAGTTAACCCCTCAACTACCGGGACCCAGGAGTTGAAGCCGGGGTTGGAGGGCTCT
                ************************************************************

E3-14-1         CTGGGGGTGGGGGACACACTGTATTTGGTCAATGG-----------------------T
E3-14-2         CTGGGGGTGGGGGACACACTGTATTTGGTCAATGGCCTCCACCCACTGACCCTGCGCTGG
PNK-Exon3       CTGGGGGTGGGGGACACACTGTATTTGGTCAATGGCCTCCACCCACTGACCCTGCGCTGG
                ************************************************************

E3-14-1         GAAGATGCC-----------------------------------------------------
E3-14-2         GAAGAGACCCGCACACCAGAATCCCAGCCAGATACTCCCGCACACCAGAATCCCAGAAGA
PNK-Exon3       GAAGAGACCCGCACACCAGAATCCCAGCCAGATACTCC----------------------
                ************************************

E3-14-1         ------------------------------------------------------------
E3-14-2         GACCCGCACACCAGAATCCCAGCCAGATACTCCCGCACACCAGAATCCCAGAAGAGACCT
PNK-Exon3       ------------------------------------------------------GCCT
                                                                        ***
```

```
E3-14-1         --------TCTGGTGTCCCAAGATGAGAAGAGAGATGCTGAGCTGCCGAAGAAGCATATG
E3-14-2         GGCACCCCTCTGGTGTCCCAAGATGAGAAGAGAGATGCTGAGCTGCCGAAGAAGCATATG
PNK-Exon3       GGCACCCCTCTGGTGTCCCAAGATGAGAAGAGAGATGCTGAGCTGCCGAAGAAGCATATG
                ************************************************************
E3-14-1         CGGAAGTCAAACCCCGGCTGGGAGAACTTGGAGAAGTTGCTAGTGTTCACCGCAGCTGGG
E3-14-2         CGGAAGTCAAACCCCGGCTGGGAGAACTTGGAGAAGTTGCTAGTGTCCACCGCAGCTGGG
PNK-Exon3       CGGAAGTCAAACCCCGGCTGGGAGAACTTGGAGAAGTTGCTAGTGTTCACCGCAGCTGGG
                ********************************************** *************

E3-14-1         GTGAAACCCCAGGGCAAG
E3-14-2         GTGAAACCCCAGGGCAAG
PNK-Exon3       GTGAAACCCCAGGGCAAG
                ******************
```

Human HeLa PNK gene knock out Confirmation by DNA sequencing

There are three copies of PNK in HeLa cells. Genomic DNA sequences around short guide RNA site of exon3 in clone 3-1-1 were sequenced.

DNA sequencing result showed that all three copies of PNK were modified.

Copy one

```
PNK3            CACTACCGGGACCCAGGAGTTGAAGCCGGGGTTGGAGGGCTCTCTGGGGGTGGGGGACAC
PNK3-1-1c       CACTACCGGGACCCAGGAGTTGAAGCCGGGGTTGGAGGGCTCTCTGGGGGTGGGGGACAC
                ************************************************************

PNK3            ACTGTATTTGGTCAATGGCCTCCACCCACTGACCCTGCGCTGGGAAGAGACCCGCACACC
PNK3-1-1c       ACTGTATTTGGTCAATGGCCTCCACCCACTGACCCTGCGCTGGGAAGAGACCCGCACACC
                ************************************************************

PNK3            AGAATCCCAGCCAGATACTCCGCCTGGCACCCCTCTGGTGTCCCAAGATGAGAAGAGAGA
PNK3-1-1c       AGAATCCCAGCCAGATACTCCGCCTGGCACCCCTCTGGTGTCCCAAGATGAGAAGAGAGA
                ************************************************************

PNK3            TGCTGAGCTGCCGAAG-AAGCGTATGCGGAAGTCAAACCCCGGCTGGGAGAACTTGGAGA
PNK3-1-1c       TGCTGAGCTGCCGAAGTAAGCGTATGCGGAAGTCAAACCCCGGCTGGGAGAACTTGGAGA
                *************** ****************************************

PNK3            AGTTGCTAGTGTTCACCGCAGCTGGGGTGAAACCCCAGGGCAAGGTGAGGGCCACGCCGA
PNK3-1-1c       AGTTGCTAGTGTTCACCGCAGCTGGGGTGAAACCCCAGGGCAAGGTGAGGGCCACGCCGA
                ************************************************************

PNK3            GGGCTGAGGGAGCCGCCACAGACTGGGACCCAATCCCACGTTTGTTGCGTGCTCTCA
PNK3-1-1c       GGGCTGAGGGAGCCGCCACAGACTGGGACCCAATCCCACGTTTGTTGCGTGCTCTCA
                ***********************************************************
1 nucleotides were inserted into clone 3-1-1.
```

Copy two

```
PNK3            ACTACCGGGACCCAGGAGTTGAAGCCGGGGTTGGAGGGCTCTCTGGGGGTGGGGGACACA
PNK3-1-1a       ACTACCGGGACCCAGGAGTTGAAGCCGGGGTTGGAGGGCTCTCTGGGGGTGGGGGACACA
                ************************************************************

PNK3            CTGTATTTGGTCAATGGCCTCCACCCACTGACCCTGCGCTGGGAAGAGACCCGCACACCA
PNK3-1-1a       CTGTATTTGGTCAATGGCCTCCACCCACTGACCCTGCGCTGGGAAGAGACCCGCACACCA
                ************************************************************

PNK3            GAATCCCAGCCAGATACTCCGCCTGGCACCCCTCTGGTGTCCCAAGATGAGAAGAGAGAT
PNK3-1-1a       GAATCCCAGCCAGATACTCCGCCTGGCACCCCTCTGGTGTCCCAAGATGAGAAGAGAGAT
                ************************************************************
```

```
PNK3            GCTGAGCTGCCGAAGA----------------------------------------------
PNK3-1-1a       GCTGAGCTGCCGAAGACCTACAACCAGCTGTTCGAGGAAAACCCCATCAACGCCAGCGGC
                ****************

PNK3            ------------------------------------------------------------
PNK3-1-1a       GTGGACGCCAAGGCCATCCTGTCTGCCAGACTGAGCAAGAGCAGACGGCTGGAAAATCTG

PNK3            ------------------------------------------------------------
PNK3-1-1a       ATCGCCCAGCTGCCCGGCGAGAAGAAGAATGGCCTGTTCGGAAACCTGATTGCCCTGAGC

PNK3            -------AGCGTATGCGGAAGTCAAACCCCGGCTGGGAGAACTTGGAGAAGTTGCTAGTG
PNK3-1-1a       CTGGGCAAGCGTATGCGGAAGTCAAACCCCGGCTGGGAGAACTTGGAGAAGTTGCTAGTG
                       ************************************************

PNK3            TTCACCGCAGCTGGGGTGAAACCCCAGGGCAAGGTGAGGGCCACGCCGAGGGCTGAGGGA
PNK3-1-1a       TTCACCGCAGCTGGGGTGAAACCCCAGGGCAAGGTGAGGGCCACGCCGAGGGCTGAGGGA
                ************************************************************

PNK3            GCCGCCACAGACTGGGACCCAATCCCACGTTTGTTGCGTGCTCTCA
PNK3-1-1a       GCCGCCACAGACTGGGACCCAATCCCACGTTTGTTGCGTGCTCTCA
                *********************************************
171 nucleotides were inserted into clone 3-1-1.
```

Copy three

```
PNK-E3          CTCCCTCTCTTTCTGCAGCTGGGAGTTAACCCCTCAACTACCGGGACCCAGGAGTTGAAG
PNK3-1-1jR      CTCCCTCTCTTTCTGCAGCTGGGAGTTAACCCCTCAACTACCGGGACCCAGGAGTTGAAG
                ************************************************************

PNK-E3          CCGGGGTTGGAGGGCTCTCTGGGGGTGGGGGACACACTGTATTTGGTCAATGGCCTCCAC
PNK3-1-1jR      CCGGGGTTGGAGGGCTCTCTGGGGGTGGGGGACACACTGTATTTGGTCAATGGCCTCCAC
                ************************************************************

PNK-E3          CCACTGACCCTGCGCTGGGAAGAGACCCGCACACCAGAATCCCAGCCAGATACTCCGCCT
PNK3-1-1jR      CCACTGACCCTGCGCTGGGAAGAGACCCGCACACCAGAATCCCAGCCAGATACTCCGCCT
                ************************************************************

PNK-E3          GGCACCCCTCTGGTGTCCCAAGATGAGAAGAGAGATGCTGAGCTGCCGAAG---------
PNK3-1-1jR      GGCACCCCTCTGGTGTCCCAAGATGAGAAGAGAGATGCTGAGCTGCCGAAGTAAGCGCGG
                *************************************************

PNK-E3          ------------------------------------------------------------
PNK3-1-1jR      CGGGTGTGGTGGTTACGCGCAGCGTGACCGCTACACTTGCCAGCGCCTTAGCGCCCGCTC

PNK-E3          ------------------------------------------------------------
PNK3-1-1jR      CTTTCGCTTTCTTCCCTTCCTTTCTCGCCACGTTCGCCGGCTTTCCCCGTCAAGCTCTAA

PNK-E3          ------------------------------------------------------------
PNK3-1-1jR      ATCGGGGGCTCCCTTTAGGGTTCCGATTTAGTGCTTTACGGCACCTCGACCCCAAAAAAC
```

```
PNK-E3          ----------------AAGCGTATGCGGAAGTCAAACCCCGGCTGGGAGAACTTGGAGAA
PNK3-1-1jR      TTGATTTGGGCGATGGAAGCGTATGCGGAAGTCAAACCCCGGCTGGGAGAACTTGGAGAA
                                ******************************************

PNK-E3          GTTGCTAGTGTTCACCGCAGCTGGGGTGAAACCCCAGGGCAAGGTGAGGGCCACGCCGAG
PNK3-1-1jR      GTTGCTAGTGTTCACCGCAGCTGGGGTGAAACCCCAGGGCAAGGTGAGGGCCACGCCGAG
                ************************************************************

PNK-E3          GGCTGAGGGAGCCGCCACAGACTGGGACCCAATCCCACGTTT
PNK3-1-1jR      GGCTGAGGGAGCCGCCACAGAC---------------------
                **********************
205 nucleotides were inserted into clone 3-1-1.
```

List of References

Aceytuno, R. D., Piett, C. G., Havali-Shahriari, Z., Edwards, R. A., Rey, M., Ye, R., Glover, J. N. M. (2017a). Structural and functional characterization of the PNKP–XRCC4–LigIV DNA repair complex. *Nucleic Acids Research*, *45*(10), 6238–6251. http://doi.org/10.1093/nar/gkx275

Adel Fahmideh, M., Lavebratt, C., Schüz, J., Röösli, M., Tynes, T., Grotzer, M. A., … Feychting, M. (2016). Common genetic variations in cell cycle and DNA repair pathways associated with pediatric brain tumor susceptibility. *Oncotarget*, *7*(39), 63640–63650. http://doi.org/10.18632/oncotarget.11575

Adelman, R., Saul, R. L., & Ames, B. N. (1988). Oxidative damage to DNA: relation to species metabolic rate and life span. *Proceedings of the National Academy of Sciences of the United States of America*, *85*(8), 2706–8. Retrieved from http://www.ncbi.nlm.nih.gov/pubmed/3128794

Ahel, I., Rass, U., El-Khamisy, S. F., Katyal, S., Clements, P. M., McKinnon, P. J., … West, S. C. (2006a). The neurodegenerative disease protein aprataxin resolves abortive DNA ligation intermediates. *Nature*, *443*(7112), 713–716. http://doi.org/10.1038/nature05164

Ali, H., Daser, A., Dear, P., Wood, H., Rabbitts, P., & Rabbitts, T. (2013). Nonreciprocal chromosomal translocations in renal cancer involve multiple DSBs and NHEJ associated with breakpoint inversion but not necessarily with transcription. *Genes, Chromosomes and Cancer*, *52*(4), 402–409. http://doi.org/10.1002/gcc.22038

Almeida, K. H., & Sobol, R. W. (2007). A unified view of base excision repair: Lesion-dependent protein complexes regulated by post-translational modification. *DNA Repair*, *6*(6), 695–711. http://doi.org/10.1016/j.dnarep.2007.01.009

Almohaini, M., Chalasani, S. L., Bafail, D., Akopiants, K., Zhou, T., Yannone, S. M., … Povirk, L. F. (2016). Nonhomologous end joining of complex DNA double-strand breaks with proximal thymine glycol and interplay with base excision repair. *DNA Repair*, *41*, 16–26. http://doi.org/10.1016/j.dnarep.2016.03.003

Andrew, A. S., Gui, J., Hu, T., Wyszynski, A., Marsit, C. J., Kelsey, K. T., … Karagas, M. R. (2015). Genetic polymorphisms modify bladder cancer recurrence and survival in a USA population-based prognostic study. *BJU International*, *115*(2), 238–247. http://doi.org/10.1111/bju.12641

Arnaudeau, C., Lundin, C., & Helleday, T. (2001). DNA double-strand breaks associated with replication forks are predominantly repaired by homologous recombination involving an exchange mechanism in mammalian cells. *Journal of Molecular Biology*, *307*(5), 1235–45. http://doi.org/10.1006/jmbi.2001.4564

Aspinwall, R., Rothwell, D. G., Roldan-Arjona, T., Anselmino, C., Ward, C. J., Cheadle, J. P., … Hickson, I. D. (1997). Cloning and characterization of a functional human homolog of Escherichia coli endonuclease III. *Proceedings of the National Academy of Sciences of the United States of America*, *94*(1), 109–14. Retrieved from http://www.ncbi.nlm.nih.gov/pubmed/8990169

Banerjee, A., Yang, W., Karplus, M., & Verdine, G. L. (2005). Structure of a repair enzyme interrogating undamaged DNA elucidates recognition of damaged DNA. *Nature*, *434*(7033), 612–618. http://doi.org/10.1038/nature03458

Barton, O., Naumann, S. C., Diemer-Biehs, R., Künzel, J., Steinlage, M., Conrad, S., … Löbrich, M. (2014). Polo-like kinase 3 regulates CtIP during DNA double-strand break repair in G1. *The Journal of Cell Biology*, *206*(7), 877–94. http://doi.org/10.1083/jcb.201401146

Basu, A. K., Loechler, E. L., Leadon, S. A., & Essigmann, J. M. (1989). Genetic effects of thymine glycol: site-specific mutagenesis and molecular modeling studies. *Proceedings of the National Academy of Sciences of the United States of America*, *86*(20), 7677–81. Retrieved from http://www.ncbi.nlm.nih.gov/pubmed/2682618

Behjati, S., Gundem, G., Wedge, D. C., Roberts, N. D., Tarpey, P. S., Cooke, S. L., … Campbell, P. J. (2016). Mutational signatures of ionizing radiation in second malignancies. *Nature Communications*, *7*, 12605. http://doi.org/10.1038/ncomms12605

Bellon, S., Shikazono, N., Cunniffe, S., Lomax, M., & O'Neill, P. (2009). Processing of thymine glycol in a clustered DNA damage site: mutagenic or cytotoxic. *Nucleic Acids Research*, *37*(13), 4430–4440. http://doi.org/10.1093/nar/gkp422

Bernstein NK, Williams RS, Rakovszky ML, Cui D, Green R, Karimi-Busheri F, Mani RS, Galicia S, Koch CA, Cass CE, Durocher D, Weinfeld M, G. J. (2005). The Molecular Architecture of the Mammalian DNA Repair Enzyme, Polynucleotide Kinase. *Molecular Cell*, *17*(5), 657–670. http://doi.org/10.1016/J.MOLCEL.2005.02.012

Beucher, A., Birraux, J., Tchouandong, L., Barton, O., Shibata, A., Conrad, S., … Löbrich, M. (2009). ATM and Artemis promote homologous recombination of radiation-induced DNA double-strand breaks in G2. *The EMBO Journal*, *28*(21), 3413–3427. http://doi.org/10.1038/emboj.2009.276

Biehs, R., Steinlage, M., Barton, O., Juhász, S., Künzel, J., Spies, J., … Löbrich, M. (2017). DNA Double-Strand Break Resection Occurs during Non-homologous End Joining in G1 but Is Distinct from Resection during Homologous Recombination. *Molecular Cell*, *65*(4), 671–684.e5. http://doi.org/10.1016/J.MOLCEL.2016.12.016

Blackford, A. N., & Jackson, S. P. (2017). ATM, ATR, and DNA-PK: The Trinity at the Heart of the DNA Damage Response. *Molecular Cell*, *66*(6), 801–817. http://doi.org/10.1016/J.MOLCEL.2017.05.015

Bras, J., Alonso, I., Barbot, C., Costa, M. M., Darwent, L., Orme, T., … Guerreiro, R. (2015). Mutations in PNKP Cause Recessive Ataxia with Oculomotor Apraxia Type 4. *The American Journal of Human Genetics*, *96*(3), 474–479. http://doi.org/10.1016/j.ajhg.2015.01.005

Buck, D., Malivert, L., de Chasseval, R., Barraud, A., Fondanèche, M.-C., Sanal, O., … Revy, P. (2006). Cernunnos, a Novel Nonhomologous End-Joining Factor, Is Mutated in Human Immunodeficiency with Microcephaly. *Cell*, *124*(2), 287–299. http://doi.org/10.1016/j.cell.2005.12.030

Calsou, P., Frit, P., Humbert, O., Muller, C., Chen, D. J., & Salles, B. (1999). The DNA-dependent protein kinase catalytic activity regulates DNA end processing by means of Ku entry into DNA. *The Journal of Biological Chemistry*, *274*(12), 7848–56. Retrieved from http://www.ncbi.nlm.nih.gov/pubmed/10075677

Cathcart, R., Schwiers, E., Saul, R. L., & Ames, B. N. (1984). Thymine glycol and thymidine glycol in human and rat urine: a possible assay for oxidative DNA damage. *Proceedings of the National Academy of Sciences of the United States of America*, *81*(18), 5633–7. Retrieved from http://www.ncbi.nlm.nih.gov/pubmed/6592579

Chanut, P., Britton, S., Coates, J., Jackson, S. P., & Calsou, P. (2016). Coordinated nuclease activities counteract Ku at single-ended DNA double-strand breaks. *Nature Communications*, *7*, 12889. http://doi.org/10.1038/ncomms12889

Chapman, J. R., Taylor, M. R. G., & Boulton, S. J. (2012). Playing the end game: DNA double-strand break repair pathway choice. *Molecular Cell*, *47*(4), 497–510. http://doi.org/10.1016/j.molcel.2012.07.029

Chappell, C., Hanakahi, L. A., Karimi-Busheri, F., Weinfeld, M., & West, S. C. (2002). Involvement of human polynucleotide kinase in double-strand break repair by non-homologous end joining. *The EMBO Journal*, *21*(11), 2827–32. http://doi.org/10.1093/emboj/21.11.2827

Chen, D. S., Herman, T., & Demple, B. (1991). Two distinct human DNA diesterases that hydrolyze 3′-blocking deoxyribose fragments from oxidized DNA. *Nucleic Acids Research*, *19*(21), 5907–14. Retrieved from http://www.ncbi.nlm.nih.gov/pubmed/1719484

Ciccia, A., & Elledge, S. J. (2010). The DNA damage response: making it safe to play with knives. *Molecular Cell*, *40*(2), 179–204. http://doi.org/10.1016/j.molcel.2010.09.019

Coquelle, N., Havali-Shahriari, Z., Bernstein, N., Green, R., & Glover, J. N. M. (2011). Structural basis for the phosphatase activity of polynucleotide kinase/phosphatase

on single- and double-stranded DNA substrates. *Proceedings of the National Academy of Sciences of the United States of America*, *108*(52), 21022–7. http://doi.org/10.1073/pnas.1112036108

Critchlow, S. E., & Jackson, S. P. (1998). DNA end-joining: from yeast to man. *Trends in Biochemical Sciences*, *23*(10), 394–8. Retrieved from http://www.ncbi.nlm.nih.gov/pubmed/9810228

D. Branzei, M. F. (2009). The checkpoint response to replication stress. *DNA Repair,* (8), 1038–1046.

Das, P., & Sutherland, B. M. (2011). Processing of abasic DNA clusters in hApeI-silenced primary fibroblasts exposed to low doses of X-irradiation. *Journal of Biosciences*, *36*(1), 105–16. Retrieved from http://www.ncbi.nlm.nih.gov/pubmed/21451252

David, S. S., O'Shea, V. L., & Kundu, S. (2007). Base-excision repair of oxidative DNA damage. *Nature*, *447*(7147), 941–950. http://doi.org/10.1038/nature05978

Davis, A. J., Chen, B. P. C., & Chen, D. J. (2014). DNA-PK: A dynamic enzyme in a versatile DSB repair pathway. *DNA Repair*, *17*, 21–29. http://doi.org/10.1016/j.dnarep.2014.02.020

Davis, A. J., & Chen, D. J. (2013). DNA double strand break repair via non-homologous end-joining. *Translational Cancer Research*, *2*(3), 130–143. http://doi.org/10.3978/j.issn.2218-676X.2013.04.02

Dianov, G. L., Sleeth, K. M., Dianova, I. I., & Allinson, S. L. (2003). Repair of abasic sites in DNA. *Mutation Research/Fundamental and Molecular Mechanisms of Mutagenesis*, *531*(1–2), 157–163. http://doi.org/10.1016/J.MRFMMM.2003.09.003

Difilippantonio, M. J., Zhu, J., Chen, H. T., Meffre, E., Nussenzweig, M. C., Max, E. E., … Nussenzweig, A. (2000). DNA repair protein Ku80 suppresses chromosomal aberrations and malignant transformation. *Nature*, *404*(6777), 510–514. http://doi.org/10.1038/35006670

Dobbs, T. A., Palmer, P., Maniou, Z., Lomax, M. E., & O'Neill, P. (2008). Interplay of two major repair pathways in the processing of complex double-strand DNA breaks. *DNA Repair*, *7*(8), 1372–1383. http://doi.org/10.1016/J.DNAREP.2008.05.001

Dobson, C. J., & Allinson, S. L. (2006). The phosphatase activity of mammalian polynucleotide kinase takes precedence over its kinase activity in repair of single strand breaks. *Nucleic Acids Research*, *34*(8), 2230–2237. http://doi.org/10.1093/nar/gkl275

Dolinnaya, N. G., Kubareva, E. A., Romanova, E. A., Trikin, R. M., & Oretskaya, T. S. (2013a). Thymidine glycol: the effect on DNA molecular structure and enzymatic processing. *Biochimie*, *95*(2), 134–147. http://doi.org/10.1016/j.biochi.2012.09.008

Dolinnaya, N. G., Kubareva, E. A., Romanova, E. A., Trikin, R. M., & Oretskaya, T. S. (2013b). Thymidine glycol: the effect on DNA molecular structure and enzymatic processing. *Biochimie*, *95*(2), 134–147. http://doi.org/10.1016/J.BIOCHI.2012.09.008

Douglas, P., Moorhead, G. B. G., Ye, R., & Lees-Miller, S. P. (2001). Protein Phosphatases Regulate DNA-dependent Protein Kinase Activity. *Journal of Biological Chemistry*, *276*(22), 18992–18998. http://doi.org/10.1074/jbc.M011703200

Drané, P., Brault, M.-E., Cui, G., Meghani, K., Chaubey, S., Detappe, A., … Chowdhury, D. (2017). TIRR regulates 53BP1 by masking its histone methyl-lysine binding function. *Nature*, *543*(7644), 211–216. http://doi.org/10.1038/nature21358

Dynan, W. S., & Yoo, S. (1998). Interaction of Ku protein and DNA-dependent protein kinase catalytic subunit with nucleic acids. *Nucleic Acids Research*, *26*(7), 1551–9. Retrieved from http://www.ncbi.nlm.nih.gov/pubmed/9512523

Eccles, L. J., Lomax, M. E., & O'Neill, P. (2010). Hierarchy of lesion processing governs the repair, double-strand break formation and mutability of three-lesion clustered DNA damage. *Nucleic Acids Research*, *38*(4), 1123–34. http://doi.org/10.1093/nar/gkp1070

Espejel, S., Martín, M., Klatt, P., Martín-Caballero, J., Flores, J. M., & Blasco, M. A. (2004). Shorter telomeres, accelerated ageing and increased lymphoma in DNA-PKcs-deficient mice. *EMBO Reports*, *5*(5), 503–509. http://doi.org/10.1038/sj.embor.7400127

Fell, V. L., & Schild-Poulter, C. (2015). The Ku heterodimer: Function in DNA repair and beyond. *Mutation Research/Reviews in Mutation Research*, *763*, 15–29. http://doi.org/10.1016/j.mrrev.2014.06.002

Feng, S., Rabii, R., Liang, G., Song, C., Chen, W., Guo, M., … Hu, S. (2016). The Expression Levels of XLF and Mutant P53 Are Inversely Correlated in Head and Neck Cancer Cells. *Journal of Cancer*, *7*(11), 1374–1382. http://doi.org/10.7150/jca.14669

Freschauf, G. K., Karimi-Busheri, F., Ulaczyk-Lesanko, A., Mereniuk, T. R., Ahrens, A., Koshy, J. M., … Weinfeld, M. (2009). Identification of a Small Molecule Inhibitor of the Human DNA Repair Enzyme Polynucleotide Kinase/Phosphatase. *Cancer Research*, *69*(19), 7739–7746. http://doi.org/10.1158/0008-5472.CAN-09-1805

Friedberg, I., Nika, K., Tautz, L., Saito, K., Cerignoli, F., Friedberg, I., … Mustelin, T. (2007). Identification and characterization of DUSP27, a novel dual-specific protein phosphatase. *FEBS Letters*, *581*(13), 2527–2533. http://doi.org/10.1016/j.febslet.2007.04.059

Gao, Y., Ferguson, D. O., Xie, W., Manis, J. P., Sekiguchi, J., Frank, K. M., … Alt, F. W.

(2000). Interplay of p53 and DNA-repair protein XRCC4 in tumorigenesis, genomic stability and development. *Nature*, *404*(6780), 897–900. http://doi.org/10.1038/35009138

Gary, R., Kim, K., Cornelius, H. L., Park, M. S., & Matsumoto, Y. (1999). Proliferating cell nuclear antigen facilitates excision in long-patch base excision repair. *The Journal of Biological Chemistry*, *274*(7), 4354–63. Retrieved from http://www.ncbi.nlm.nih.gov/pubmed/9933638

Georgakilas, A. G. (2008). Processing of DNA damage clusters in human cells: current status of knowledge. *Mol. BioSyst.*, *4*(1), 30–35. http://doi.org/10.1039/B713178J

Georgakilas, A. G., O'Neill, P., & Stewart, R. D. (2013a). Induction and repair of clustered DNA lesions: what do we know so far? *Radiation Research*, *180*(1), 100–9. http://doi.org/10.1667/RR3041.1

Georgakilas, A. G., O'Neill, P., & Stewart, R. D. (2013b). Induction and Repair of Clustered DNA Lesions: What Do We Know So Far? *Radiation Research*, *180*(1), 100–109. http://doi.org/10.1667/RR3041.1

Groth, P., Orta, M. L., Elvers, I., Majumder, M. M., Lagerqvist, A., & Helleday, T. (2012). Homologous recombination repairs secondary replication induced DNA double-strand breaks after ionizing radiation. *Nucleic Acids Research*, *40*(14), 6585–94. http://doi.org/10.1093/nar/gks315

GRUPP, K., ROETTGER, L., KLUTH, M., HUBE-MAGG, C., SIMON, R., LEBOK, P., … KRECH, T. (2015). Expression of DNA ligase IV is linked to poor prognosis and characterizes a subset of prostate cancers harboring TMPRSS2:ERG fusion and PTEN deletion. *Oncology Reports*, *34*(3), 1211–1220. http://doi.org/10.3892/or.2015.4080

H. Vakifahmetoglu, M. Olsson, B. Z. (2008). Death through a tragedy: mitotic catastrophe. *Cell Death Differ*, (15), 1153–1162.

Harper, J. W., & Elledge, S. J. (2007). The DNA Damage Response: Ten Years After. *Molecular Cell*, *28*(5), 739–745. http://doi.org/10.1016/j.molcel.2007.11.015

Harper, J. V, Anderson, J. A., & O'Neill, P. (2010). Radiation induced DNA DSBs: Contribution from stalled replication forks? *DNA Repair*, *9*(8), 907–13. http://doi.org/10.1016/j.dnarep.2010.06.002

Harrison, L., Hatahet, Z., Purmal, A. A., & Wallace, S. S. (1998). Multiply damaged sites in DNA: interactions with Escherichia coli endonucleases III and VIII. *Nucleic Acids Research*, *26*(4), 932–41. Retrieved from http://www.ncbi.nlm.nih.gov/pubmed/9461450

Hayes, R. C., & Leclerc, J. E. (1986). Sequence dependence for bypass of thymine glycols in DNA by DNA polymerase I. *Nucleic Acids Research*, *14*(2), 1045–1061.

http://doi.org/10.1093/nar/14.2.1045

Hayes, R. C., & LeClerc, J. E. (1986). Sequence dependence for bypass of thymine glycols in DNA by DNA polymerase I. *Nucleic Acids Research*, *14*(2), 1045–61. Retrieved from http://www.ncbi.nlm.nih.gov/pubmed/3945552

Hazra, T. K., Izumi, T., Boldogh, I., Imhoff, B., Kow, Y. W., Jaruga, P., … Mitra, S. (2002). Identification and characterization of a human DNA glycosylase for repair of modified bases in oxidatively damaged DNA. *Proceedings of the National Academy of Sciences of the United States of America*, *99*(6), 3523–8. http://doi.org/10.1073/pnas.062053799

Hsiang, Y. H., Hertzberg, R., Hecht, S., & Liu, L. F. (1985). Camptothecin induces protein-linked DNA breaks via mammalian DNA topoisomerase I. *The Journal of Biological Chemistry*, *260*(27), 14873–8. Retrieved from http://www.ncbi.nlm.nih.gov/pubmed/2997227

Hsu, C.-F., Tseng, H.-C., Chiu, C.-F., Liang, S.-Y., Tsai, C.-W., Tsai, M.-H., & Bau, D.-T. (2009). Association between DNA double strand break gene Ku80 polymorphisms and oral cancer susceptibility. *Oral Oncology*, *45*(9), 789–793. http://doi.org/10.1016/j.oraloncology.2008.12.002

Hu, S., Qu, Y., Xu, X., Xu, Q., Geng, J., & Xu, J. (2013). Nuclear Survivin and Its Relationship to DNA Damage Repair Genes in Non-Small Cell Lung Cancer Investigated Using Tissue Array. *PLoS ONE*, *8*(9), e74161. http://doi.org/10.1371/journal.pone.0074161

Huang, H., Imoto, S., & Greenberg, M. M. (2009). The mutagenicity of thymidine glycol in Escherichia coli is increased when it is part of a tandem lesion. *Biochemistry*, *48*(33), 7833–41. http://doi.org/10.1021/bi900927d

Huertas, P. (2010). DNA resection in eukaryotes: deciding how to fix the break. *Nature Structural & Molecular Biology*, *17*(1), 11–6. http://doi.org/10.1038/nsmb.1710

Ide, H., Kow, Y. W., & Wallace, S. S. (1985). Thymine glycols and urea residues in M13 DNA constitute replicative blocks in vitro. *Nucleic Acids Research*, *13*(22), 8035–52. Retrieved from http://www.ncbi.nlm.nih.gov/pubmed/3906566

Ikeda, S., Biswas, T., Roy, R., Izumi, T., Boldogh, I., Kurosky, A., … Mitra, S. (1998). Purification and characterization of human NTH1, a homolog of Escherichia coli endonuclease III. Direct identification of Lys-212 as the active nucleophilic residue. *The Journal of Biological Chemistry*, *273*(34), 21585–93. http://doi.org/10.1074/JBC.273.34.21585

Isobe, S.-Y., Nagao, K., Nozaki, N., Kimura, H., & Obuse, C. (2017). Inhibition of RIF1 by SCAI Allows BRCA1-Mediated Repair. *Cell Reports*, *20*(2), 297–307. http://doi.org/10.1016/j.celrep.2017.06.056

Jackson, S. P., & Bartek, J. (2009). The DNA-damage response in human biology and disease. *Nature*, *461*(7267), 1071–1078. http://doi.org/10.1038/nature08467

Jeggo, P. A., & Löbrich, M. (2017). DNA non-homologous end-joining enters the resection arena. *Oncotarget*, *8*(55), 93317–93318. http://doi.org/10.18632/oncotarget.22075

JF, W. (1988). DNA damage produced by ionizing radiation in mammalian cells: identities, mechanisms of formation, and repairability. *Prog Nucleic Acid Res Mol Biol*, *35*, 95–125.

Jin, Y., Xu, X., Wang, X., Kuang, H., Osterman, M., Feng, S., … Guo, H. (2016). Increasing sensitivity to DNA damage is a potential driver for human ovarian cancer. *Oncotarget*, *7*(31), 49710–49721. http://doi.org/10.18632/oncotarget.10436

Jun, S., Jung, Y.-S., Suh, H. N., Wang, W., Kim, M. J., Oh, Y. S., … Park, J.-I. (2016). LIG4 mediates Wnt signalling-induced radioresistance. *Nature Communications*, *7*, 10994. http://doi.org/10.1038/ncomms10994

Kao, J. Y., Goljer, I., Phan, T. A., & Bolton, P. H. (1993a). Characterization of the effects of a thymine glycol residue on the structure, dynamics, and stability of duplex DNA by NMR. *The Journal of Biological Chemistry*, *268*(24), 17787–93. Retrieved from http://www.ncbi.nlm.nih.gov/pubmed/8349663

Kao, J. Y., Goljer, I., Phan, T. A., & Bolton, P. H. (1993b). Characterization of the effects of a thymine glycol residue on the structure, dynamics, and stability of duplex DNA by NMR. *The Journal of Biological Chemistry*, *268*(24), 17787–93. Retrieved from http://www.ncbi.nlm.nih.gov/pubmed/8349663

Karimi-Busheri, F., & Weinfeld, M. (1997). Purification and substrate specificity of polydeoxyribonucleotide kinases isolated from calf thymus and rat liver. *Journal of Cellular Biochemistry*, *64*(2), 258–72. Retrieved from http://www.ncbi.nlm.nih.gov/pubmed/9027586

Katafuchi, A., Nakano, T., Masaoka, A., Terato, H., Iwai, S., Hanaokaţ, F., & Ide, H. (2004). Differential Specificity of Human and Escherichia coli Endonuclease III and VIII Homologues for Oxidative Base Lesions*. http://doi.org/10.1074/jbc.M400393200

Kuhmann, C., Li, C., Kloor, M., Salou, M., Weigel, C., Schmidt, C. R., … Popanda, O. (2014). Altered regulation of DNA ligase IV activity by aberrant promoter DNA methylation and gene amplification in colorectal cancer. *Human Molecular Genetics*, *23*(8), 2043–2054. http://doi.org/10.1093/hmg/ddt599

Kung, H. C., & Bolton, P. H. (1997). Structure of a duplex DNA containing a thymine glycol residue in solution. *The Journal of Biological Chemistry*, *272*(14), 9227–36. Retrieved from http://www.ncbi.nlm.nih.gov/pubmed/9083056

Kutuzov, M. M., Ilina, E. S., Sukhanova, M. V, Pyshnaya, I. A., Pyshnyi, D. V, Lavrik, O.

I., & Khodyreva, S. N. (2011). Interaction of poly(ADP-ribose) polymerase 1 with apurinic/apyrimidinic sites within clustered DNA damage. *Biochemistry. Biokhimiia*, *76*(1), 147–56. Retrieved from http://www.ncbi.nlm.nih.gov/pubmed/21568846

Lamarche, B. J., Orazio, N. I., & Weitzman, M. D. (2010). The MRN complex in double-strand break repair and telomere maintenance. *FEBS Letters*, *584*(17), 3682–3695. http://doi.org/10.1016/j.febslet.2010.07.029

Lan, T., Zhao, Z., Qu, Y., Zhang, M., Wang, H., Zhang, Z., … Song, Y. (2016). Targeting hyperactivated DNA-PKcs by KU0060648 inhibits glioma progression and enhances temozolomide therapy via suppression of AKT signaling. *Oncotarget*, *7*(34), 55555–55571. http://doi.org/10.18632/oncotarget.10864

Leahy, J. J. J., Golding, B. T., Griffin, R. J., Hardcastle, I. R., Richardson, C., Rigoreau, L., & Smith, G. C. M. (2004). Identification of a highly potent and selective DNA-dependent protein kinase (DNA-PK) inhibitor (NU7441) by screening of chromenone libraries. *Bioorganic & Medicinal Chemistry Letters*, *14*(24), 6083–6087. http://doi.org/10.1016/j.bmcl.2004.09.060

Lee, K. C., Padget, K., Curtis, H., Cowell, I. G., Moiani, D., Sondka, Z., … Austin, C. A. (2012). MRE11 facilitates the removal of human topoisomerase II complexes from genomic DNA. *Biology Open*, *1*(9), 863–73. http://doi.org/10.1242/bio.20121834

Li, L., Poon, H.-Y., Hildebrandt, M. R., Monckton, E. A., Germain, D. R., Fahlman, R. P., & Godbout, R. (2017). Role for RIF1-interacting partner DDX1 in BLM recruitment to DNA double-strand breaks. *DNA Repair*, *55*, 47–63. http://doi.org/10.1016/j.dnarep.2017.05.001

Lieber, M. R. (2010). The Mechanism of Double-Strand DNA Break Repair by the Nonhomologous DNA End-Joining Pathway. *Annual Review of Biochemistry*, *79*(1), 181–211. http://doi.org/10.1146/annurev.biochem.052308.093131

Lieber, M. R., Gu, J., Lu, H., Shimazaki, N., & Tsai, A. G. (2010). Nonhomologous DNA End Joining (NHEJ) and Chromosomal Translocations in Humans. In *Sub-cellular biochemistry* (Vol. 50, pp. 279–296). http://doi.org/10.1007/978-90-481-3471-7_14

Lindahl, T., & Wood, R. D. (1999). Quality control by DNA repair. *Science (New York, N.Y.)*, *286*(5446), 1897–905. Retrieved from http://www.ncbi.nlm.nih.gov/pubmed/10583946

Lomax, M. E., Cunniffe, S., & O'Neill, P. (2004). 8-OxoG retards the activity of the ligase III/XRCC1 complex during the repair of a single-strand break, when present within a clustered DNA damage site. *DNA Repair*, *3*(3), 289–99. http://doi.org/10.1016/j.dnarep.2003.11.006

Lustig, M. J., Cadet, J., Boorstein, R. J., & Teebor, G. W. (1992). Synthesis of the diastereomers of thymidine glycol, determination of concentrations and rates of interconversion of their cis-trans epimers at equilibrium and demonstration of

differential alkali lability within DNA. *Nucleic Acids Research*, *20*(18), 4839–45. Retrieved from http://www.ncbi.nlm.nih.gov/pubmed/1408799

M. Hada, B. M. S. (2006). Spectrum of complex DNA damages depends on the incident radiation. *Radiat. Res., 165*, 223–230.

Mackay, D. R., Howa, A. C., Werner, T. L., & Ullman, K. S. (2017). Nup153 and Nup50 promote recruitment of 53BP1 to DNA repair foci by antagonizing BRCA1-dependent events. *Journal of Cell Science*, jcs.203513. http://doi.org/10.1242/jcs.203513

Mahaney, B. L., Hammel, M., Meek, K., Tainer, J. A., & Lees-Miller, S. P. (2013). XRCC4 and XLF form long helical protein filaments suitable for DNA end protection and alignment to facilitate DNA double strand break repair. *Biochemistry and Cell Biology*, *91*(1), 31–41. http://doi.org/10.1139/bcb-2012-0058

Mailand, N., Bekker-Jensen, S., Faustrup, H., Melander, F., Bartek, J., Lukas, C., & Lukas, J. (2007). RNF8 ubiquitylates histones at DNA double-strand breaks and promotes assembly of repair proteins. *Cell*, *131*(5), 887–900. http://doi.org/10.1016/j.cell.2007.09.040

Mani, R. S., Yu, Y., Fang, S., Lu, M., Fanta, M., Zolner, A. E., … Weinfeld, M. (2010a). Dual modes of interaction between XRCC4 and polynucleotide kinase/phosphatase: implications for nonhomologous end joining. *The Journal of Biological Chemistry*, *285*(48), 37619–29. http://doi.org/10.1074/jbc.M109.058719

Marenstein, D. R., Chan, M. K., Altamirano, A., Basu, A. K., Boorstein, R. J., Cunningham, R. P., & Teebor, G. W. (2003). Substrate specificity of human endonuclease III (hNTH1). Effect of human APE1 on hNTH1 activity. *The Journal of Biological Chemistry*, *278*(11), 9005–12. http://doi.org/10.1074/jbc.M212168200

McVey, M., & Lee, S. E. (2008). MMEJ repair of double-strand breaks (director's cut): deleted sequences and alternative endings. *Trends in Genetics : TIG*, *24*(11), 529–38. http://doi.org/10.1016/j.tig.2008.08.007

Menon, V., & Povirk, L. F. (2016). End-processing nucleases and phosphodiesterases: An elite supporting cast for the non-homologous end joining pathway of DNA double-strand break repair. *DNA Repair*, *43*, 57–68. http://doi.org/10.1016/J.DNAREP.2016.05.011

Mohapatra, S., Yannone, S. M., Lee, S.-H., Hromas, R. A., Akopiants, K., Menon, V., … Povirk, L. F. (2013). Trimming of damaged 3′ overhangs of DNA double-strand breaks by the Metnase and Artemis endonucleases. *DNA Repair*, *12*(6), 422–32. http://doi.org/10.1016/j.dnarep.2013.03.005

Mol, C. D., Arvai, A. S., Slupphaug, G., Kavli, B., Alseth, I., Krokan, H. E., & Tainer, J. A. (1995). Crystal structure and mutational analysis of human uracil-DNA glycosylase: structural basis for specificity and catalysis. *Cell*, *80*(6), 869–78. Retrieved from http://www.ncbi.nlm.nih.gov/pubmed/7697717

Nikjoo, H., O'Neill, P., Wilson, W. E., & Goodhead, D. T. (2001). Computational approach for determining the spectrum of DNA damage induced by ionizing radiation. *Radiation Research*, *156*(5 Pt 2), 577–83. Retrieved from http://www.ncbi.nlm.nih.gov/pubmed/11604075

Nilsen, L., Forstrøm, R. J., Bjørås, M., & Alseth, I. (2012). AP endonuclease independent repair of abasic sites in Schizosaccharomyces pombe. *Nucleic Acids Research*, *40*(5), 2000–9. http://doi.org/10.1093/nar/gkr933

Pannunzio, N. R., Watanabe, G., & Lieber, M. R. (2017). Nonhomologous DNA End Joining for Repair of DNA Double-Strand Breaks. *Journal of Biological Chemistry*, jbc.TM117.000374. http://doi.org/10.1074/jbc.TM117.000374

Pearson, C. G., Shikazono, N., Thacker, J., & O'Neill, P. (2004). Enhanced mutagenic potential of 8-oxo-7,8-dihydroguanine when present within a clustered DNA damage site. *Nucleic Acids Research*, *32*(1), 263–270. http://doi.org/10.1093/nar/gkh150

Plo, I., Liao, Z. Y., Barceló, J. M., Kohlhagen, G., Caldecott, K. W., Weinfeld, M., & Pommier, Y. (2003). Association of XRCC1 and tyrosyl DNA phosphodiesterase (Tdp1) for the repair of topoisomerase I-mediated DNA lesions. *DNA Repair*, *2*(10), 1087–100. Retrieved from http://www.ncbi.nlm.nih.gov/pubmed/13679147

Rasouli-Nia, A., Karimi-Busheri, F., & Weinfeld, M. (2004). Stable down-regulation of human polynucleotide kinase enhances spontaneous mutation frequency and sensitizes cells to genotoxic agents. *Proceedings of the National Academy of Sciences*, *101*(18), 6905–6910. http://doi.org/10.1073/pnas.0400099101

Reid, D. A., Keegan, S., Leo-Macias, A., Watanabe, G., Strande, N. T., Chang, H. H., … Rothenberg, E. (2015). Organization and dynamics of the nonhomologous end-joining machinery during DNA double-strand break repair. *Proceedings of the National Academy of Sciences of the United States of America*, *112*(20), E2575-84. http://doi.org/10.1073/pnas.1420115112

Riabinska, A., Daheim, M., Herter-Sprie, G. S., Winkler, J., Fritz, C., Hallek, M., … Reinhardt, H. C. (2013). Therapeutic Targeting of a Robust Non-Oncogene Addiction to PRKDC in ATM-Defective Tumors. *Science Translational Medicine*, *5*(189), 189ra78-189ra78. http://doi.org/10.1126/scitranslmed.3005814

Roddam, P. L., Rollinson, S., O'Driscoll, M., Jeggo, P. A., Jack, A., & Morgan, G. J. (2002). Genetic variants of NHEJ DNA ligase IV can affect the risk of developing multiple myeloma, a tumour characterised by aberrant class switch recombination. *Journal of Medical Genetics*, *39*(12), 900–5. Retrieved from http://www.ncbi.nlm.nih.gov/pubmed/12471202

Romick-Rosendale, L. E., Hoskins, E. E., Privette Vinnedge, L. M., Foglesong, G. D., Brusadelli, M. G., Potter, S. S., … Wells, S. I. (2016). Defects in the Fanconi Anemia Pathway in Head and Neck Cancer Cells Stimulate Tumor Cell Invasion through DNA-PK and Rac1 Signaling. *Clinical Cancer Research*, *22*(8), 2062–2073.

http://doi.org/10.1158/1078-0432.CCR-15-2209

Rothkamm, K., Kühne, M., Jeggo, P. A., & Löbrich, M. (2001). Radiation-induced genomic rearrangements formed by nonhomologous end-joining of DNA double-strand breaks. *Cancer Research*, *61*(10), 3886–93. Retrieved from http://www.ncbi.nlm.nih.gov/pubmed/11358801

Rouse, J., & Jackson, S. P. (2002). Interfaces Between the Detection, Signaling, and Repair of DNA Damage. *Science*, *297*(5581), 547–551. http://doi.org/10.1126/science.1074740

Rulten, S. L., Fisher, A. E. O., Robert, I., Zuma, M. C., Rouleau, M., Ju, L., … Caldecott, K. W. (2011). PARP-3 and APLF function together to accelerate nonhomologous end-joining. *Molecular Cell*, *41*(1), 33–45. http://doi.org/10.1016/j.molcel.2010.12.006

Rulten, S. L., & Grundy, G. J. (2017). Non-homologous end joining: Common interaction sites and exchange of multiple factors in the DNA repair process. *BioEssays*, *39*(3), 1600209. http://doi.org/10.1002/bies.201600209

Sacco, E. (2009). Cancer and aging: The molecular pathways. *Urologic Oncology: Seminars and Original Investigations*, *27*(6), 620–627. http://doi.org/10.1016/J.UROLONC.2009.07.013

Sage, E., & Shikazono, N. (2017). Radiation-induced clustered DNA lesions: Repair and mutagenesis. *Free Radical Biology and Medicine*, *107*, 125–135. http://doi.org/10.1016/J.FREERADBIOMED.2016.12.008

Schildkraut, J. M., Iversen, E. S., Wilson, M. A., Clyde, M. A., Moorman, P. G., Palmieri, R. T., … Berchuck, A. (2010). Association between DNA Damage Response and Repair Genes and Risk of Invasive Serous Ovarian Cancer. *PLoS ONE*, *5*(4), e10061. http://doi.org/10.1371/journal.pone.0010061

Shao, C.-J., Fu, J., Shi, H.-L., Mu, Y.-G., & Chen, Z.-P. (2008). Activities of DNA-PK and Ku86, but not Ku70, may predict sensitivity to cisplatin in human gliomas. *Journal of Neuro-Oncology*, *89*(1), 27–35. http://doi.org/10.1007/s11060-008-9592-7

Shao, R.-G., Cao, C.-X., Zhang, H., Kohn, K. W., Wold, M. S., & Pommier, Y. (1999). Replication-mediated DNA damage by camptothecin induces phosphorylation of RPA by DNA-dependent protein kinase and dissociates RPA:DNA-PK complexes. *The EMBO Journal*, *18*(5), 1397–1406. Retrieved from http://emboj.embopress.org/content/embojnl/18/5/1397.full.pdf

Shen, J., Gilmore, E. C., Marshall, C. A., Haddadin, M., Reynolds, J. J., Eyaid, W., … Walsh, C. A. (2010). Mutations in PNKP cause microcephaly, seizures and defects in DNA repair. *Nature Genetics*, *42*(3), 245–249. http://doi.org/10.1038/ng.526

Shibata, A. (2017). Regulation of repair pathway choice at two-ended DNA double-strand

breaks. *Mutation Research/Fundamental and Molecular Mechanisms of Mutagenesis*. http://doi.org/10.1016/j.mrfmmm.2017.07.011

Shimada, M., Dumitrache, L. C., Russell, H. R., & McKinnon, P. J. (2015). Polynucleotide kinase-phosphatase enables neurogenesis via multiple DNA repair pathways to maintain genome stability. *The EMBO Journal*, *34*(19), 2465–80. http://doi.org/10.15252/embj.201591363

Shintani, S., Mihara, M., Li, C., Nakahara, Y., Hino, S., Nakashiro, K.-I., & Hamakawa, H. (2003). Up-regulation of DNA-dependent protein kinase correlates with radiation resistance in oral squamous cell carcinoma. *Cancer Science*, *94*(10), 894–900. Retrieved from http://www.ncbi.nlm.nih.gov/pubmed/14556663

Sishc, B. J., & Davis, A. J. (2017). The Role of the Core Non-Homologous End Joining Factors in Carcinogenesis and Cancer. *Cancers*, *9*(7), 81. http://doi.org/10.3390/cancers9070081

Smith, G. C., & Jackson, S. P. (1999). The DNA-dependent protein kinase. *Genes & Development*, *13*(8), 916–34. Retrieved from http://www.ncbi.nlm.nih.gov/pubmed/10215620

Sutherland, B. M., Bennett, P. V., Sutherland, J. C., & Laval, J. (2002). Clustered DNA Damages Induced by X Rays in Human Cells. *Radiation Research*, *157*(6), 611–616. http://doi.org/10.1667/0033-7587(2002)157[0611:CDDIBX]2.0.CO;2

Tahbaz, N., Subedi, S., & Weinfeld, M. (2012). Role of polynucleotide kinase/phosphatase in mitochondrial DNA repair. *Nucleic Acids Research*, *40*(8), 3484–3495. http://doi.org/10.1093/nar/gkr1245

Takahashi, T., Tada, M., Igarashi, S., Koyama, A., Date, H., Yokoseki, A., … Onodera, O. (2007). Aprataxin, causative gene product for EAOH/AOA1, repairs DNA single-strand breaks with damaged 3′-phosphate and 3′-phosphoglycolate ends. *Nucleic Acids Research*, *35*(11), 3797–3809. http://doi.org/10.1093/nar/gkm158

Tarish, F. L., Schultz, N., Tanoglidi, A., Hamberg, H., Letocha, H., Karaszi, K., … Helleday, T. (2015). Castration radiosensitizes prostate cancer tissue by impairing DNA double-strand break repair. *Science Translational Medicine*, *7*(312), 312re11-312re11. http://doi.org/10.1126/scitranslmed.aac5671

Thayer, M. M., Ahern, H., Xing, D., Cunningham, R. P., & Tainer, J. A. (1995). Novel DNA binding motifs in the DNA repair enzyme endonuclease III crystal structure. *The EMBO Journal*, *14*(16), 4108–20. Retrieved from http://www.ncbi.nlm.nih.gov/pubmed/7664751

Tsuji, T., Sapinoso, L. M., Tran, T., Gaffney, B., Wong, L., Sankar, S., … Xu, S. (2017). CC-115, a dual inhibitor of mTOR Kinase and DNA-PK, blocks DNA damage repair pathways and selectively inhibits ATM-deficient cell growth <i>in vitro</i> *Oncotarget*, *8*(43). http://doi.org/10.18632/oncotarget.20342

Uziel, T., Lerenthal, Y., Moyal, L., Andegeko, Y., Mittelman, L., & Shiloh, Y. (2003). Requirement of the MRN complex for ATM activation by DNA damage. *The EMBO Journal*, *22*(20), 5612–5621. http://doi.org/10.1093/emboj/cdg541

Vaishnav, Y., Holwitt, E., Swenberg, C., Lee, H. C., & Kan, L. S. (1991). Synthesis and characterization of stereoisomers of 5,6-dihydro-5,6-dihydroxy-thymidine. *Journal of Biomolecular Structure & Dynamics*, *8*(5), 935–51. http://doi.org/10.1080/07391102.1991.10507858

Walker, J. R., Corpina, R. A., & Goldberg, J. (2001). Structure of the Ku heterodimer bound to DNA and its implications for double-strand break repair. *Nature*, *412*(6847), 607–614. http://doi.org/10.1038/35088000

Wallace, S. S. (2002). Biological consequences of free radical-damaged DNA bases. *Free Radical Biology & Medicine*, *33*(1), 1–14. Retrieved from http://www.ncbi.nlm.nih.gov/pubmed/12086677

Wang, S.-Y., Peng, L., Li, C.-P., Li, A.-P., Zhou, J.-W., Zhang, Z.-D., & Liu, Q.-Z. (2008). Genetic variants of the XRCC7 gene involved in DNA repair and risk of human bladder cancer. *International Journal of Urology*, *15*(6), 534–539. http://doi.org/10.1111/j.1442-2042.2008.02049.x

Ward, J. F. (1988). DNA damage produced by ionizing radiation in mammalian cells: identities, mechanisms of formation, and reparability. *Progress in Nucleic Acid Research and Molecular Biology*, *35*, 95–125. Retrieved from http://www.ncbi.nlm.nih.gov/pubmed/3065826

Weinfeld, M., Mani, R. S., Abdou, I., Aceytuno, R. D., & Glover, J. N. M. (2011). Tidying up loose ends: the role of polynucleotide kinase/phosphatase in DNA strand break repair. *Trends in Biochemical Sciences*, *36*(5), 262–271. http://doi.org/10.1016/J.TIBS.2011.01.006

Weinstock, D. M., Richardson, C. A., Elliott, B., & Jasin, M. (2006). Modeling oncogenic translocations: Distinct roles for double-strand break repair pathways in translocation formation in mammalian cells. *DNA Repair*, *5*(9–10), 1065–1074. http://doi.org/10.1016/j.dnarep.2006.05.028

Williams, R. S., Dodson, G. E., Limbo, O., Yamada, Y., Williams, J. S., Guenther, G., … Tainer, J. A. (2009). Nbs1 flexibly tethers Ctp1 and Mre11-Rad50 to coordinate DNA double-strand break processing and repair. *Cell*, *139*(1), 87–99. http://doi.org/10.1016/j.cell.2009.07.033

Winkler, J., Hofmann, K., & Chen, S. (2014). Novel targets for ATM-deficient malignancies. *Molecular & Cellular Oncology*, *1*(1), e29905. http://doi.org/10.4161/mco.29905

Yan, C. T., Kaushal, D., Murphy, M., Zhang, Y., Datta, A., Chen, C., … Alt, F. W. (2006). XRCC4 suppresses medulloblastomas with recurrent translocations in p53-deficient

mice. *Proceedings of the National Academy of Sciences*, *103*(19), 7378–7383. http://doi.org/10.1073/pnas.0601938103

Yanai, M., Makino, H., Ping, B., Takeda, K., Tanaka, N., Sakamoto, T., … Shimizu, E. (2017). DNA-PK Inhibition by NU7441 Enhances Chemosensitivity to Topoisomerase Inhibitor in Non-Small Cell Lung Carcinoma Cells by Blocking DNA Damage Repair. *Yonago Acta Medica*, *60*(1), 9–15. Retrieved from http://www.ncbi.nlm.nih.gov/pubmed/28331416

Yoon, J.-H., Roy Choudhury, J., Park, J., Prakash, S., & Prakash, L. (2014). A role for DNA polymerase θ in promoting replication through oxidative DNA lesion, thymine glycol, in human cells. *The Journal of Biological Chemistry*, *289*(19), 13177–85. http://doi.org/10.1074/jbc.M114.556977

You, Z., & Bailis, J. M. (2010). DNA damage and decisions: CtIP coordinates DNA repair and cell cycle checkpoints. *Trends in Cell Biology*, *20*(7), 402–409. http://doi.org/10.1016/j.tcb.2010.04.002

Zhou, R.-Z., Blanco, L., Garcia-Diaz, M., Bebenek, K., Kunkel, T. A., & Povirk, L. F. (2008b). Tolerance for 8-oxoguanine but not thymine glycol in alignment-based gap filling of partially complementary double-strand break ends by DNA polymerase λ in human nuclear extracts. *Nucleic Acids Research*, *36*(9), 2895–2905. http://doi.org/10.1093/nar/gkn126

Zhou, T., Akopiants, K., Mohapatra, S., Lin, P.-S., Valerie, K., Ramsden, D. A., … Povirk, L. F. (2009). Tyrosyl-DNA phosphodiesterase and the repair of 3′-phosphoglycolate-terminated DNA double-strand breaks. *DNA Repair*, *8*(8), 901–911. http://doi.org/10.1016/j.dnarep.2009.05.003

Zolner, A. E., Abdou, I., Ye, R., Mani, R. S., Fanta, M., Yu, Y., … Lees-Miller, S. P. (2011b). Phosphorylation of polynucleotide kinase/ phosphatase by DNA-dependent protein kinase and ataxia-telangiectasia mutated regulates its association with sites of DNA damage. *Nucleic Acids Research*, *39*(21), 9224–37. http://doi.org/10.1093/nar/gkr647